

ELECTRONIC SUPPORTING INFORMATION

Rigid, Biconical Hydrogen-bonded Dimers that Encapsulate Cationic Guests in Solution and the Solid State

Jordan N. Smith, Courtney Ennis and Nigel T. Lucas

MacDiarmid Institute for Advanced Materials and Nanotechnology, Department of
Chemistry, University of Otago, Union Place, Dunedin 9016, New Zealand

Contents

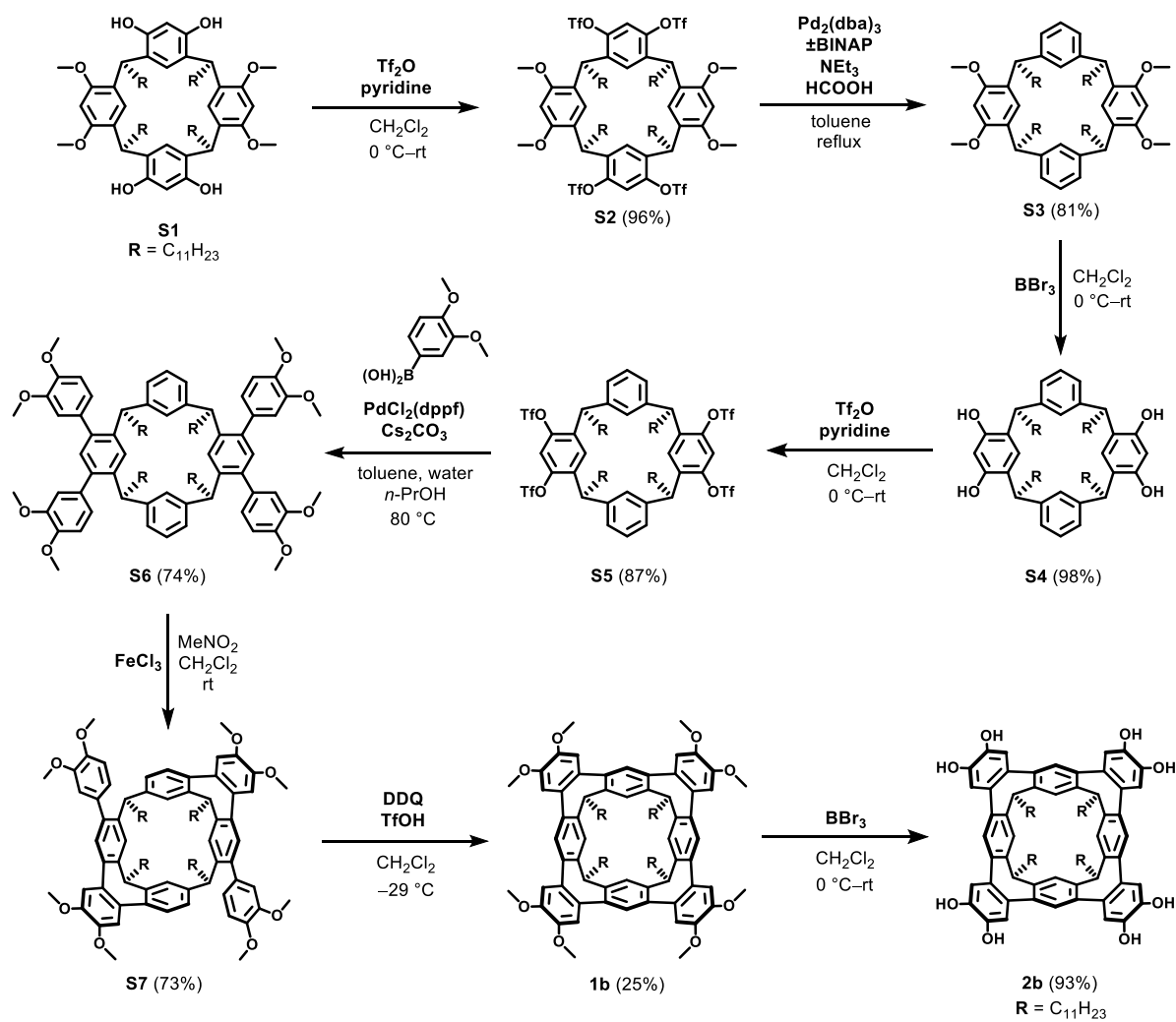
1. General	2
2. Synthesis and Characterization.....	2
3. ^1H and ^{13}C NMR spectra of new compounds.....	11
4. Supramolecular Behaviour Including Guest Binding	29
5. Calculations.....	46
6. X-ray Crystallography	54
7. References	56

1. General

All commercially purchased starting materials were used as received unless otherwise noted. Solvents listed as “dry” were dried using a Pure-Solv MD-6 solvent purification system. All other solvents were LR grade unless otherwise noted. Solvents were removed under “reduced pressure” by rotary evaporation and “*in vacuo*” under high vacuum via a Schlenk line. Standard Schlenk techniques were employed where an inert atmosphere of argon or nitrogen was required. ^1H , ^{13}C and ^{19}F NMR spectra were recorded in 5 mm diameter tubes at 25 °C, on a Varian 400 MR spectrometer (400, 100 and 376, MHz, respectively) or a Varian 500 AR spectrometer (500, 126 and 470 MHz, respectively). ^1H NMR signals were referenced against residual non-perdeuterated solvent and ^{13}C NMR against a signal of the deuterated solvent.¹ 2-Dimensional NMR spectra (COSY, NOESY, HSQC, HMBC) were recorded for all new compounds to assist in assignments. HR MS (ESI) mass spectra were recorded on a Bruker MicrOTOF-Q or Shimadzu LCMS-9030 Q-TOF electrospray ionisation mass spectrometer. IR spectra were recorded on a Bruker Alpha FT-IR spectrometer. Elemental analyses were measured on a Carlo Erba 1108 CHNS combustion analyser at the Campbell Microanalytical Laboratory, University of Otago, Dunedin with an absolute uncertainty of $\pm 0.3\%$, and are omitted where satisfactory analysis could not be obtained.

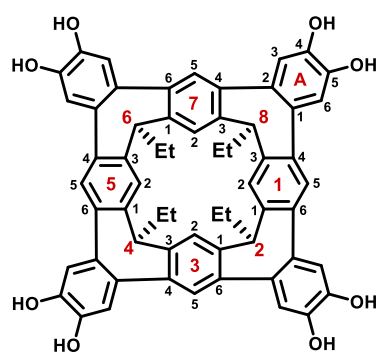
2. Synthesis and Characterization

Compounds **1a**² and **S1**³ were synthesised using reported procedures or minor variations thereof. Compounds **1b** and **2b** were prepared as shown in Scheme S1.



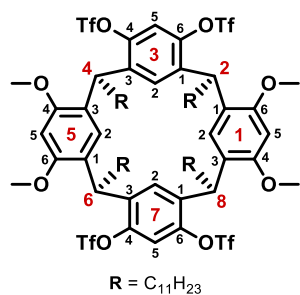
Scheme S1. The synthesis of **1b** and **2b** from C_{2v} -symmetric precursor **S1**.

1⁴,7⁴:1⁶,3⁶:3⁴,5⁶:5⁴,7⁶-Tetrakis(4,5-dihydroxy[1,2]benzeno)-2,4,6,8-tetraethyl-1,3,5,7(1,3)-tetrabenzenacyclooctaphane (2a)



Octamethoxy **1a** (30 mg, 0.030 mmol) was dissolved in dry CH₂Cl₂ (20 mL) under an argon atmosphere and the solution cooled in an ice-water bath. Boron tribromide in CH₂Cl₂ (1.0 M, 0.71 mL, 0.71 mmol) was added dropwise and the resulting dark solution allowed to warm to rt over 18 h. The reaction was quenched with MeOH (1 mL) causing a white precipitate to form. The volatiles were removed under reduced pressure and the solid dried *in vacuo* affording **2a** as an off-white solid (26 mg, 0.029 mmol, 96%). ¹H NMR (400 MHz, *d*₆-DMSO): δ 9.13 (s (br), 8H, OH), 7.14 (s, 4H, *H*-1²,3²,5²,7²), 6.95 (s, 8H, *H*-A³,A⁶), 6.74 (s, 4H, *H*-1⁵,3⁵,5⁵,7⁵), 3.27 (t, *J* = 7.7 Hz, 4H, CH), 2.51–2.48 (m, 8H, CH₂), 1.05 (t, *J* = 7.1 Hz, 12H, CH₃). ¹³C NMR (101 MHz, *d*₆-DMSO): δ 144.78 (*C*-A⁴,A⁵), 142.67 (*C*-1¹,1³,3¹,3³,5¹,5³,7¹,7³), 134.59 (*C*-1⁴,1⁶,3⁴,3⁶,5⁴,5⁶,7⁴,7⁶), 129.97 (*C*-A¹,A²), 129.46 (*C*-1⁵,3⁵,5⁵,7⁵), 115.04 (*C*-A³,A⁶), 114.15 (*C*-1²,3²,5²,7²), 44.38 (2,4,6,8-CH), 20.08 (CH₂), 12.29 (CH₃). HR-ESI-MS: calcd [M+Na]⁺ (C₆₀H₄₈NaO₈) *m/z* 919.324; found 919.323. IR (neat): 3485 (w, OH), 3375 (m, br, OH), 2956 (m, CH), 2921 (s, CH), 2851 (s, CH) cm⁻¹.

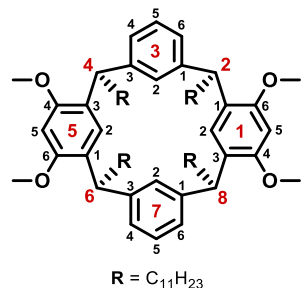
1⁴,1⁶,5⁴,5⁶-Tetramethoxy-3⁴,3⁶,7⁴,7⁶-tetratriflyloxy-2,4,6,8-tetra(*n*-undecyl)-1,3,5,7(1,3)-tetrabenzenacyclooctaphane (S2)



Tetrol **S1** (3.60 g, 3.10 mmol) was dissolved in dry CH₂Cl₂ (120 mL), pyridine (6.0 mL, 5.88 g, 74.4 mmol) added and the solution cooled in an ice-water bath under an argon atmosphere. Triflic anhydride (2.60 mL, 4.37 g, 15.5 mmol) was added dropwise and the resulting deep-purple solution stirred cold for 30 min before allowing to warm to rt over 16 h. The reaction was quenched by the dropwise addition of aqueous HCl (5 M, 30 mL) with vigorous stirring, diluted with Et₂O, the organic phase washed with water, brine, then dried over MgSO₄ and filtered. The solvents were removed under reduced pressure affording **S2** as an off-white solid (5.02 g, 2.95 mmol, 96%). ¹H NMR (500 MHz, CDCl₃): δ 7.18 (s, 2H, *H*-3⁵,7⁵), 7.05 (s, 2H, *H*-1²,5²), 6.55 (s, 2H, *H*-3²,7²), 6.10 (s, 2H, *H*-1⁵,5⁵), 4.44 (dd, *J* = 8.8, 6.1 Hz, 4H, CH), 3.44 (s, 12H, OCH₃), 2.02–1.95 (m, 4H, CHCHH), 1.80–1.73 (m, 4H, CHCHH), 1.44–1.22 (m, 72H, (CH₂)₉), 0.88 (t, *J* = 7.0 Hz, 12H, CH₃). ¹³C NMR (126 MHz, CDCl₃): δ 157.17 (*C*-1⁴,1⁶,5⁴,5⁶), 144.87 (*C*-3⁴,3⁶,7⁴,7⁶), 140.21 (*C*-3¹,3³,7¹,7³), 128.46 (*C*-3²,7²), 124.93 (*C*-1²,5²), 121.17 (*C*-1¹,1³,5¹,5³), 118.65 (q, *J*_{CF} = 320 Hz, CF₃), 113.48 (*C*-3⁵,7⁵), 95.78 (*C*-1⁵,5⁵), 55.26 (OCH₃), 36.58 (2,4,6,8-CH), 34.76 (CH₂), 32.08 (CH₂), 29.91 (CH₂), 29.87 (CH₂), 29.86 (CH₂), 29.83 (CH₂), 29.77 (CH₂), 29.52 (CH₂),

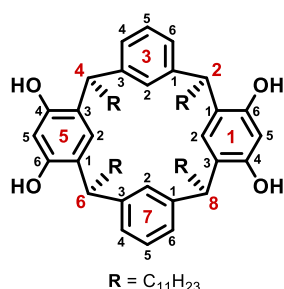
27.96 (CH₂), 22.84 (CH₂), 14.24 (CH₃). ¹⁹F NMR (376 MHz, CDCl₃): δ -74.6 (s, CF₃). HR-ESI-MS: calcd [M+Na]⁺ (C₈₀H₁₁₆F₁₂NaO₁₆S₄) *m/z* 1711.685; found 1711.689.

1⁴,1⁶,5⁴,5⁶-Tetramethoxy-2,4,6,8-tetra(*n*-undecyl-1,3,5,7(1,3)-tetrabenzenacyclooctaphane (S3)



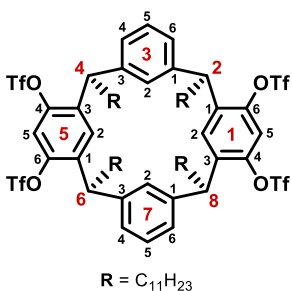
Tetratriflate **S2** (3.40 g, 2.07 mmol) was dissolved in toluene (15 mL) and triethylamine (3.5 mL, 2.51 g, 24.9 mmol) under an argon atmosphere, and the solution deoxygenated by gentle argon bubbling for 10 min. Formic acid (0.95 mL, 1.15 g, 24.9 mmol) was added dropwise, followed by tris(dibenzylideneacetone)-dipalladium(0) (189 mg, 0.21 mmol) and (±)-BINAP (255 mg, 0.41 mmol), and the dark-purple mixture heated at reflux until judged complete by TLC (24–48 h). After cooling, the mixture was diluted with CH₂Cl₂, the organic phase washed with water, brine, then dried over MgSO₄, filtered and the solvents removed under reduced pressure. The crude residue was purified by column chromatography (SiO₂, 30% CH₂Cl₂/petrol) affording **S3** as a white solid (1.85 g, 1.67 mmol, 81%). ¹H NMR (500 MHz, CDCl₃): δ 7.16–7.13 (m, 6H, *H*-3⁴,3⁵,3⁶,7⁴,7⁵,7⁶), 6.77 (s, 2H, *H*-1²,5²), 6.71 (s, 2H, *H*-3²,7²), 6.25 (s, 2H, *H*-1⁵,5⁵), 4.14 (t, *J* = 7.8 Hz, 4H, CH), 3.70 (s, 12H, OCH₃), 1.93–1.85 (m, 8H, CHCH₂), 1.32–1.20 (m, 72H, (CH₂)₉), 0.89 (t, *J* = 6.9 Hz, 12H, CH₃). ¹³C NMR (126 MHz, CDCl₃): δ 155.54 (C-1⁴,1⁶,5⁴,5⁶), 145.25 (C-3¹,3³,7¹,7³), 127.07 (C-3⁵,7⁵), 126.74 (C-1²,5²), 126.42 (C-3⁴,3⁶,7⁴,7⁶), 126.05 (C-1¹,1³,5¹,5³), 125.75 (C-3²,7²), 95.44 (C-1⁵,5⁵), 55.75 (OCH₃), 42.64 (2,4,6,8-CH), 35.07 (CH₂), 32.10 (CH₂), 29.92 (CH₂), 29.90 (CH₂), 29.89 (CH₂), 29.87 (CH₂), 29.85 (CH₂), 29.77 (CH₂), 29.55 (CH₂), 28.22 (CH₂), 14.27 (CH₃). HR-ESI-MS: calcd [M+K]⁺ (C₇₆H₁₂₀KO₄) *m/z* 1135.882; found 1135.878. Anal. calcd [C₇₆H₁₂₀O₄]: C 83.15, H 11.02; found C 83.05, H 11.32.

2,4,6,8-Tetra(*n*-undecyl)-1,3,5,7(1,3)-tetrabenzenacyclooctaphane-1⁴,1⁶,5⁴,5⁶-tetrol (**S4**)



Tetramethoxy **S3** (600 mg, 0.55 mmol) was dissolved in dry CH₂Cl₂ (30 mL) under argon and the solution cooled in an ice-water bath. Boron tribromide in CH₂Cl₂ (1.0 M, 3.30 mL, 3.30 mmol) was added dropwise and the resulting deep-purple solution stirred for 30 min before allowing to warm to rt over 20 h. The reaction was quenched by the dropwise addition of MeOH (3 mL) and diluted with Et₂O, the organic phase washed with water, brine, then dried over MgSO₄ and filtered. The removal of solvents under reduced pressure afforded **S4** as an off-white solid (570 mg, 0.54 mmol, 98%). ¹H NMR (500 MHz, *d*₆-acetone): δ 7.71 (s, 4H, OH), 7.15 (dd, *J* = 7.4, 1.6 Hz, 4H, *H*-3⁴,3⁶,7⁴,7⁶), 7.12 (s, 2H, *H*-1²,5²), 7.11 (s, 2H, *H*-3²,7²), 7.05 (t, *J* = 7.4 Hz, 2H, *H*-3⁵,7⁵), 6.16 (s, 2H, *H*-1⁵,5⁵), 4.20 (t, *J* = 7.9 Hz, 4H, CH), 2.03–2.00 (m, 8H, CHCH₂), 1.33–1.23 (m, 72H, (CH₂)₉), 0.89 (t, *J* = 7.0 Hz, 12H, CH₃). ¹³C NMR (126 MHz, *d*₆-acetone): δ 153.74 (*C*-1⁴,1⁶,5⁴,5⁶), 146.74 (*C*-3¹,3³,7¹,7³), 127.53 (*C*-3⁴,3⁶,7⁴,7⁶), 127.51 (*C*-3⁵,7⁵), 126.16 (*C*-3²,7²), 125.93 (*C*-1²,5²), 123.87 (*C*-1¹,1³,5¹,5³), 102.95 (*C*-1⁵,5⁵), 43.58 (2,4,6,8-CH), 36.00 (CH₂), 32.70 (CH₂), 30.58 (CH₂), 30.50 (CH₂), 30.49 (CH₂), 30.47 (CH₂), 30.46 (CH₂), 30.17 (CH₂), 28.97 (CH₂), 23.39 (CH₂), 14.41 (CH₃). HR-ESI-MS: calcd [M+Na]⁺ (C₇₂H₁₁₂NaO₄) *m/z* 1063.845; found 1063.844.

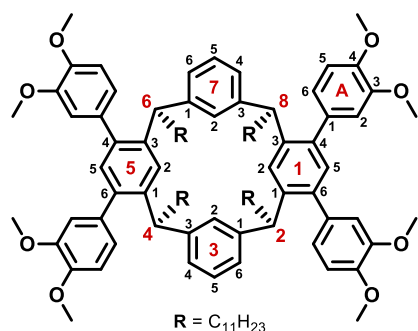
1⁴,1⁶,5⁴,5⁶-Tetratriflyloxy-2,4,6,8-tetra(*n*-undecyl)-1,3,5,7(1,3)-tetrabenzenacyclooctaphane (**S5**)



Tetrahydroxy **S4** (520 mg, 0.49 mmol) was dissolved in dry CH₂Cl₂ (60 mL), pyridine (1.36 mL, 1.34 g, 11.8 mmol) added and the solution cooled in an ice-water bath under an argon atmosphere. Triflic anhydride (0.41 mL, 695 mg, 2.46 mmol) was added dropwise and the resulting pale-yellow solution stirred cold for 30 min before allowing to warm to rt over 8 h. The reaction was quenched by the dropwise addition of aqueous HCl (2 M, 20 mL) with vigorous stirring, the organic phase washed with water, brine, then dried over MgSO₄ and filtered. The solvents were removed under reduced pressure affording **S5** as a pale-yellow solid (670 mg, 0.43 mmol, 87%). ¹H NMR (500 MHz, CDCl₃): δ 7.33 (t, *J* = 7.7 Hz, 2H, *H*-3⁵,7⁵), 7.23 (dd, *J* = 7.7, 1.7 Hz, 4H, *H*-3⁴,3⁶,7⁴,7⁶), 7.04 (s, 2H, *H*-1⁵,5⁵), 6.89 (s, 2H, *H*-1²,5²), 6.27 (s, 2H, *H*-3²,7²), 4.16 (t, *J* = 7.6 Hz, 4H, CH), 1.95–1.79 (m, 8H, CHCH₂), 1.31–1.25 (m, 72H, (CH₂)₉), 0.88 (t, *J* = 6.8 Hz, 12H, CH₃). ¹³C NMR (126 MHz, CDCl₃): δ 145.12 (*C*-1⁴,1⁶,5⁴,5⁶), 142.68 (*C*-3¹,3³,7¹,7³), 138.25 (*C*-1¹,1³,5¹,5³), 129.01 (*C*-1²,5²), 128.67 (*C*-3⁵,7⁵), 127.30 (*C*-3²,7²), 126.81 (*C*-3⁴,3⁶,7⁴,7⁶), 118.51 (q, *J*_{CF} = 320 Hz, CF₃), 114.72 (*H*-1⁵,5⁵), 43.83 (2,4,6,8-CH), 34.97 (CH₂), 32.07 (CH₂),

29.80 (CH₂), 29.97 (CH₂), 29.76 (CH₂), 29.65 (CH₂), 29.61 (CH₂), 29.51 (CH₂), 27.77 (CH₂), 22.84 (CH₂), 14.25 (CH₃). ¹⁹F NMR (376 MHz, CDCl₃): δ -74.0 (s, CF₃). HR-ESI-MS: calcd [M+Na]⁺ (C₇₆H₁₀₅F₁₂NaO₁₂S₄) *m/z* 1591.642; found 1591.640. Anal. calcd [C₇₆H₁₀₅F₁₂O₁₂S₄]: C 58.15, H 6.93, S 8.17; found C 57.78, H 7.28, S 8.03.

1⁴,1⁶,5⁴,5⁶-Tetrakis(3,4-dimethoxyphenyl)-2,4,6,8-tetra(*n*-undecyl)-1,3,5,7(1,3)-tetrabenzenacyclooctaphane (S6)



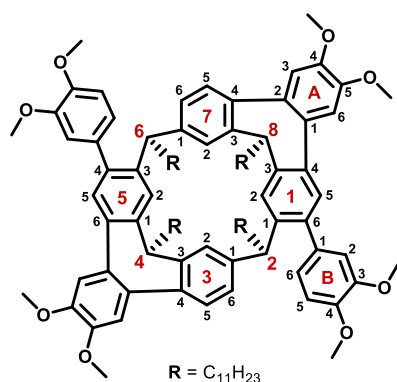
Tetratrilate **S5** (500 mg, 0.32 mmol), 3,4-dimethoxyphenylboronic acid (870 mg, 4.78 mmol) and caesium carbonate (3.11 g, 9.56 mmol) were suspended in toluene (20 mL), water (10 mL) and *n*-PrOH (1 mL), and the mixture deoxygenated with gentle argon bubbling for 10 min.

Dichloro[1,1'-bis(diphenylphosphino)ferrocene]-

palladium(II) dichloromethane solvate (58 mg, 0.071 mmol)

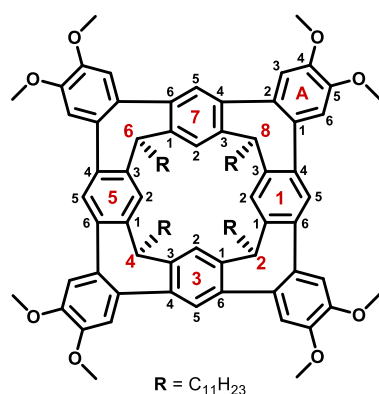
was added and the mixture heated at 80 °C for 18 h with vigorous stirring. After cooling, the dark mixture was diluted with CH₂Cl₂, the organic phase washed with water, brine, then dried over MgSO₄, filtered and the solvents removed under reduced pressure. The crude residue was purified by column chromatography (SiO₂, 1% acetone/CH₂Cl₂) affording **S6** as a colourless oil (360 mg, 0.24 mmol, 74%). ¹H NMR (500 MHz, CDCl₃): δ 7.20 (s, 2H, *H*-3²,7²), 7.00–6.98 (m, 6H, *H*-1²,1⁵,3⁵,5²,5⁵,7⁵), 6.82 (d, *J* = 8.3 Hz, 4H, *H*-A⁵), 6.76–6.74 (m, 8H, *H*-A²,A⁶), 6.67 (dd, *J* = 7.7, 1.5 Hz, 4H, *H*-3⁴,3⁶,7⁴,7⁶), 4.11 (t, *J* = 7.7 Hz, 4H, *CH*), 3.91 (s, 12H, A⁴-OCH₃), 3.76 (s, 12H, A³-OCH₃), 1.96–1.91 (m, 8H, CHCH₂), 1.29–1.20 (m, 72H, (CH₂)₉), 0.88 (t, *J* = 7.0 Hz, 12H, CH₃). ¹³C NMR (126 MHz, CDCl₃): δ 148.36 (C-A⁴), 148.07 (C-A³), 145.53 (C-3¹,3³,7¹,7³), 141.66 (C-1¹,1³,5¹,5³/1⁴,1⁶,5⁴,5⁶), 139.38 (C-1¹,1³,5¹,5³/1⁴,1⁶,5⁴,5⁶), 134.53 (C-A¹), 131.83 (C-1²,5²/1⁵,5⁵), 127.49 (C-3⁵,7⁵), 126.78 (C-3⁴,3⁶,7⁴,7⁶), 126.34 (C-3²,7²), 126.03 (C-1²,5²/1⁵,5⁵), 122.17 (C-A⁶), 113.59 (C-A²), 110.73 (C-A⁵), 56.04 (A⁴-OCH₃), 55.99 (A³-OCH₃), 46.68 (2,4,6,8-CH), 37.01 (CH₂), 32.09 (CH₂), 29.91 (CH₂), 29.90 (CH₂), 29.87 (CH₂), 29.85 (CH₂), 29.76 (CH₂), 29.54 (CH₂), 28.23 (CH₂), 22.84 (CH₂), 14.26 (CH₃). HR-ESI-MS: calcd [M+Na]⁺ (C₁₀₄H₁₁₄NaO₈) *m/z* 1544.075; found 1544.076. Anal. calcd [C₁₀₄H₁₁₄O₈]: C 82.06, H 9.54; found C 82.07, H 9.88.

***rac*-1⁴,7⁴:3⁴,5⁶-Bis(4,5-dimethoxy[1,2]benzeno)-1⁶,5⁴-bis(3,4-dimethoxyphenyl)-2,4,6,8-tetra(*n*-undecyl)-1,3,5,7(1,3)tetrabenzenacyclooctaphane (**S7**)**



Macrocycle **S6** (640 mg, 0.42 mmol) was dissolved in CH₂Cl₂ (150 mL, AR grade) and the solution deoxygenated with gentle argon bubbling for 10 min. FeCl₃ (1.36 g, 8.41 mmol) in MeNO₂ (3 mL) was added dropwise and the resulting dark green solution stirred at rt with continued argon bubbling. After 30 min, the reaction was quenched with MeOH (10 mL), the organic phase washed with water, brine, then dried over MgSO₄, filtered and the solvents removed under reduced pressure. The crude product was purified by column chromatography (SiO₂, 1% acetone/CH₂Cl₂) affording **S7** as a pale-yellow oil with a minor, inseparable impurity (465 mg, 0.31 mmol, 73%). ¹H NMR (500 MHz, CDCl₃): δ 7.69 (s, 2H, *H*-1²,5²), 7.59 (s, 2H, *H*-3²,7²), 7.17 (s, 2H, *H*-1⁵,5⁵), 7.07 (s, 2H, *H*-A⁶), 7.05 (d, *J* = 7.8 Hz, 2H, *H*-3⁵,7⁵), 7.02 (s, 2H, *H*-A³), 6.96–6.73 (m (br), 6H, *H*-B²,B⁵,B⁶), 6.41 (d, *J* = 7.8 Hz, 2H, *H*-3⁶,7⁶), 4.11 (t, *J* = 7.9 Hz, 2H, 4,8-CH), 3.97 (s, 6H, B⁴-OCH₃), 3.94 (s, 6H, A⁴-OCH₃), 3.91 (s, 6H, A⁵-OCH₃), 3.81 (s (br), 6H, B³-OCH₃), 3.48 (t, *J* = 7.6 Hz, 2H, 2,6-CH), 2.64–2.58 (m, 4H, 4,8-CHCH₂), 2.34–2.26 (m, 4H, 2,6-CHCH₂), 1.64–1.56 (m, 8H, 2,4,6,8-CHCH₂CH₂), 1.38–1.21 (m, 64H, (CH₂)₈), 0.89 (t, *J* = 6.8 Hz, 12H, CH₃). ¹³C NMR (126 MHz, CDCl₃): δ 148.46 (C-B³), 148.23 (C-A⁵), 148.20 (C-A⁴), 148.03 (C-B⁴), 145.35 (C-3¹,7¹), 144.33 (C-3³,7³), 143.12 (C-1³,5¹), 142.79 (C-1¹,5³), 138.59 (C-1⁶,5⁴), 136.26 (C-3⁴,7⁴), 135.27 (C-1⁴,5⁶), 134.69 (C-A¹), 131.72 (C-A²), 131.17 (C-B¹), 130.20 (C-1⁵,5⁵), 128.46 (C-3⁵,7⁵), 126.56 (C-3⁶,7⁶), 121.96 (C-B²), 119.81 (C-1²,5²), 118.85 (C-3²,7²), 113.54 (C-B⁵), 112.03 (C-A³), 111.76 (C-A⁶), 110.81 (C-B⁶), 56.16 (B⁴-OCH₃), 56.08 (A⁴-OCH₃), 56.06 (A⁵-OCH₃), 56.02 (B³-OCH₃), 46.14 (2,6-CH), 43.13 (4,8-CH), 36.81 (2,6-CH₂), 32.13 (CH₂), 32.10 (CH₂), 30.69 (CH₂), 30.19 (CH₂), 30.14 (CH₂), 30.11 (CH₂), 30.08 (CH₂), 29.98 (CH₂), 29.96 (CH₂), 29.92 (CH₂), 29.88 (CH₂), 29.85 (CH₂), 29.64 (CH₂), 29.55 (CH₂), 29.03 (4,8-CH₂), 28.63 (CH₂), 28.03 (CH₂), 22.86 (CH₂), 22.85 (CH₂), 14.26 (CH₃ × 2). HR-ESI-MS: calcd [M+Na]⁺ (C₁₀₄H₁₄₀NaO₈) *m/z* 1541.044; found 1541.044. Anal. calcd [C₁₀₄H₁₄₀O₈]: C 82.27, H 9.29; found C 82.46, H 9.68.

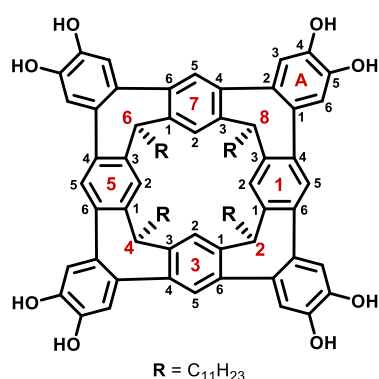
1⁴,7⁴:1⁶,3⁶:3⁴,5⁶:5⁴,7⁶-Tetrakis(4,5-dimethoxy[1,2]benzeno)-2,4,6,8-tetra(*n*-undecyl)-1,3,5,7(1,3)-tetrabenzenacyclooctaphane (1b**)**



Macrocycle **S7** (900 mg, 0.59 mmol) was dissolved in dry CH₂Cl₂ (80 mL) under an argon atmosphere and cooled to -29 °C in a *o*-xylene/dry ice bath. Triflic acid (5.20 mL, 8.85 g, 59.0 mmol) was added dropwise giving a dark solution. DDQ (605 mg, 2.67 mmol) was added immediately in one aliquot and the resulting deep blue solution was stirred at -29 °C for 4.5 h. The reaction was quenched with aqueous NaHCO₃ (sat.), the organic phase washed with water, brine, then dried over

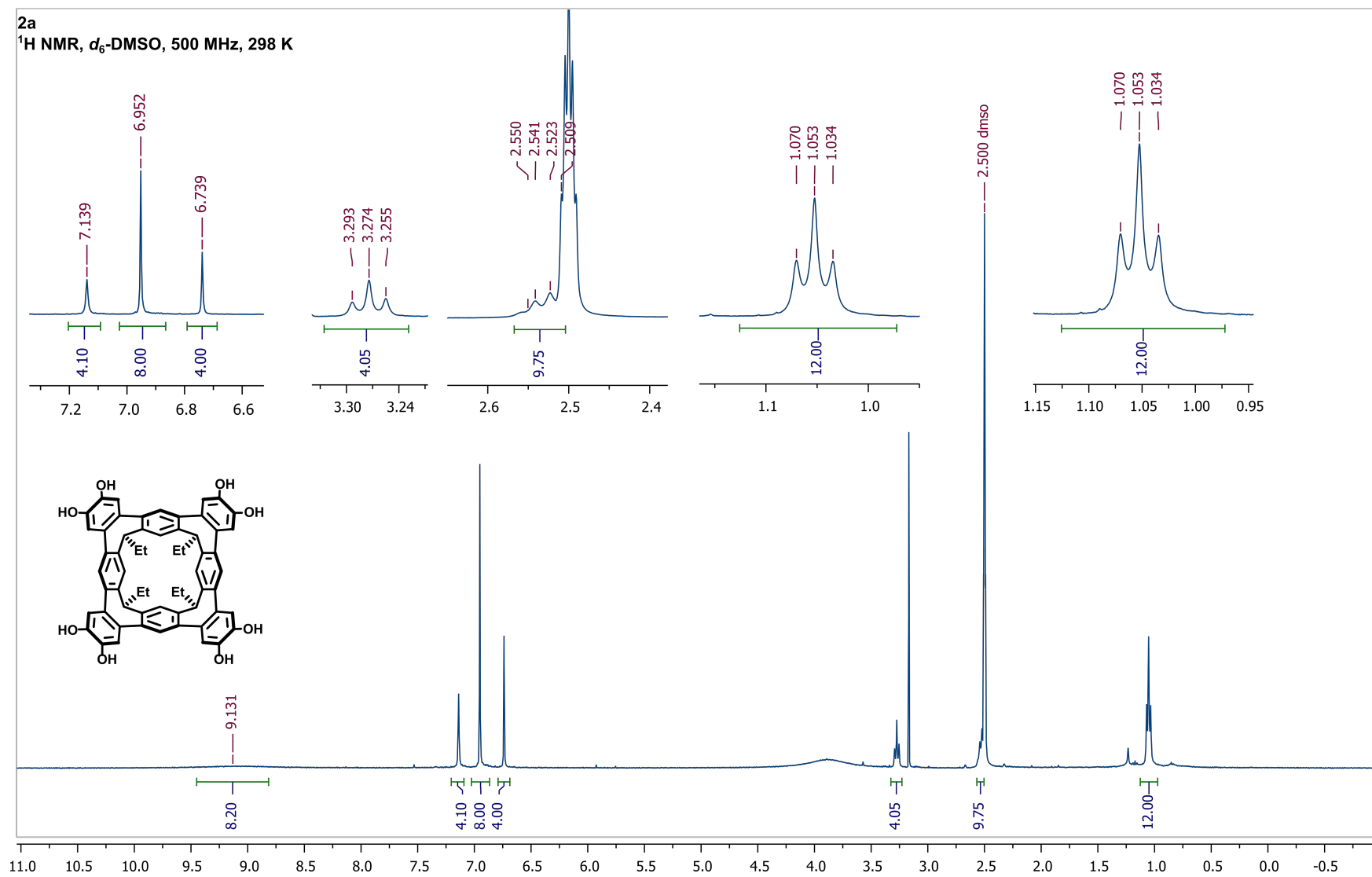
MgSO₄, filtered and the solvents removed under reduced pressure. The crude residue was purified by column chromatography (SiO₂, 7% EtOAc/CH₂Cl₂) affording **1b** as an off-white solid (220 mg, 0.15 mmol, 25%). ¹H NMR (400 MHz, CDCl₃): δ 7.14 (s, 8H, *H*-A³,A⁶), 7.09 (s, 4H, *H*-1⁵,3⁵,5⁵,7⁵), 7.07 (s, 4H, *H*-1²,3²,5²,7²), 3.98 (s, 24H, OCH₃), 3.56 (t, *J*=7.6 Hz, 4H, CH), 2.46–2.44 (m, 8H, CHCH₂), 1.54–1.52 (m, 16H, (CH₂)₂), 1.33–1.28 (m, 56H, (CH₂)₇), 0.89 (t, *J* = 7.0 Hz, 12H, CH₃). ¹³C NMR (101 MHz, CDCl₃): δ 148.32 (C-A⁴,A⁵), 143.49 (C-1¹,1³,3¹,3³,5¹,5³,7¹,7³), 135.41 (C-1⁴,1⁶,3⁴,3⁶,5⁴,5⁶,7⁴,7⁶), 131.88 (C-A¹,A²), 130.05 (C-1⁵,3⁵,5⁵,7⁵), 113.71 (C-1²,3²,5²,7²), 111.60 (C-A³,A⁶), 56.37 (OCH₃), 43.15 (2,4,6,8-CH), 32.10 (CH₂), 30.53 (CH₂), 30.06 (CH₂), 29.94 (CH₂), 29.93 (CH₂), 29.90 (CH₂), 29.85 (CH₂), 29.57 (CH₂), 28.24 (CH₂), 22.85 (CH₂), 14.27 (CH₃). HR-ESI-MS: calcd [M+Na]⁺ (C₁₀₄H₁₃₆NaO₈) *m/z* 1536.013; found 1536.010.

1⁴,7⁴:1⁶,3⁶:3⁴,5⁶:5⁴,7⁶-Tetrakis(4,5-dihydroxy[1,2]benzeno)-2,4,6,8-tetra(*n*-undecyl)-1,3,5,7(1,3)-tetrabenzenacyclooctaphane (2b**)**

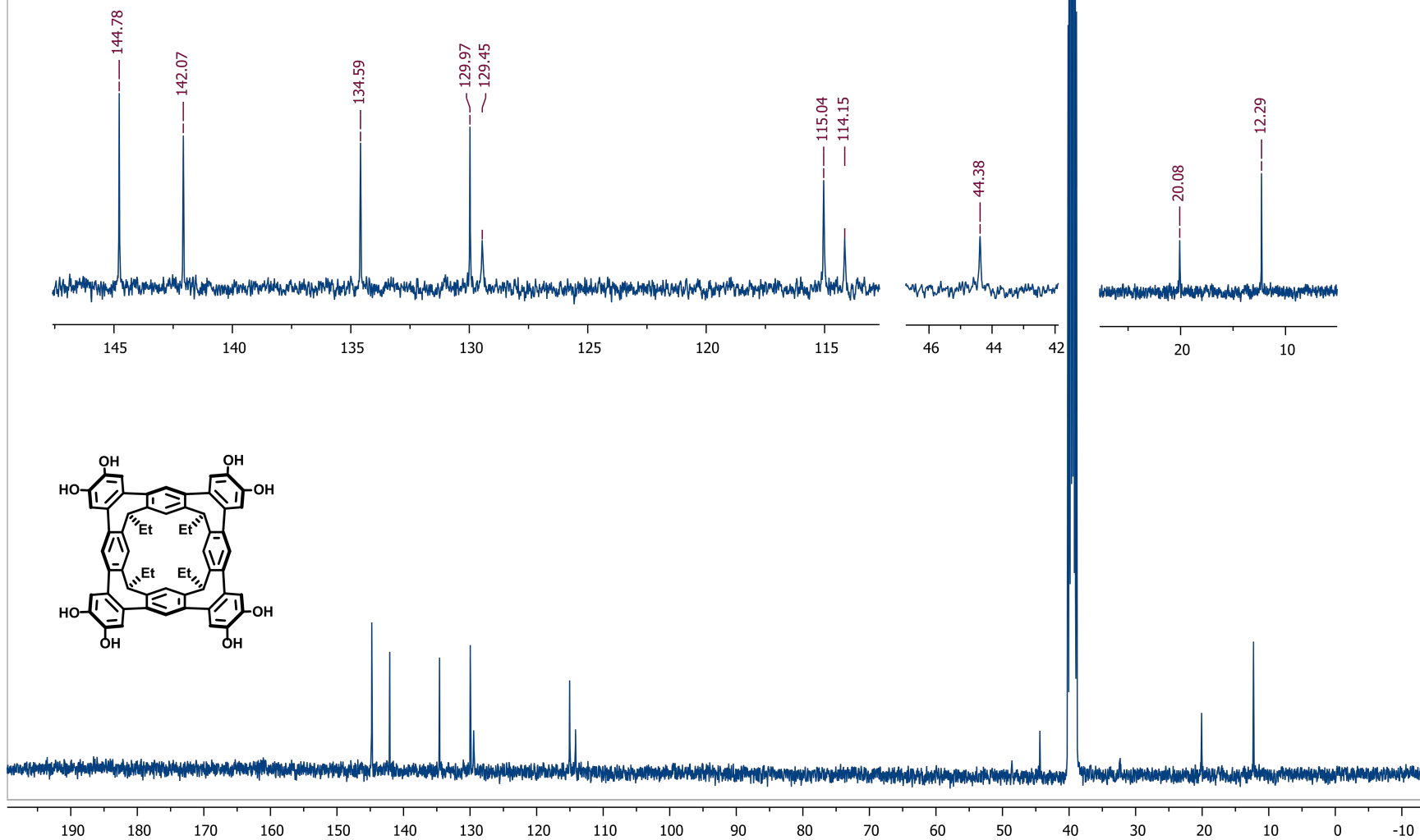


Octamethoxy **2a** (220 mg, 0.15 mmol) was dissolved in dry CH₂Cl₂ (50 mL) under an argon atmosphere and the solution cooled in an ice-water bath. Boron tribromide in CH₂Cl₂ (1.0 M, 1.74 mL, 1.74 mmol) was added dropwise and the resulting dark solution allowed to warm to rt over 20 h. The reaction was quenched with MeOH (1 mL) added dropwise, diluted with Et₂O and the organic phase washed with water, brine, then dried over MgSO₄ and filtered. The solvents were removed under reduced pressure affording **2b** as an off-white solid (188 mg, 0.13 mmol, 93%). ¹H NMR (400 MHz, CDCl₃): δ 7.18 (s, 8H, *H*-A³,A⁶), 6.93 (s, 8H, -OH), 6.81 (s, 4H, *H*-1²,3²,5²,7²), 6.06 (s, 4H, *H*-1⁵,3⁵,5⁵,7⁵), 3.38 (t, *J* = 7.6 Hz, 4H, CH), 2.32–2.26 (m, 8H, CHCH₂), 1.43–1.26 (m, 72H, (CH₂)₉), 0.88 (t, *J* = 7.6 Hz, 12H, CH₃). ¹³C NMR (400 MHz, CDCl₃): δ 142.96 (*C*-A⁴,A⁵), 141.41 (*C*-A¹,A²), 134.43 (*C*-1⁴,1⁶,3⁴,3⁶,5⁴,5⁶,7⁴,7⁶), 132.56 (*C*-1¹,1³,3¹,3³,5¹,5³,7¹,7³), 129.74 (*C*-1⁵,3⁵,5⁵,7⁵), 114.53 (*C*-A³,A⁶), 113.14 (*C*-1²,3²,5²,7²), 42.85 93 (CH), 32.09 (CH₂), 30.46 (CH₂), 30.00 (CH₂), 29.91 (CH₂), 29.89 (CH₂), 29.88 (CH₂), 29.55 (CH₂), 28.15 (CH₂), 27.96 (CH₂), 22.85 (CH₂), 14.26 (CH₃). ¹H NMR (500 MHz, *d*₆-acetone): δ 8.02 (s, 8H, -OH), 7.22 (s, 4H, *H*-1²,3²,5²,7²), 7.12 (s, 8H, *H*-A³,A⁶), 6.93 (s, 4H, *H*-1⁵,3⁵,5⁵,7⁵), 3.54 (t, *J* = 7.8 Hz, 4H, CH), 2.55–2.50 (m, 8H, CHCH₂), 1.41–1.29 (m, 72H, (CH₂)₉), 0.90 (t, *J* = 6.9 Hz, 12H, CH₃). ¹³C NMR (500 MHz, *d*₆-acetone): δ 145.41 (*C*-A⁴,A⁵), 143.66 (*C*-A¹,A²), 136.01 (*C*-1⁴,1⁶,3⁴,3⁶,5⁴,5⁶,7⁴,7⁶), 132.22 (*C*-1¹,1³,3¹,3³,5¹,5³,7¹,7³), 130.88 (*C*-1⁵,3⁵,5⁵,7⁵), 115.77 (*C*-A³,A⁶), 114.74 (*C*-1²,3²,5²,7²), 43.93 (CH), 32.72 (CH₂), 31.06 (CH₂), 30.69 (CH₂), 30.59 (CH₂), 30.55 (CH₂), 30.51 (CH₂), 30.19 (CH₂), 28.99 (CH₂), 28.59 (CH₂), 23.39 (CH₂), 14.42 (CH₃). HR-ESI-MS: calcd [M+K]⁺ (C₉₆H₁₂₀KO₈) *m/z* 1439.862; found 1439.859. Anal. calcd [C₉₆H₁₂₀O₈·1.3CH₂Cl₂·2Me₂CO]: C 76.19, H 8.33; found C 76.05, H 8.67. IR (neat): 3547 (w, OH), 3423 (br, OH), 2953 (m, CH), 2919 (s, CH), 2850 (s, CH) cm⁻¹.

3. ^1H and ^{13}C NMR spectra of new compounds

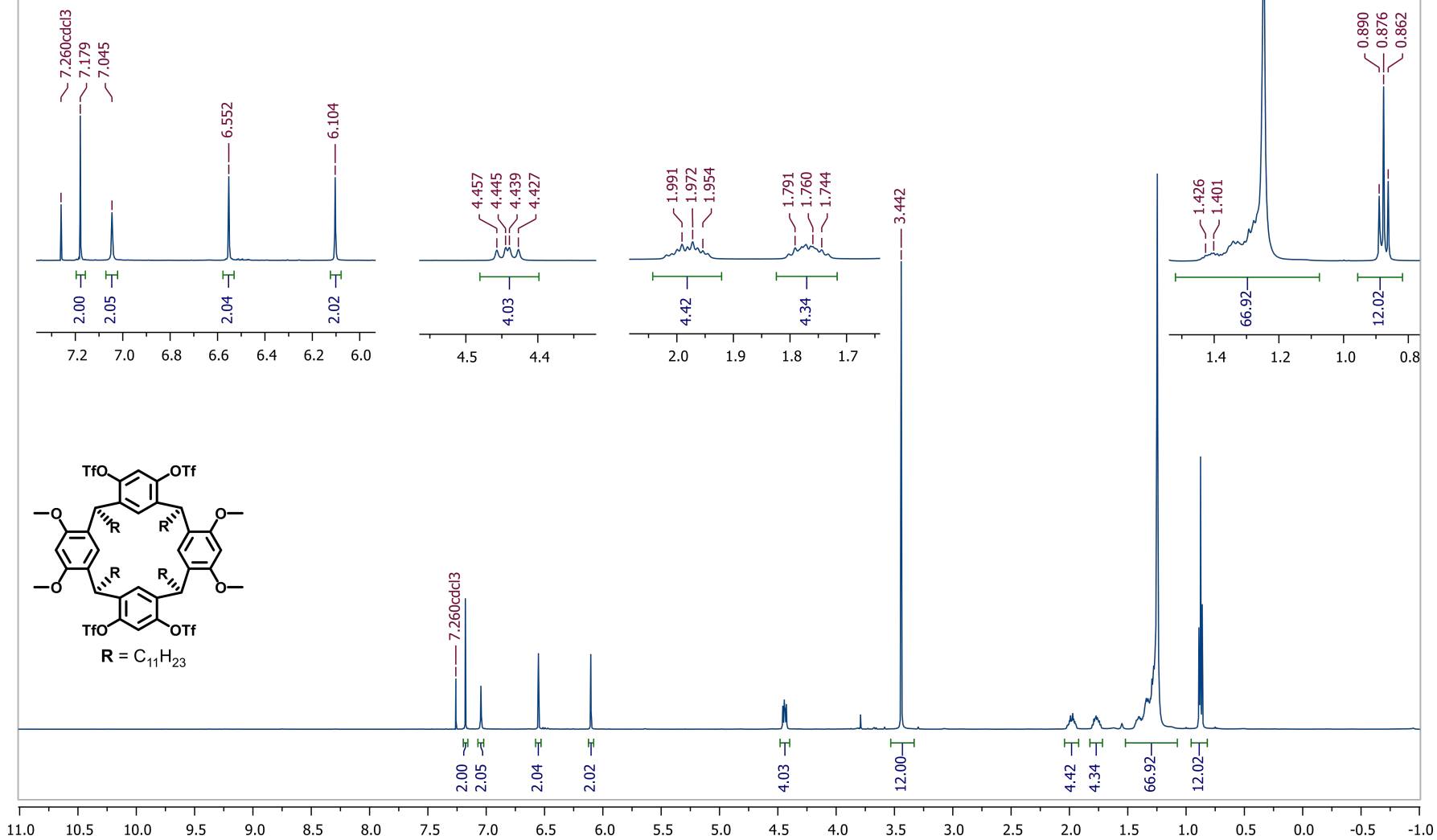


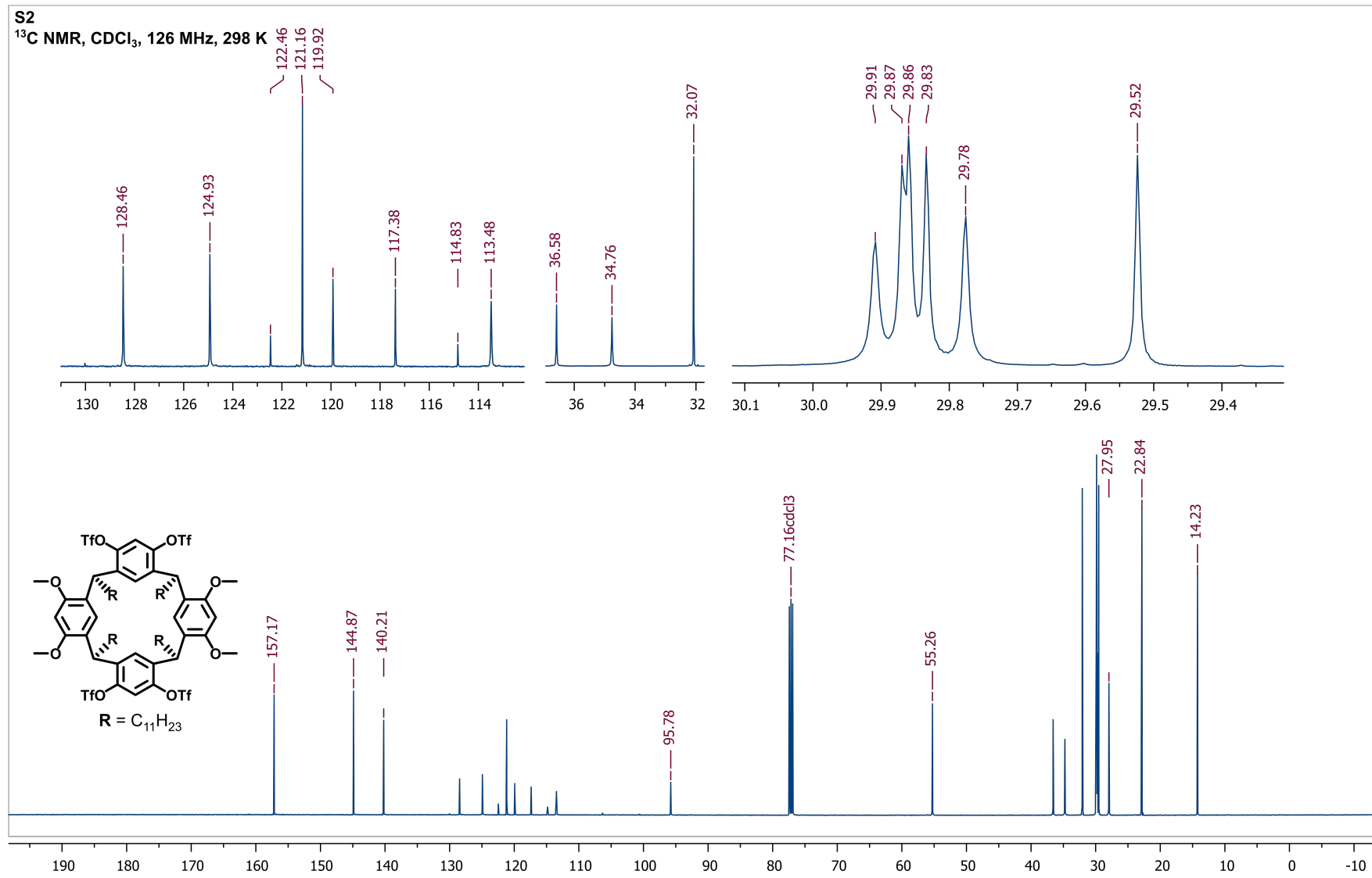
2a
¹³C NMR, d₆-DMSO, 126 MHz, 298 K



S2

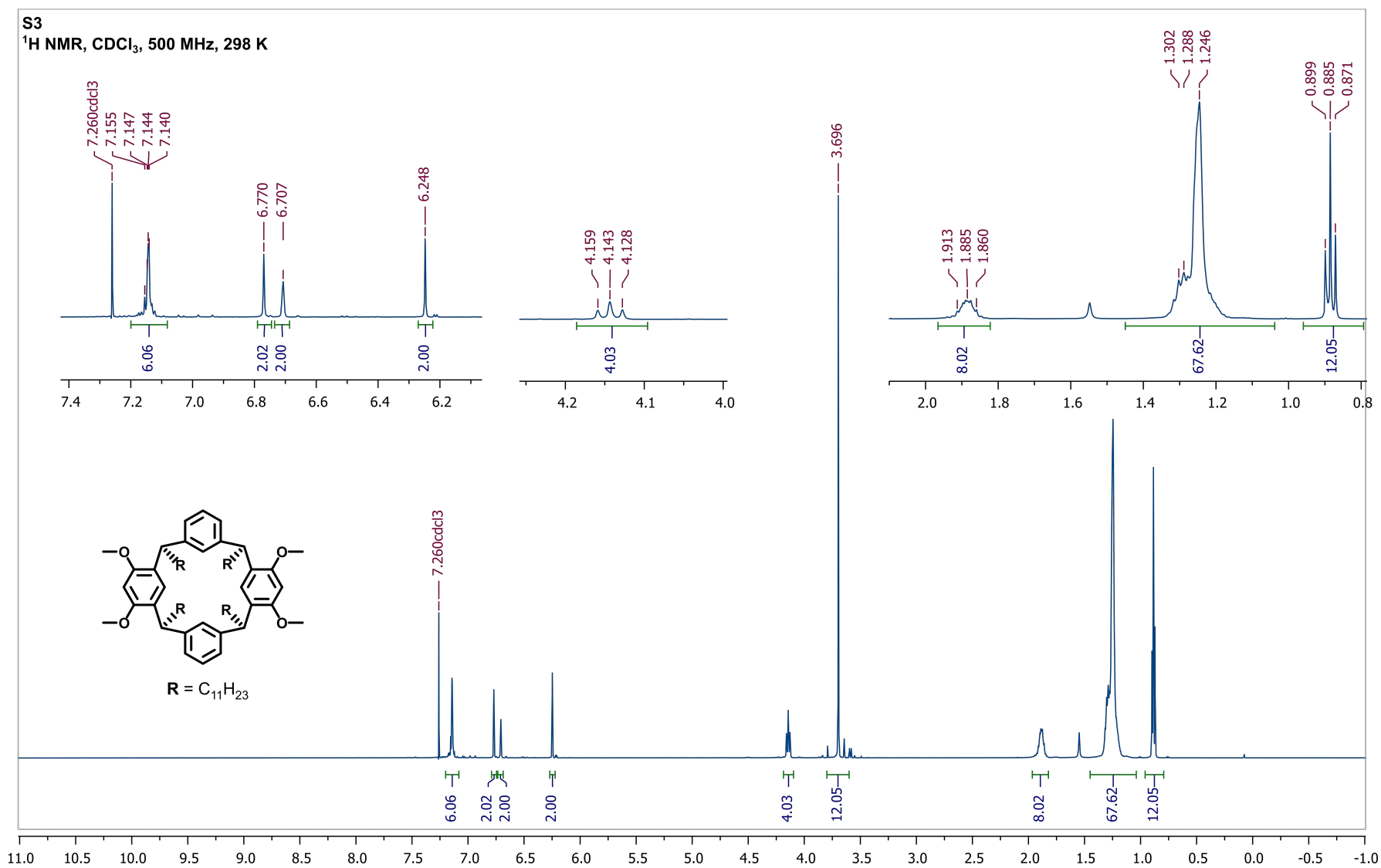
^1H NMR, CDCl_3 , 500 MHz, 298 K



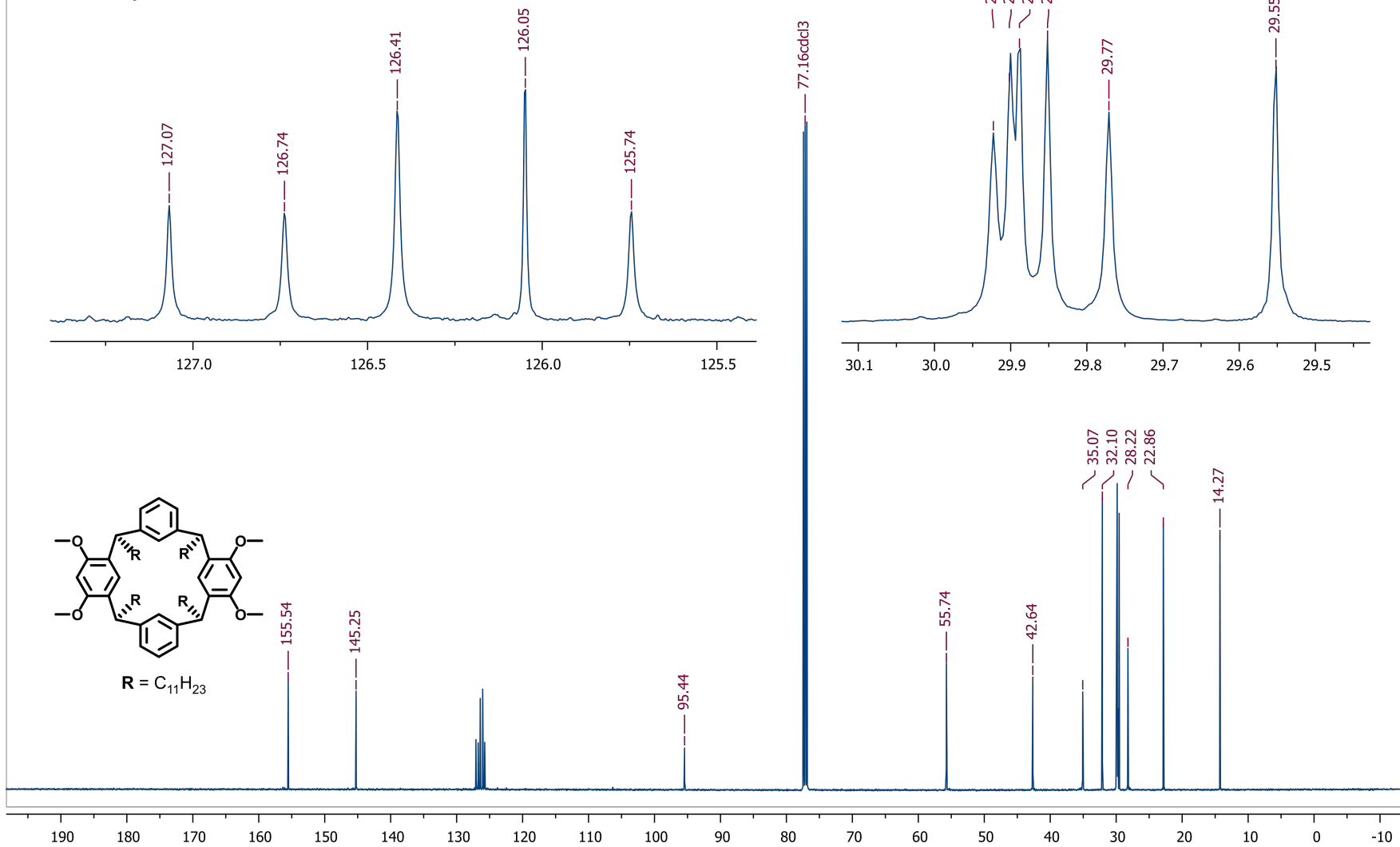


S3

$^1\text{H NMR}$, CDCl_3 , 500 MHz, 298 K

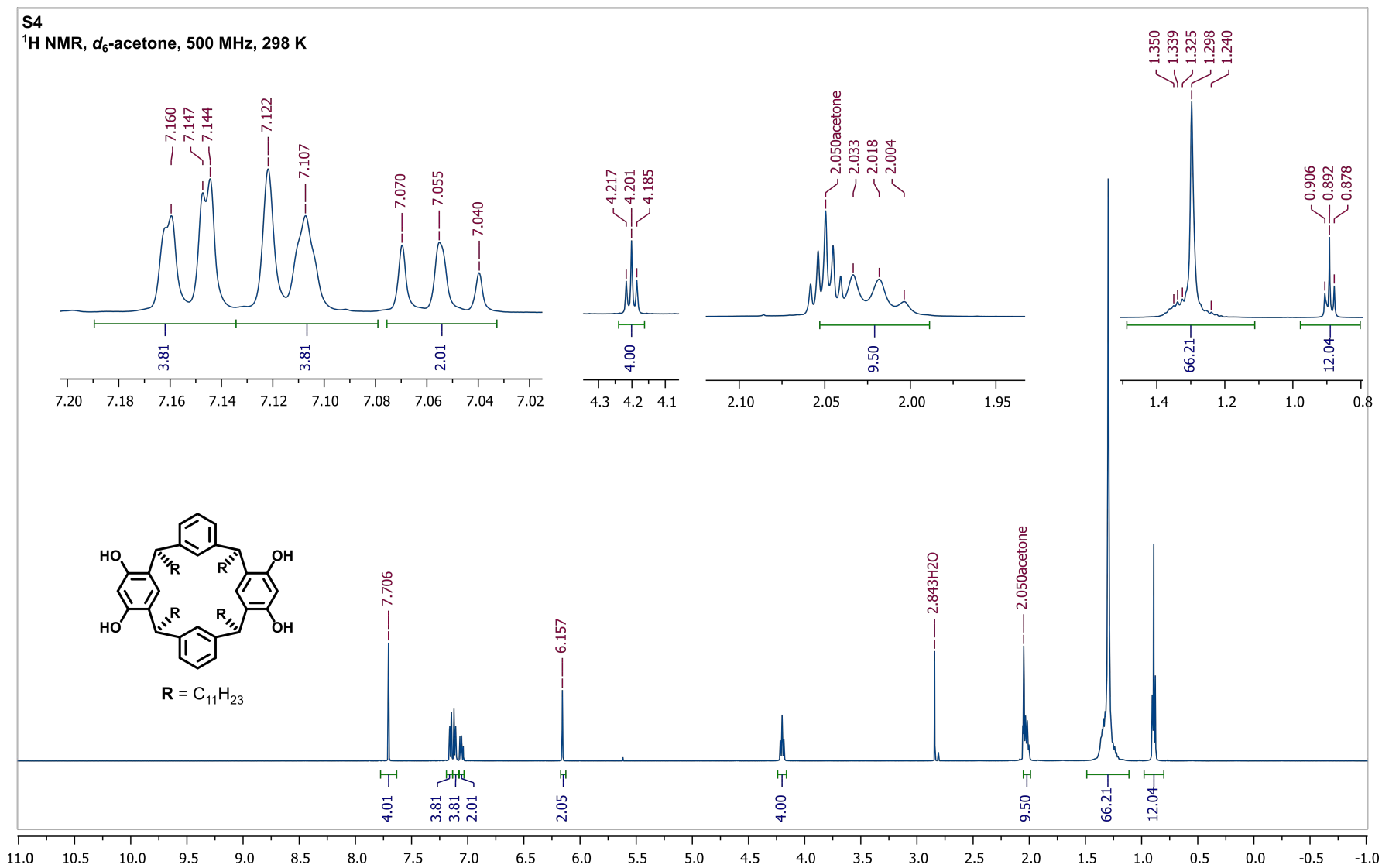


S3
¹³C NMR, CDCl₃, 126 MHz, 298 K



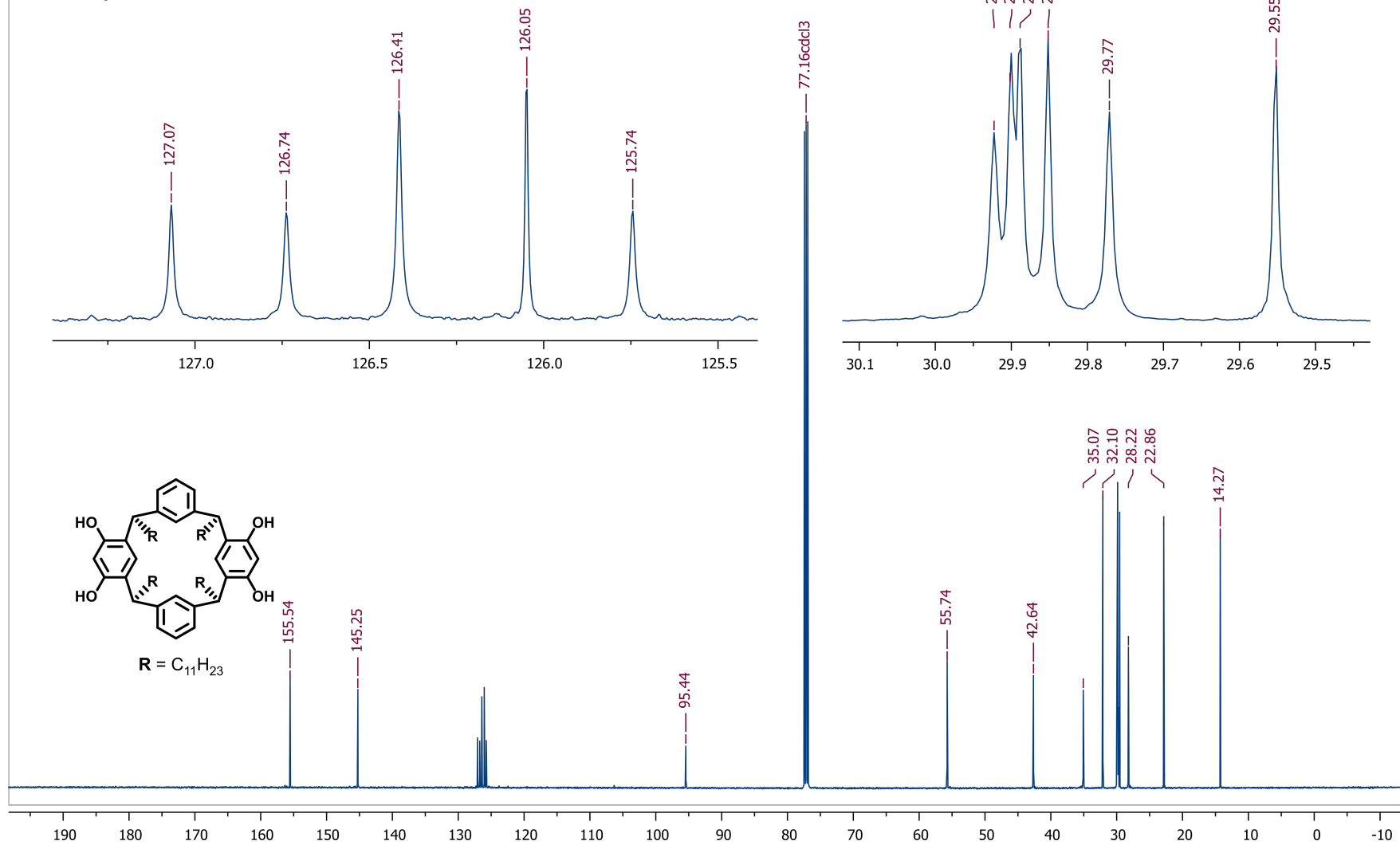
S4

^1H NMR, d_6 -acetone, 500 MHz, 298 K



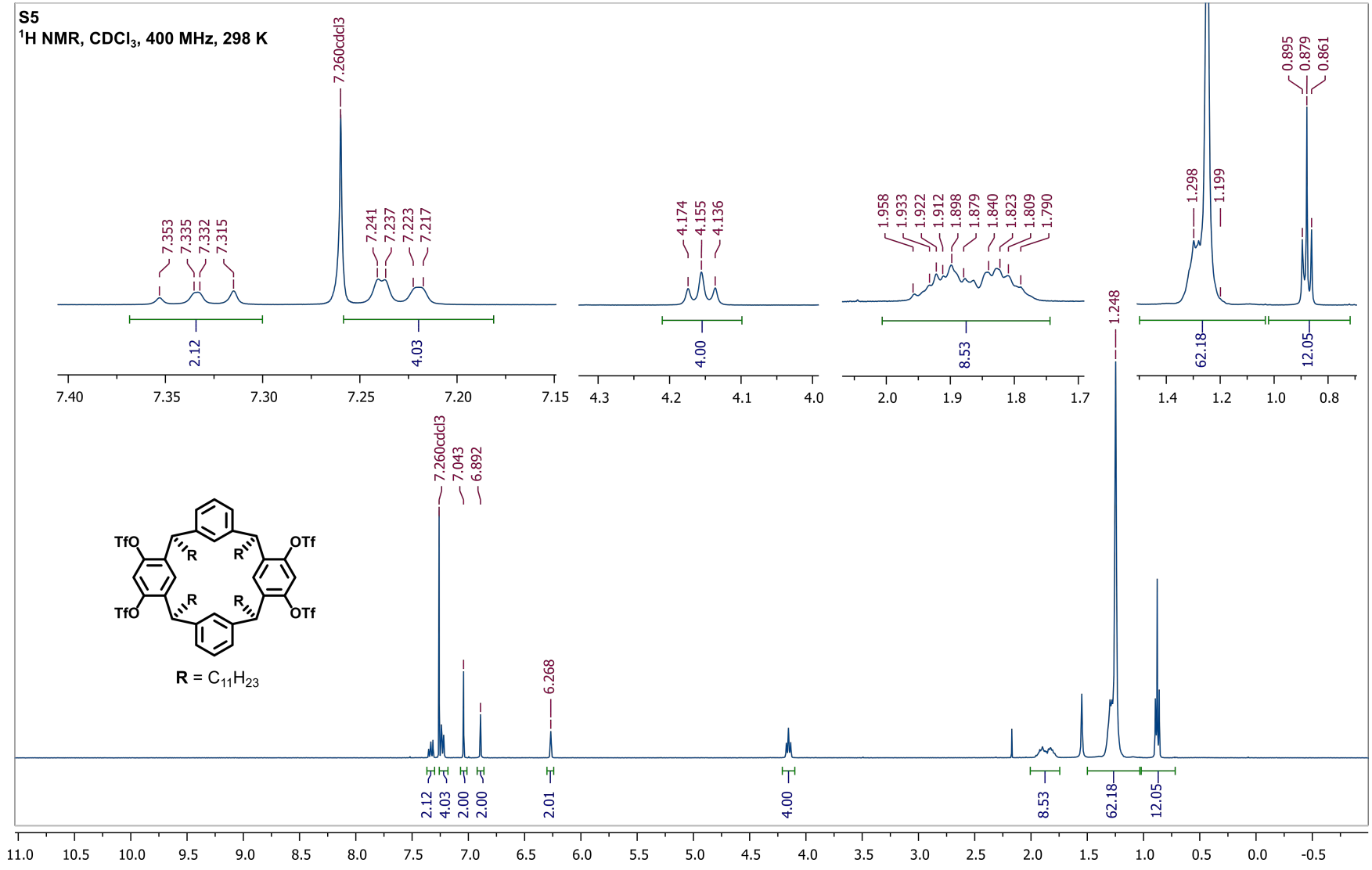
S4

^{13}C NMR, d_6 -acetone, 126 MHz, 298 K



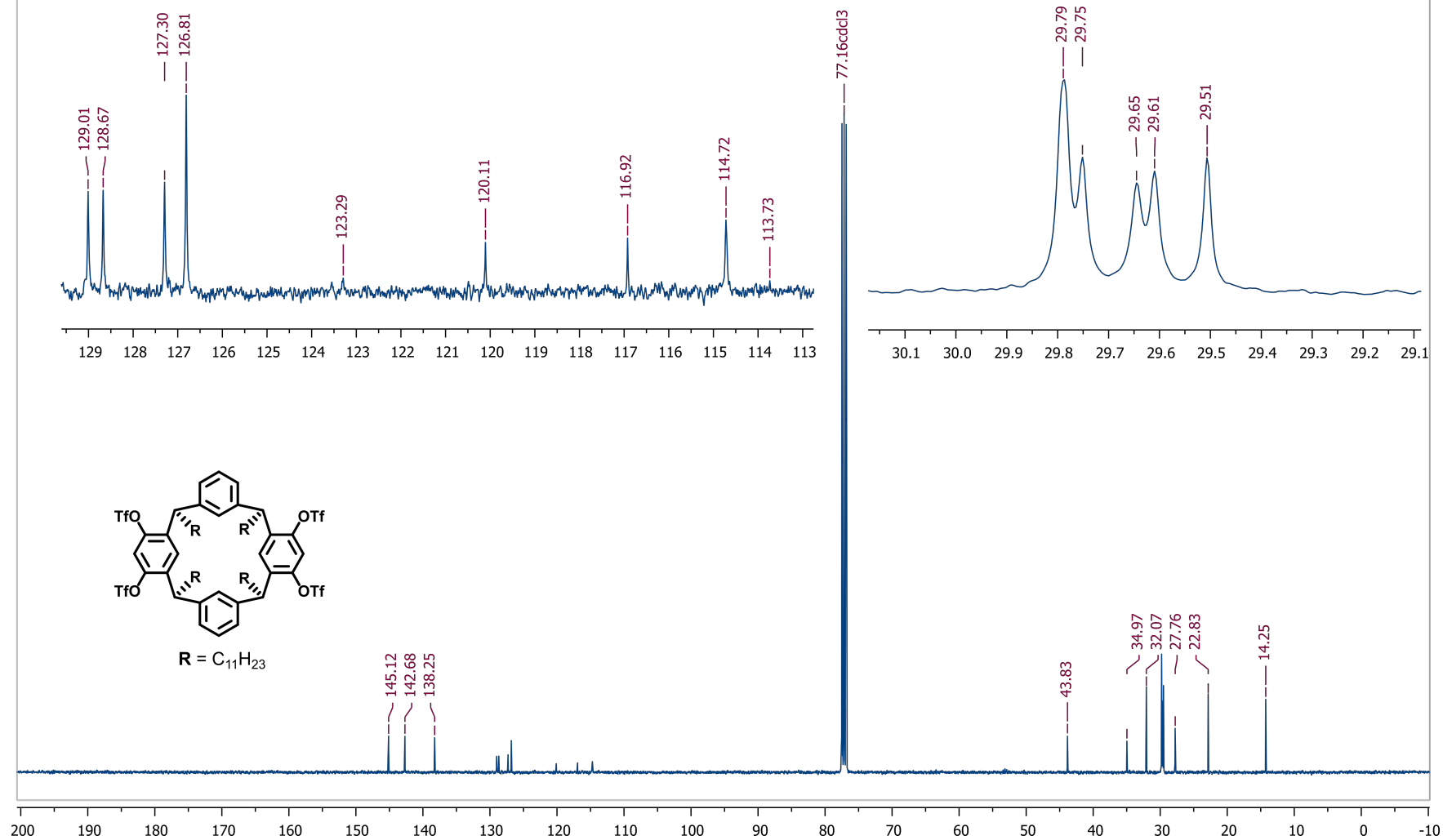
S5

¹H NMR, CDCl₃, 400 MHz, 298 K



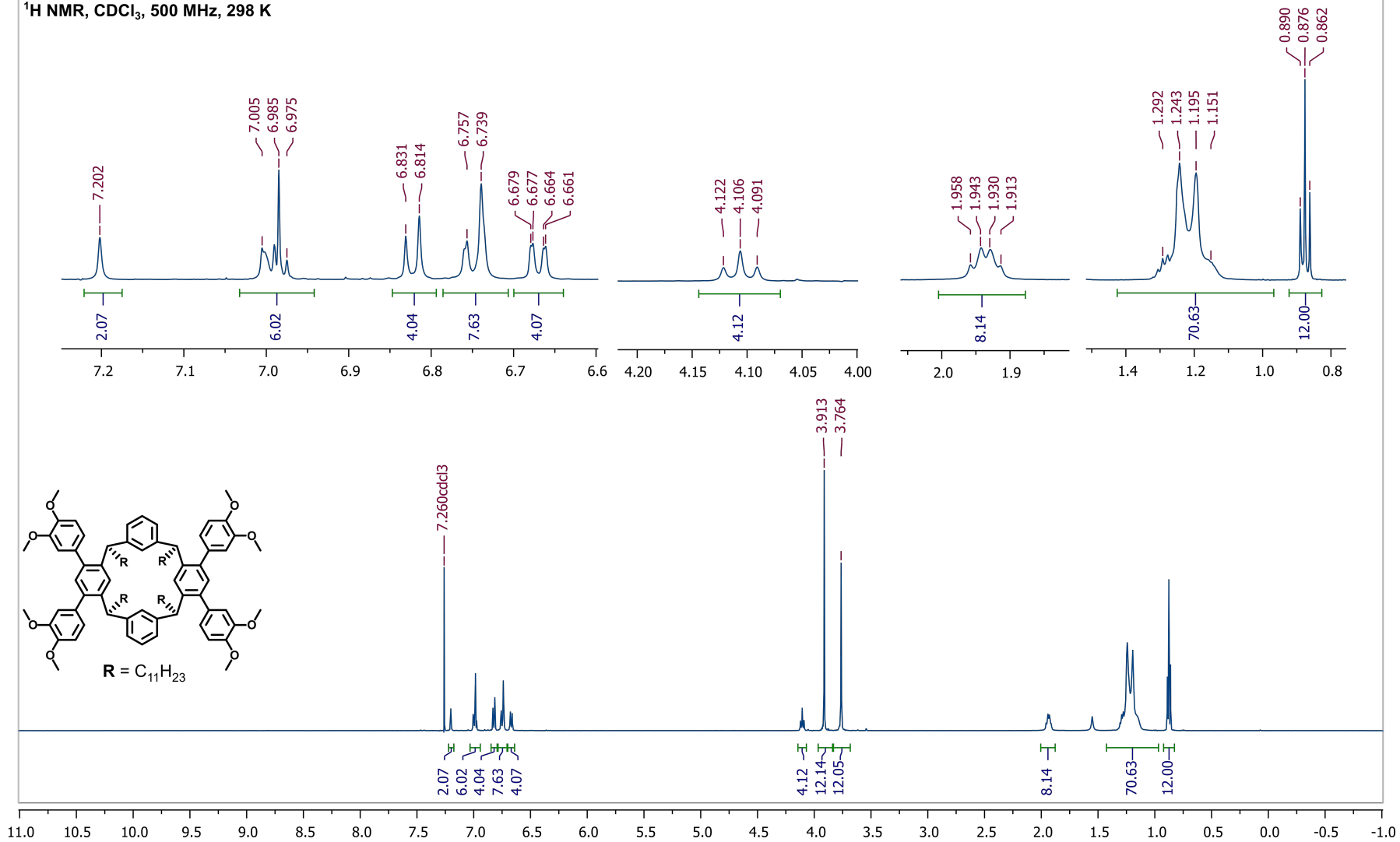
S5

^{13}C NMR, CDCl_3 , 101 MHz, 298 K



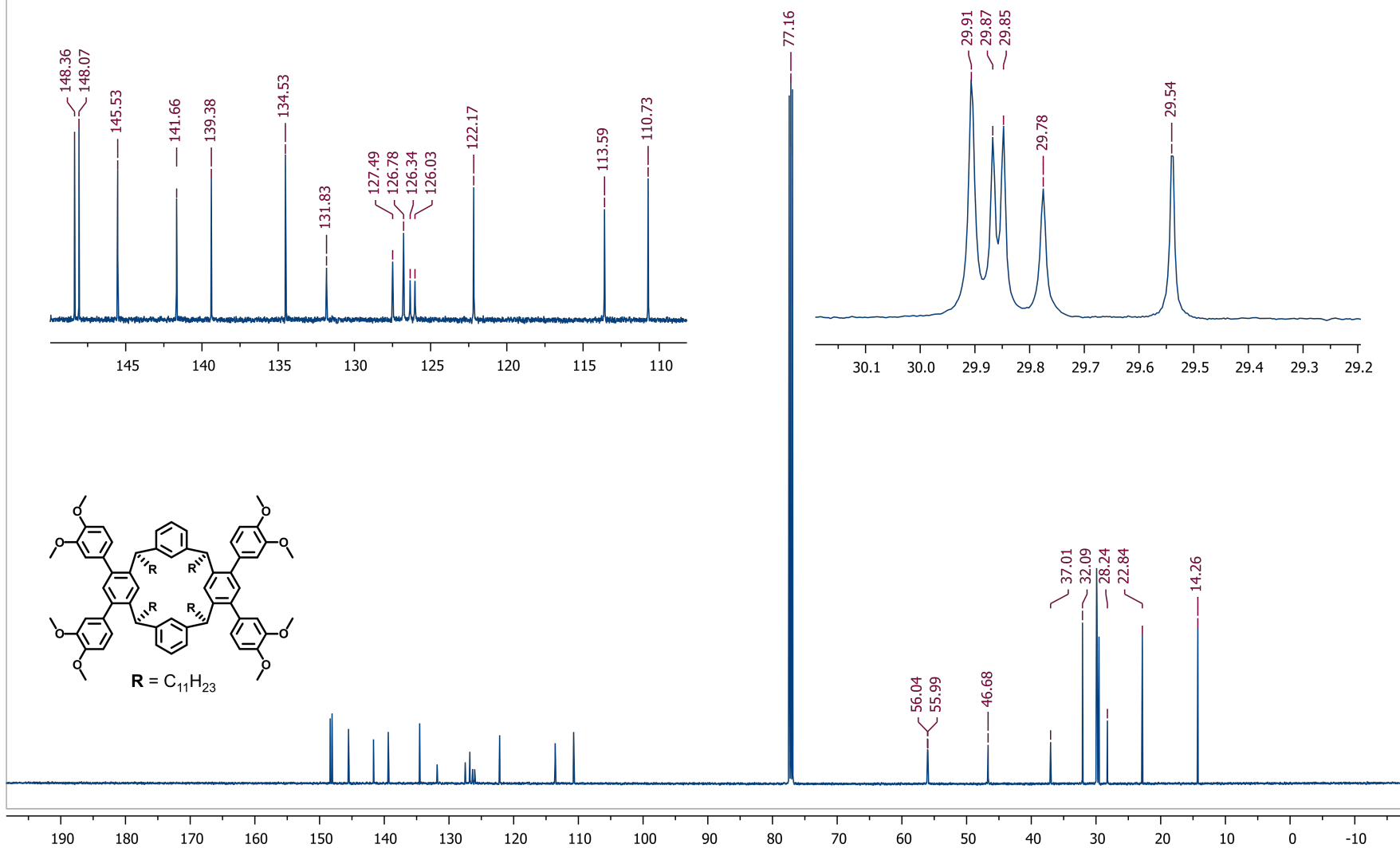
S6

$^1\text{H NMR}$, CDCl_3 , 500 MHz, 298 K



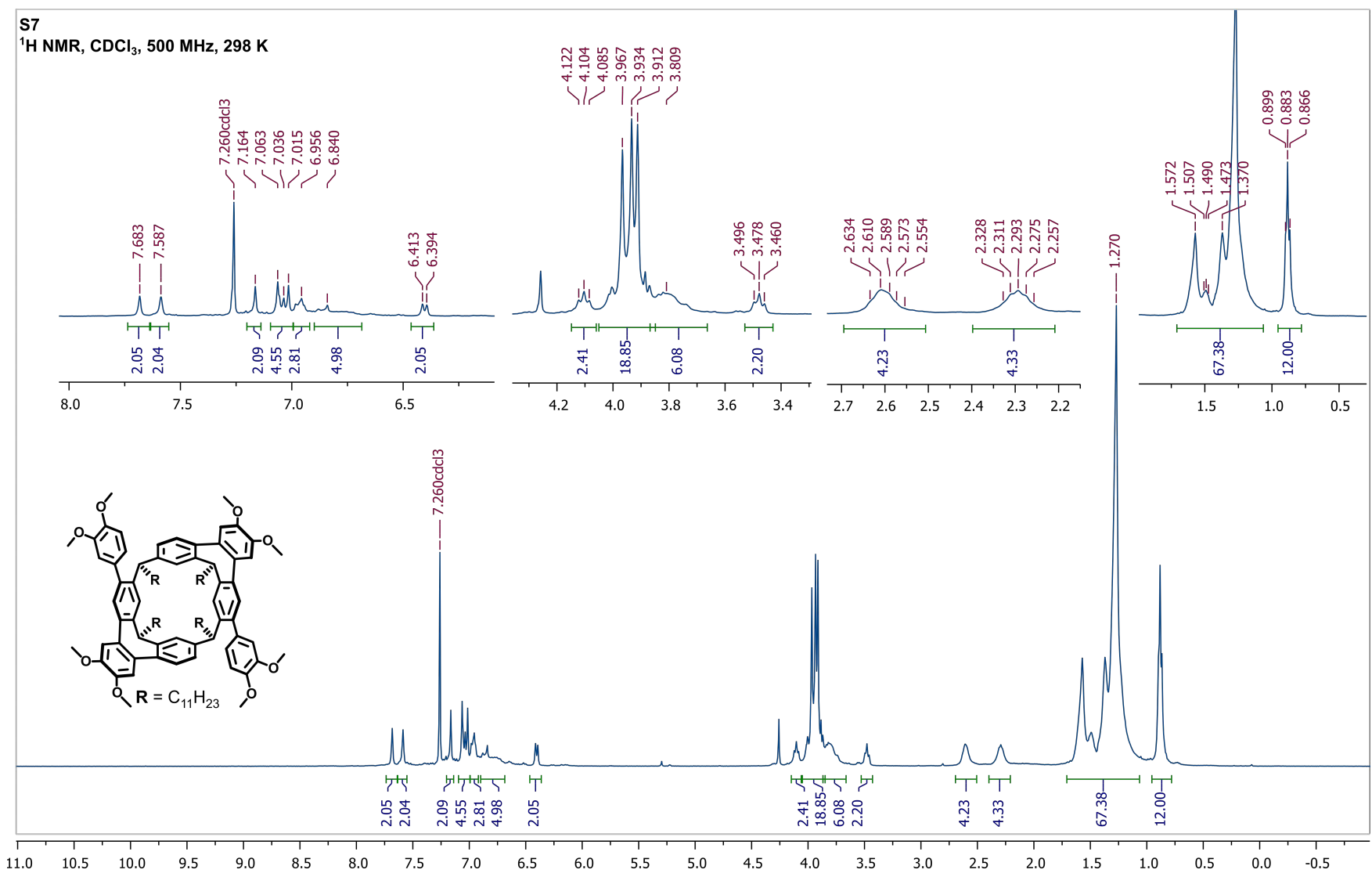
S6

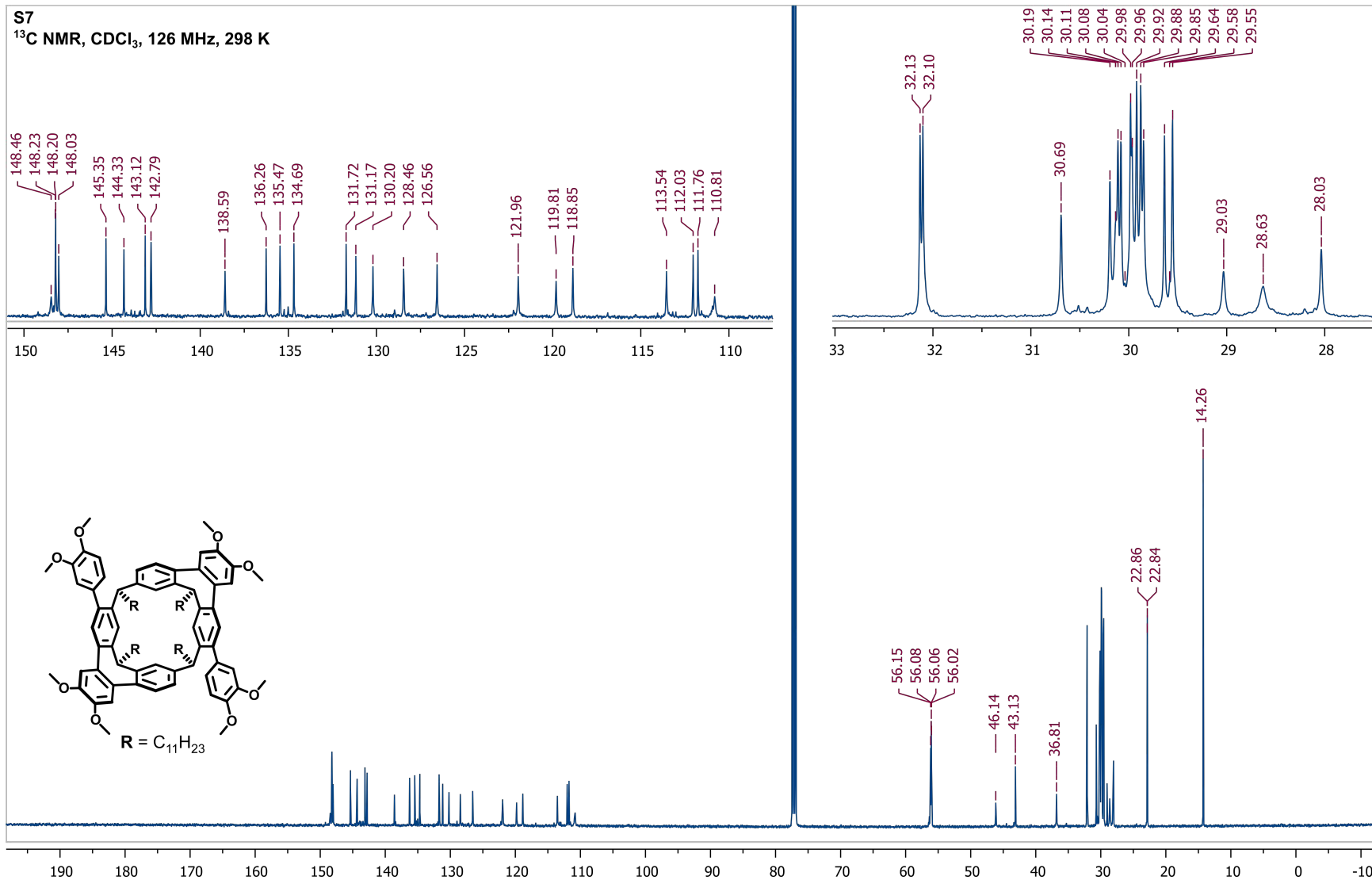
^{13}C NMR, CDCl_3 , 126 MHz, 298 K



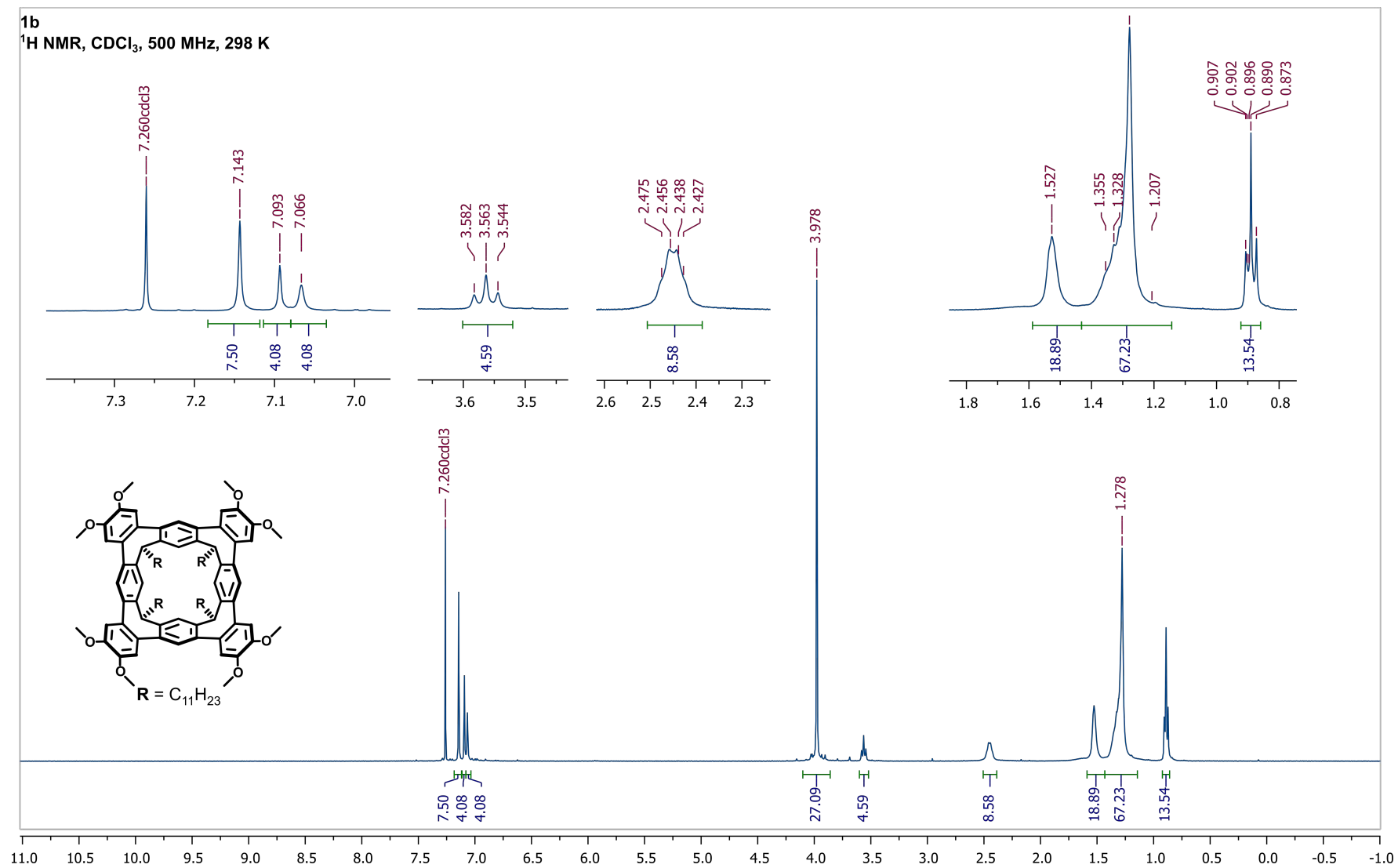
S7

¹H NMR, CDCl₃, 500 MHz, 298 K

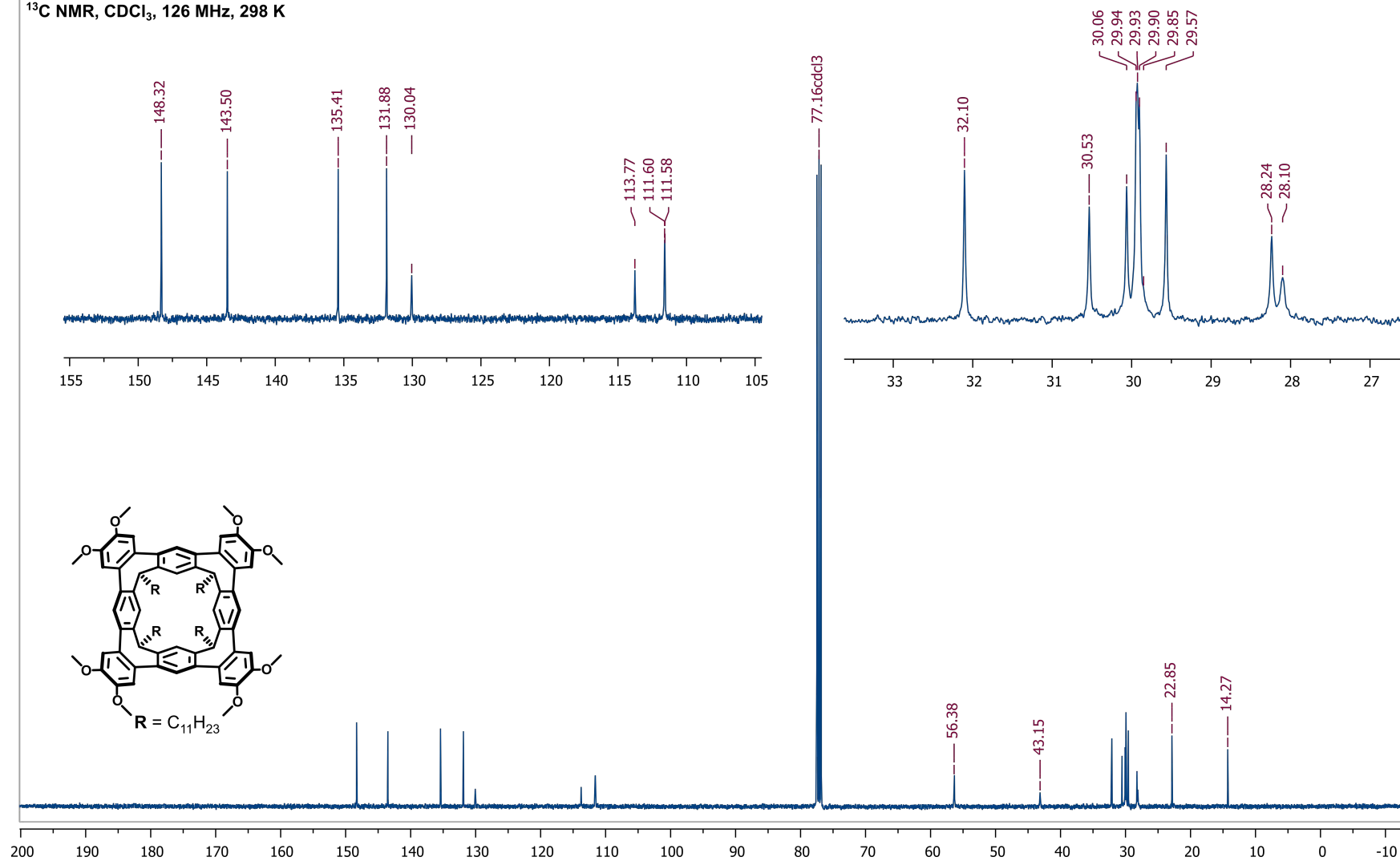




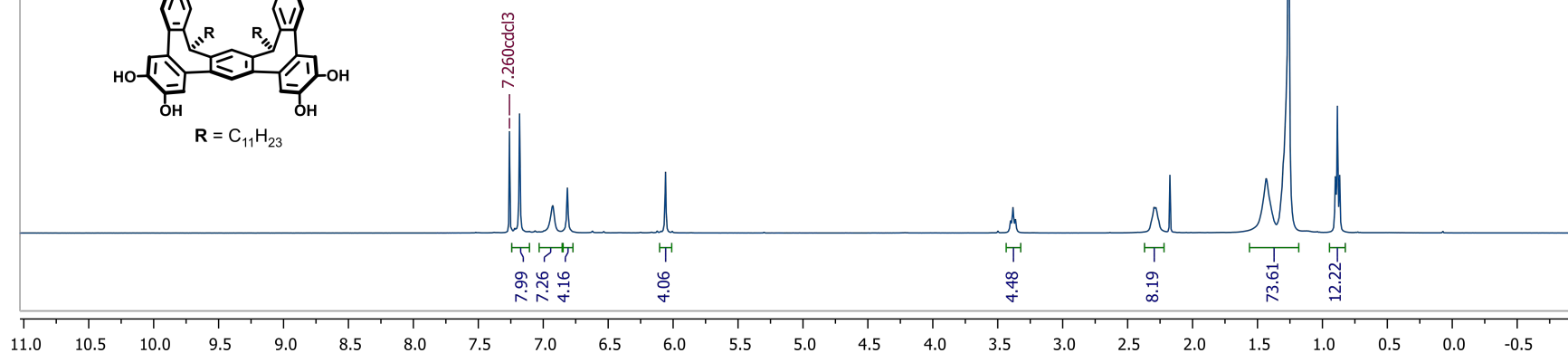
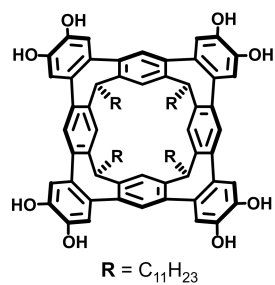
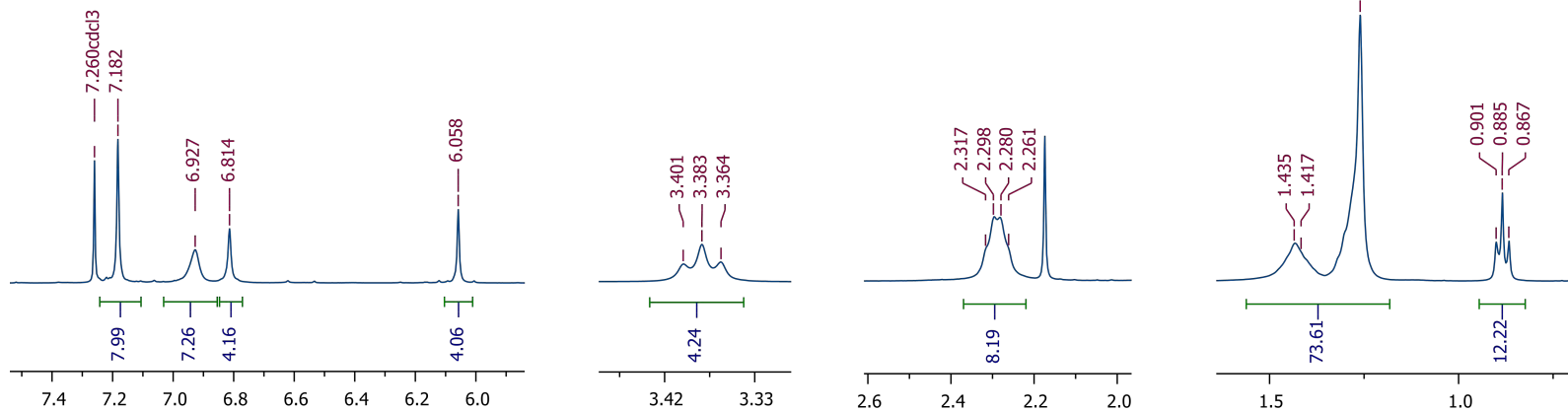
1b
¹H NMR, CDCl₃, 500 MHz, 298 K

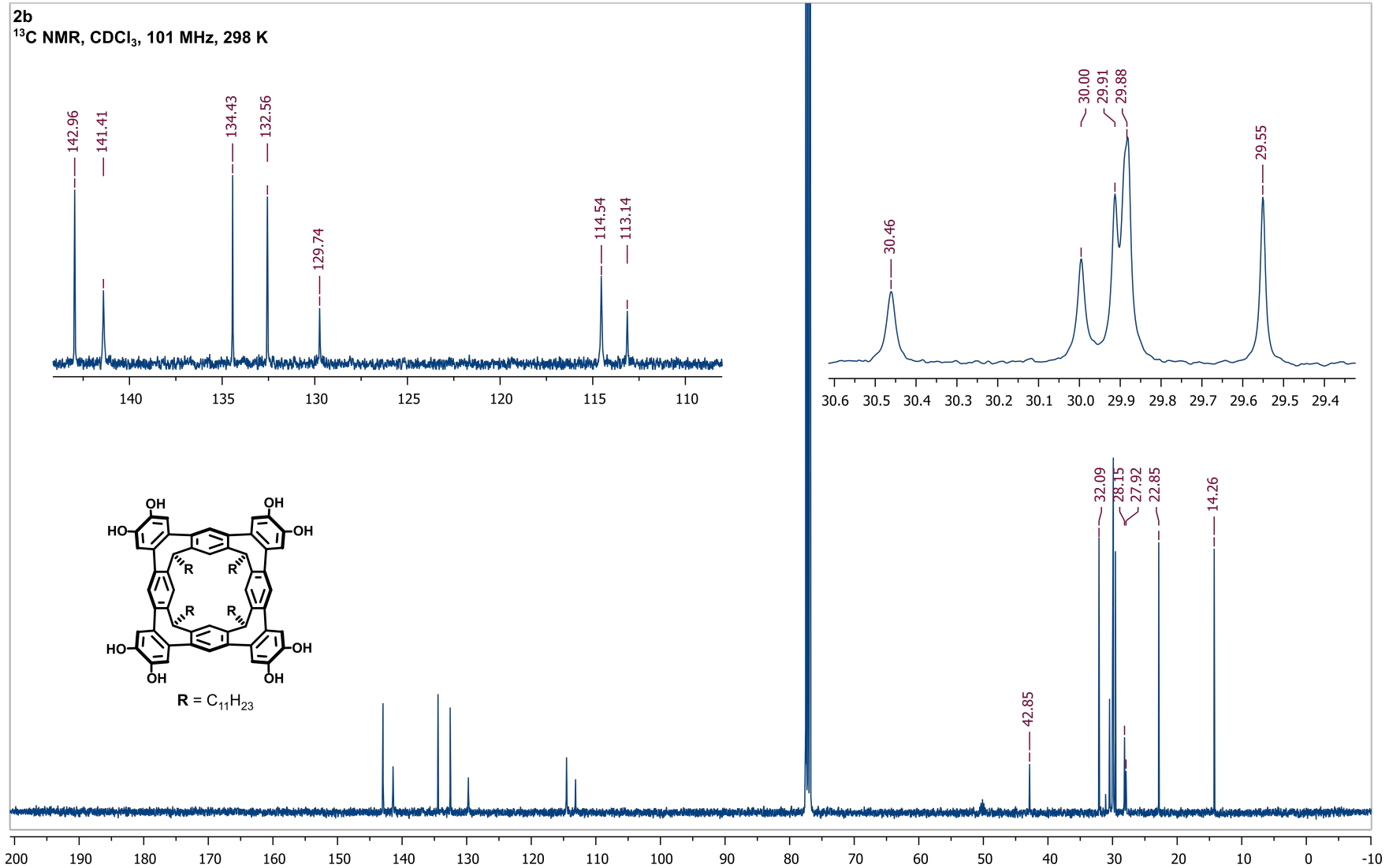


1b
¹³C NMR, CDCl₃, 126 MHz, 298 K



2b
¹H NMR, CDCl₃, 400 MHz, 298 K





4. Supramolecular Behaviour Including Guest Binding

General: Bulk samples of **2b** dried from acetone often contained solvent residues that could not be removed *in vacuo* with heating: when present, the acetone signal appears at 2.17 ppm in CDCl₃. Unless stated otherwise, samples for NMR spectroscopy experiments were allowed to equilibrate for at least 1 hour before analysis. Samples for UV-visible spectroscopy experiments were allowed to equilibrate for at least 15 hours before analysis. DOSY NMR spectra were recorded in 5 mm diameter tubes at 25 °C on a Varian 500 AR spectrometer (500 MHz) and processed using Varian VnmrJ or MestReNova software with corrections for non-uniform gradients. Reported diffusion coefficient values (*D*) are the average of all signals corresponding to each species of interest.

Dimerization of 2b: Upon dissolution in CDCl₃, **2b** initially shows three species of C_{4v}-symmetry in slow exchange (Figure S1). Equilibrium, in which only **2b·2b** is observed, is reached within 30 minutes.

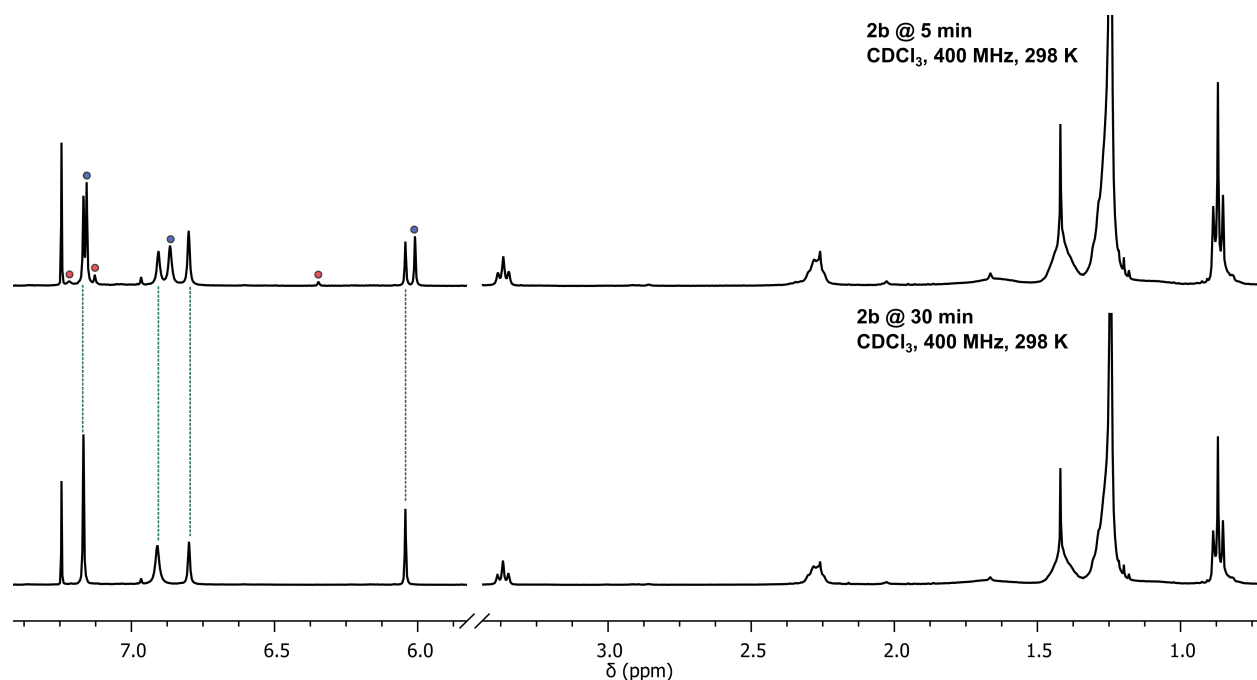


Figure S1. Truncated ¹H NMR spectra of **2b** recorded 5 and 30 minutes after preparation. The two species which are not observed at equilibrium are marked with red and blue circles.

The self-assembly of **2b** was investigated by DOSY NMR. Comparison of the diffusion coefficient, D , of **2b** with **1b**—which cannot form intermolecular hydrogen bonds and is a good surrogate for the monomer—shows **2b** diffuses more slowly consistent with a higher molecular weight (Figure S2). Approximation of the volume of the diffusing particles was calculated from the radius determined from the Stokes-Einstein equation (1; k_B = Boltzmann constant, T = temperature, η = solvent viscosity, r = radius) and the formula for the volume of a sphere (2). The volume of **2b** (6880 Å³) is ca 1.7 times that of **1b** (4060 Å³) consistent with dimerization (**2b**·**2b**). In the polar bulk solvent *d*₆-acetone, the similar diffusion coefficients of **1b** and **2b** evidence the monomer in each case (Figure S3).

$$D = \frac{k_B T}{6\pi\eta r} \quad (1)$$

$$V = \frac{4}{3}\pi r^3 \quad (2)$$

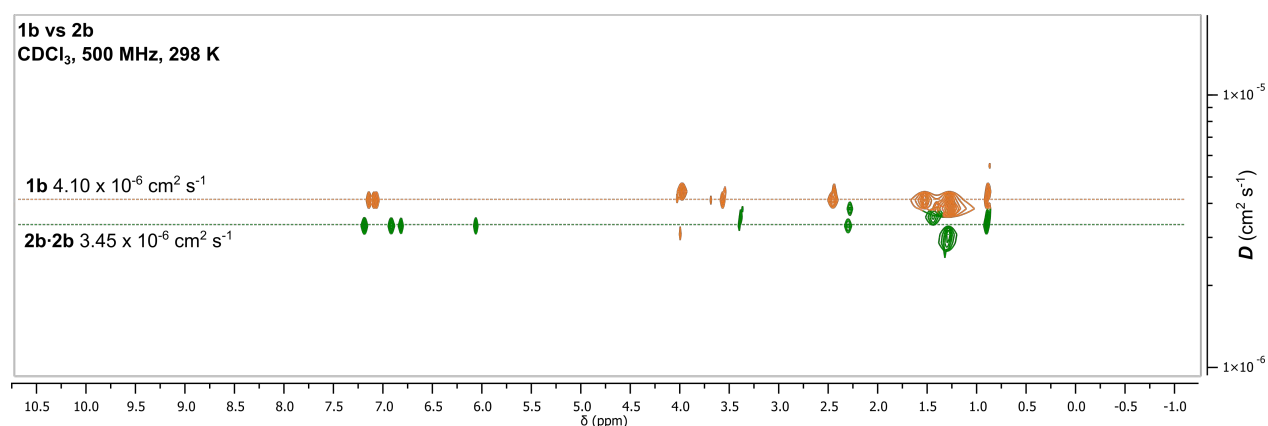


Figure S2. Overlaid DOSY NMR spectra (CDCl₃, 500 MHz, 298 K) showing the different diffusion rates of **1b** (orange trace) and **2b**·**2b** (green trace).

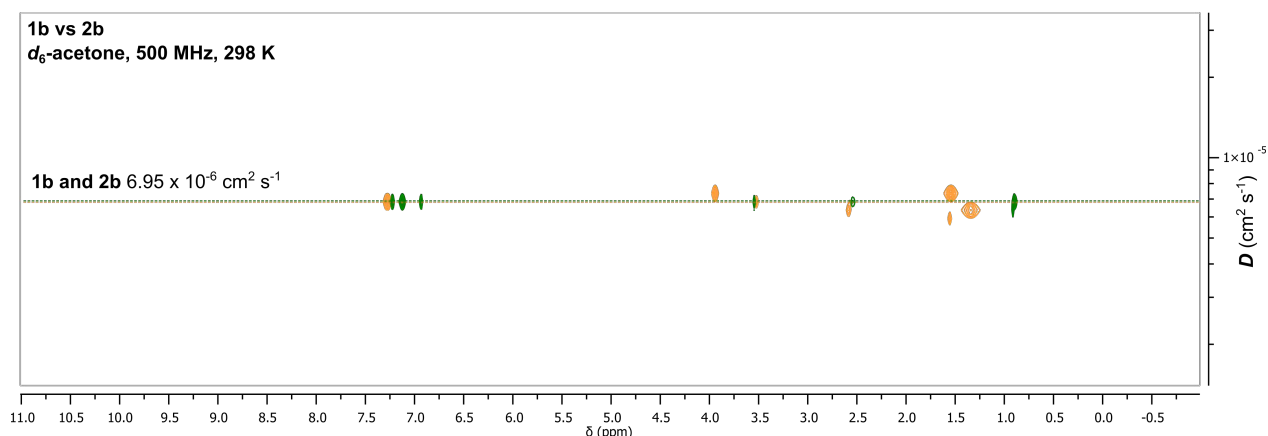


Figure S3. Overlaid DOSY NMR spectra (*d*₆-acetone, 500 MHz, 298 K) showing co-diffusion of **1b** (orange trace) vs **2b** (green trace).

Concentration dependence of OH resonance: Samples of **2b** were prepared across the range 1–14 mM and allowed to equilibrate for at least 1 hour. The spectra show the OH signal is largely independent of concentration, varying only 0.05 ppm (Figure S4).

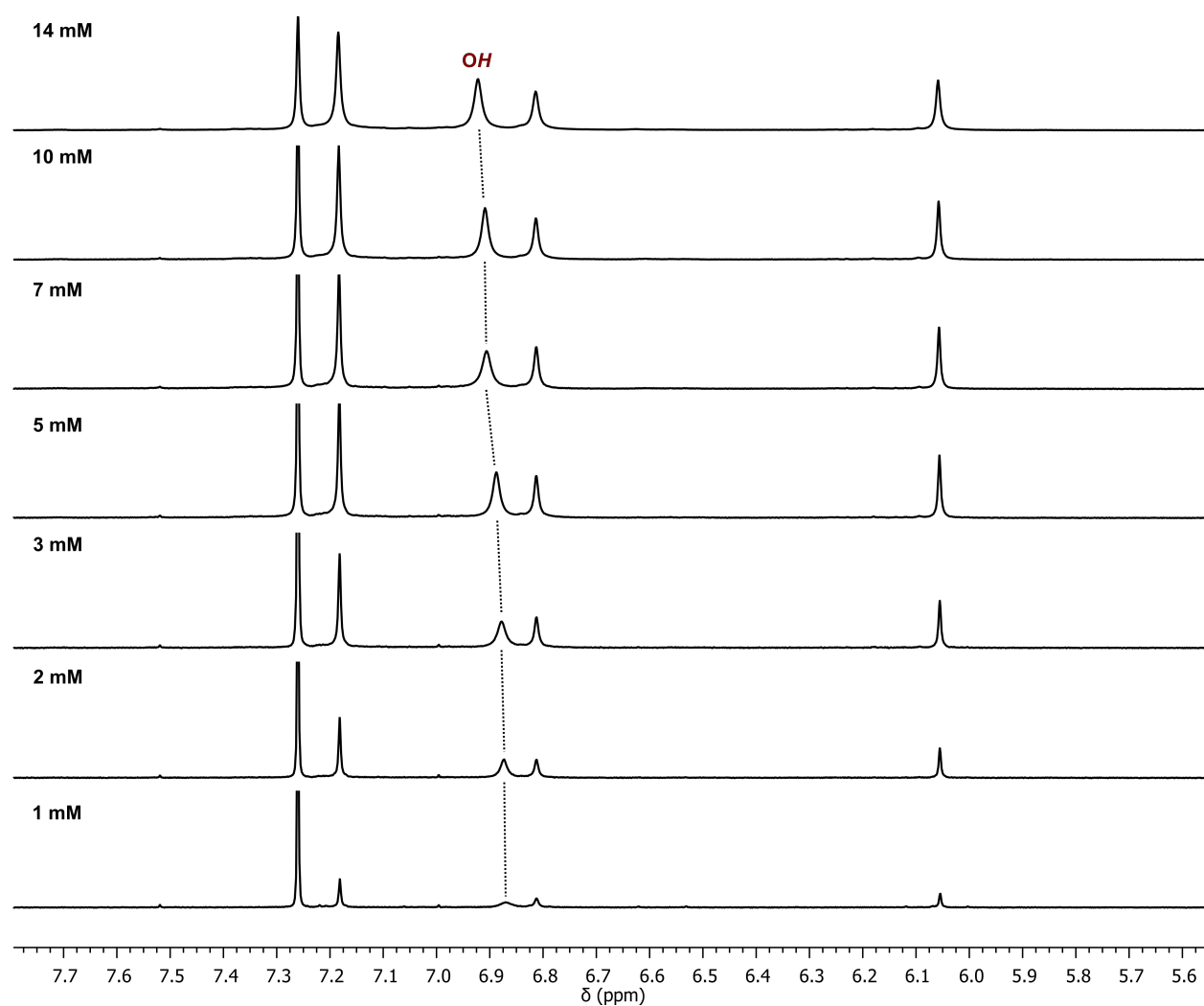


Figure S4. Truncated ¹H NMR spectra (400 MHz, CDCl₃, 298 K) of **2b** across the concentration range 1-14 mM.

Solvent encapsulation ($\text{CHCl}_3/\text{CDCl}_3$): compound **2b** in 20% v/v $\text{CHCl}_3/\text{CDCl}_3$ shows a new resonance at 3.02 ppm that increases in relative intensity in 50% v/v $\text{CHCl}_3/\text{CDCl}_3$ (Figure S5). The spectrum of solvent only shows this is not an impurity. Due to the low intensity of these signals the binding stoichiometry was not interpreted.

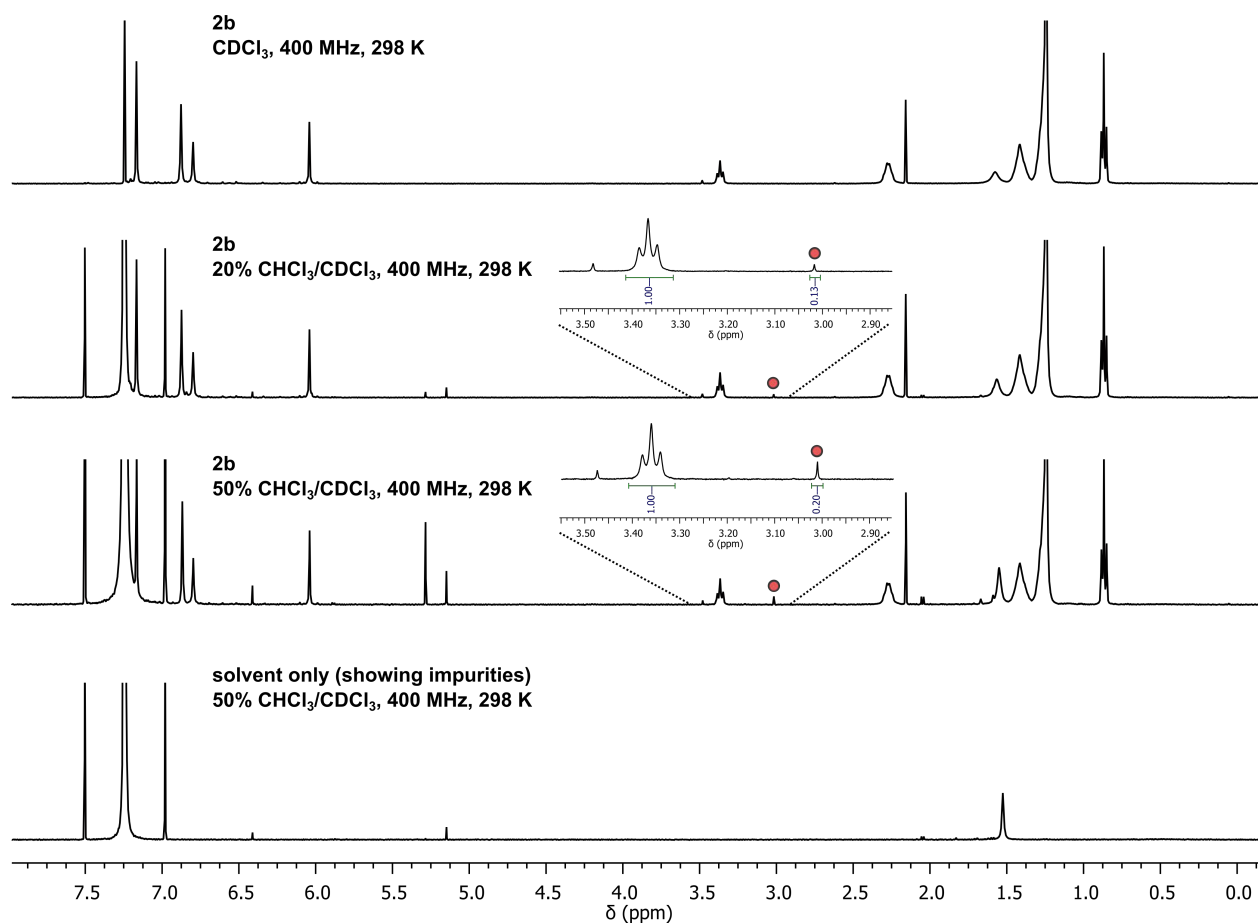


Figure S5. ^1H NMR spectra of **2b** in $\text{CHCl}_3/\text{CDCl}_3$ mixtures, with expansions showing the relative intensity of the host methine proton and encapsulated CHCl_3 . The blank solvent is shown to account for solvent impurities.

Solvent encapsulation (CDCl₃/C₆D₆): **2b** in C₆D₆ shows a single species (Figure S6). Upon addition of CDCl₃ to the sample (1:1 v/v) a second species appears in slow exchange, indicative of the individual encapsulation of C₆D₆ or CDCl₃. Equilibrium is reached within 60 minutes, showing the two species in a 5:1 ratio. The rapid loss of the minor species is consistent with the process $2b \cdot 2b \subset C_6D_6 \rightarrow 2b \cdot 2b \subset CDCl_3$.

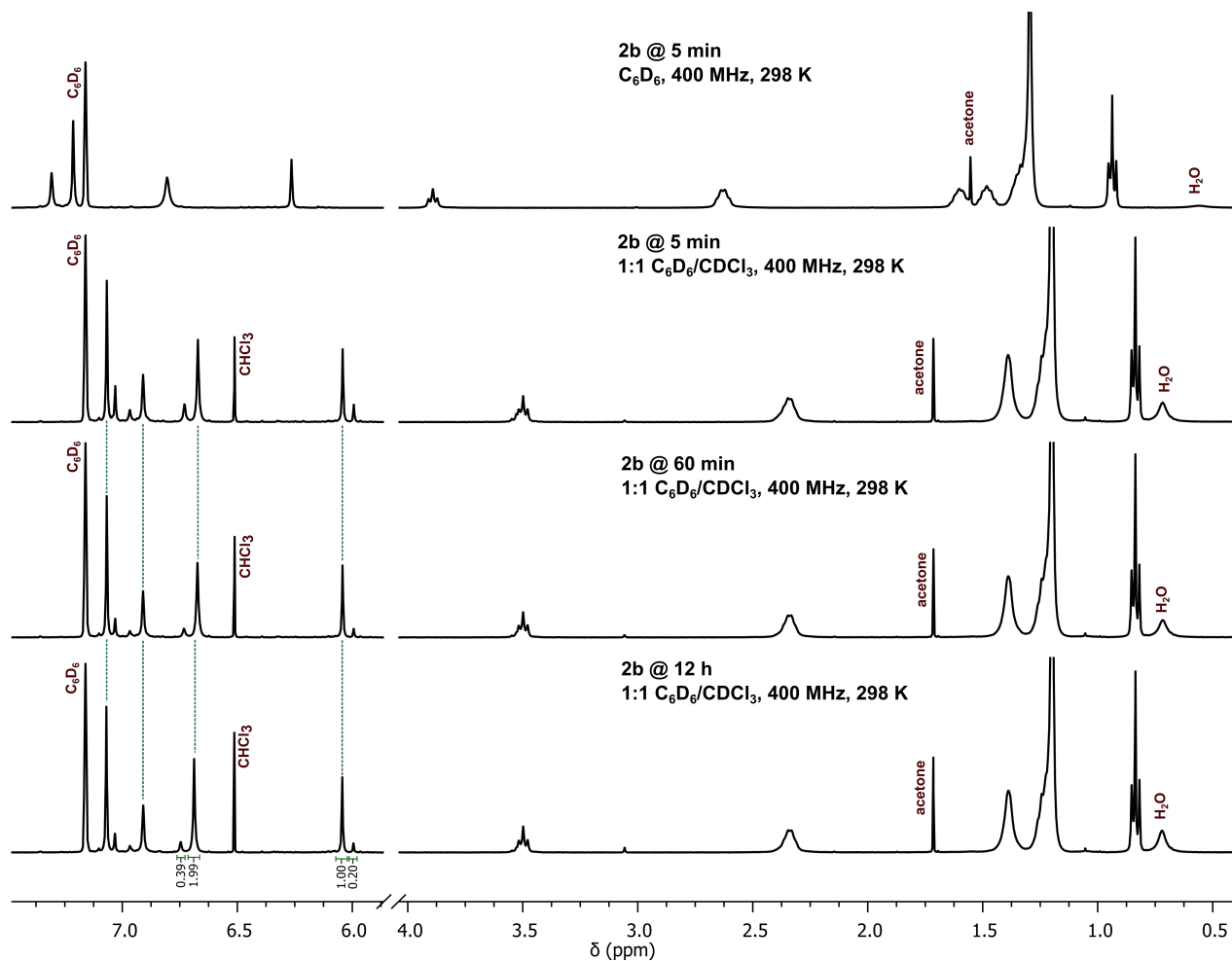


Figure S6. Truncated ¹H NMR spectra of **2b** in C₆D₆, and following the addition of CDCl₃ to 1:1 v/v measured at 5 minutes, 60 minutes and 12 hours. All spectra referenced to the C₆D₆ residual signal at 7.16 ppm. Integrations of the two species are shown for the equilibrium mixture.

In an attempt to measure the dimerization constant K_{dimer} , of **2b**, UV-visible spectra at various concentrations were recorded on an Edinburgh Instruments FS5 Fluorimeter in 1 cm quartz cells at room temperature (20–21 °C). In both CHCl_3 (Figure S7) and 5% v/v MeOH/ CHCl_3 (Figure S8) the isotherm (absorbance vs concentration) was linear in the Beer-Lambert region.

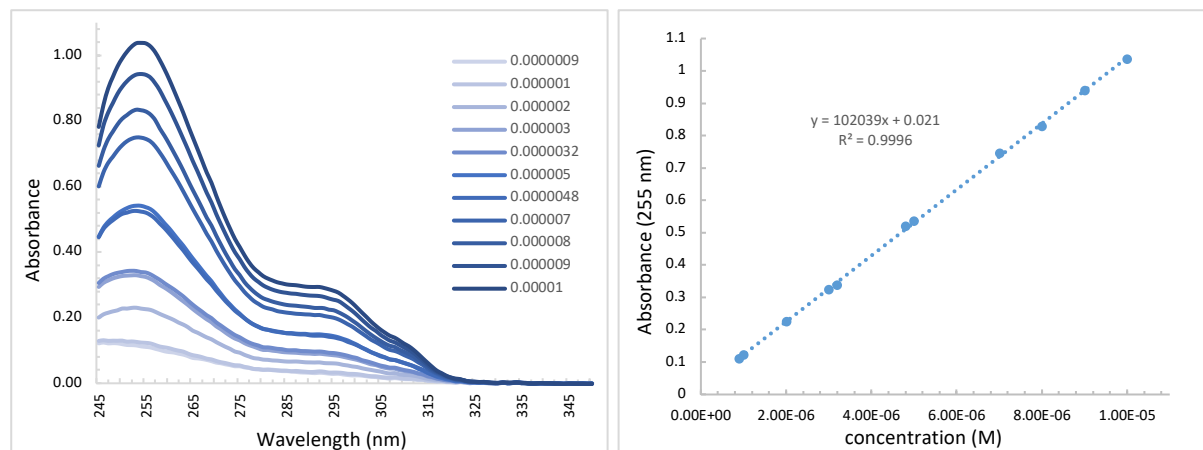


Figure S7. UV-visible spectra of **2b** in CHCl_3 at concentrations 0.90×10^{-6} to 11.0×10^{-6} M, and plot of absorbance at 255 nm vs concentration (M).

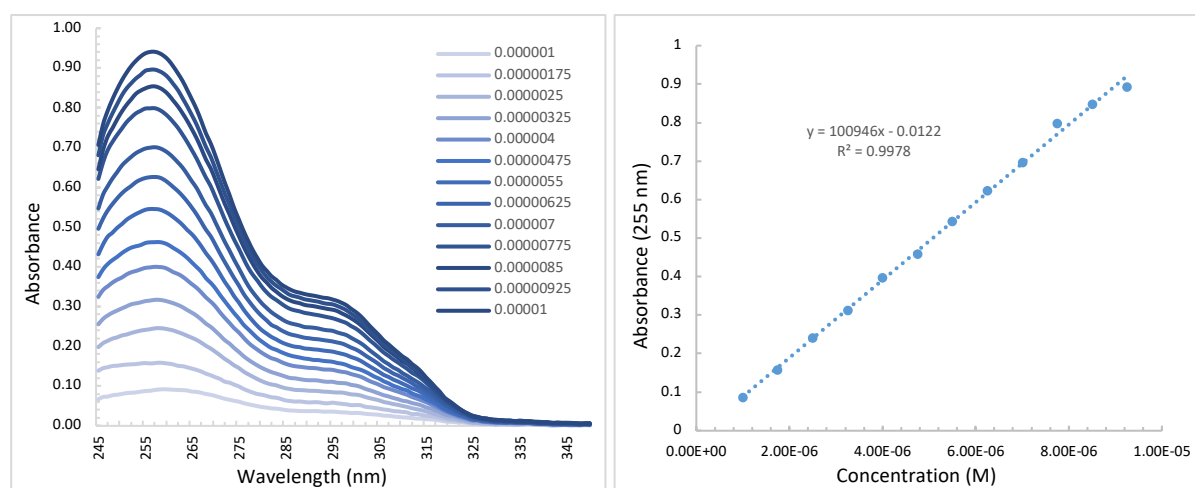


Figure S8. UV-visible spectra of **2b** in 5% MeOH/ CHCl_3 at concentrations 0.10×10^{-5} to 1.10×10^{-5} M, and plot of absorbance at 255 nm vs concentration (M).

Stability in polar solvent mixtures: a stock solution of **2b** (0.0166 mmol/mL) in CDCl₃ was prepared and allowed to equilibrate for 1 h. CD₃OD (130, 200, 400, 600, 800 or 1600 equiv.) and CDCl₃ were added to a total volume of 700 μL, and the solutions allowed to equilibrate for at least 1 hour before the DOSY spectra were measured. The diffusion coefficient, *D*, vs equivalents CD₃OD is shown in Figure S9; *D* did not change significantly ($3.4\text{--}3.5 \times 10^{-6} \text{ cm}^2 \text{ s}^{-1}$) across the experimental range (ca 0–35% CD₃OD in CDCl₃).

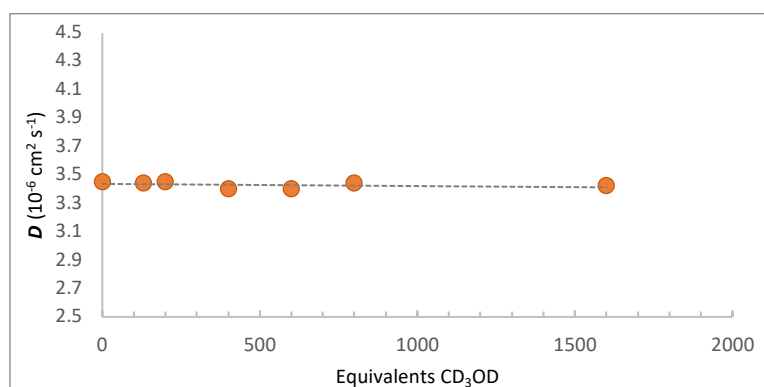


Figure S9. Diffusion coefficient of **2b·2b** measured by DOSY NMR spectroscopy in CDCl₃ solutions containing increasing amounts of CD₃OD.

Guest binding: All ammonium salts were dried under vacuum at 100 °C for at least 2 h before use. Neutral guests were used as supplied. Stock solutions of host (0.0166 mmol/mL) and guest (0.0125 mmol/mL) in the required solvent mixture were combined in the appropriate ratios to a total volume of 700 μ L. The solutions were allowed to equilibrate for at least 1 h before the spectra were measured. As NMe₄Cl and choline chloride are only sparingly soluble in CDCl₃, a 5% CD₃OD/CDCl₃ mixture was used.

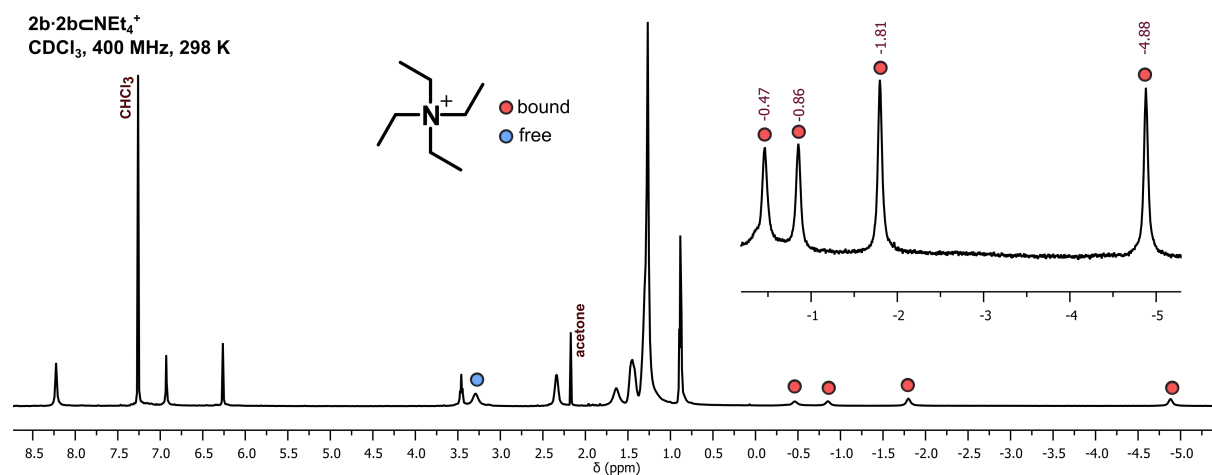


Figure S10. ¹H NMR spectrum (CDCl₃, 400 MHz, 298 K) of **2b** and NEt₄Br (1:1). Signals corresponding to the encapsulated and free guest are marked with red and blue circles, respectively. An aromatic signal of the host and the methyl signal of the free guest are obscured by the solvent residual signal and the alkyl signals of the host, respectively.

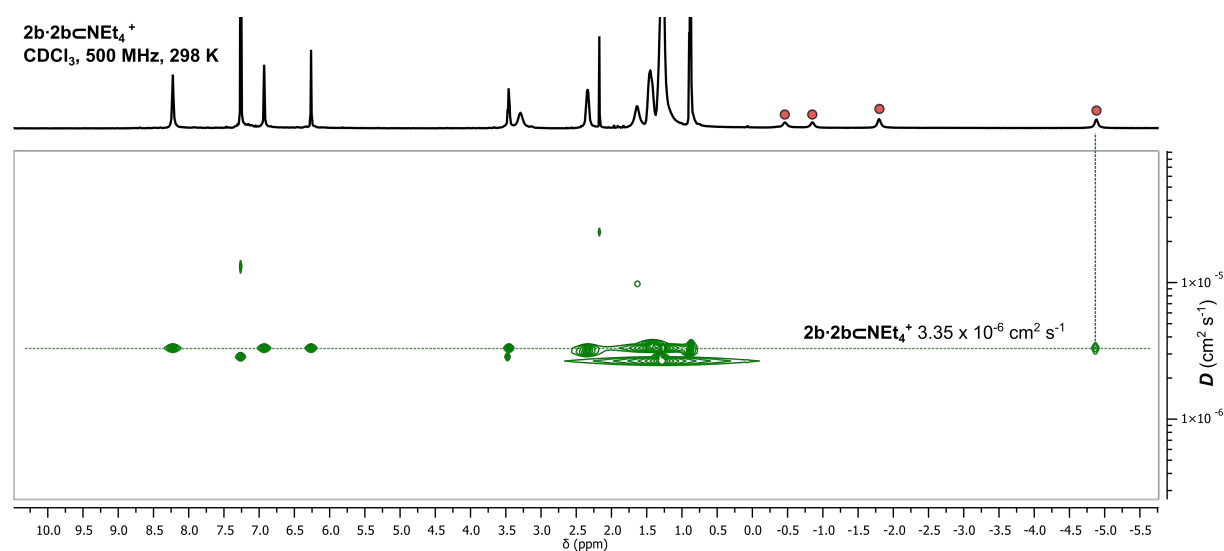


Figure S11. DOSY NMR spectrum (CDCl₃, 500 MHz, 298 K) of **2b** and NEt₄Br (1:1). Signals corresponding to the encapsulated guest are marked with red circles.

Cavitand **2b** failed to dimerize in neat d_6 -acetone based on DOSY NMR; however, upon the addition of excess NEt_4Br (ca 4 equivalents; NEt_4Br is only sparingly soluble in d_6 -acetone) the complex $\mathbf{2b}\cdot\mathbf{2b}\subset\text{NEt}_4^+$ formed quantitatively (Figure S12). The diffusion coefficient (D) of the complex $\mathbf{2b}\cdot\mathbf{2b}\subset\text{NEt}_4^+$ in d_6 -acetone ($5.50 \times 10^{-6} \text{ cm}^2 \text{ s}^{-1}$) is less than that of the monomer **2b** ($6.95 \times 10^{-6} \text{ cm}^2 \text{ s}^{-1}$) consistent with a larger diffusion radius (Figure S12).

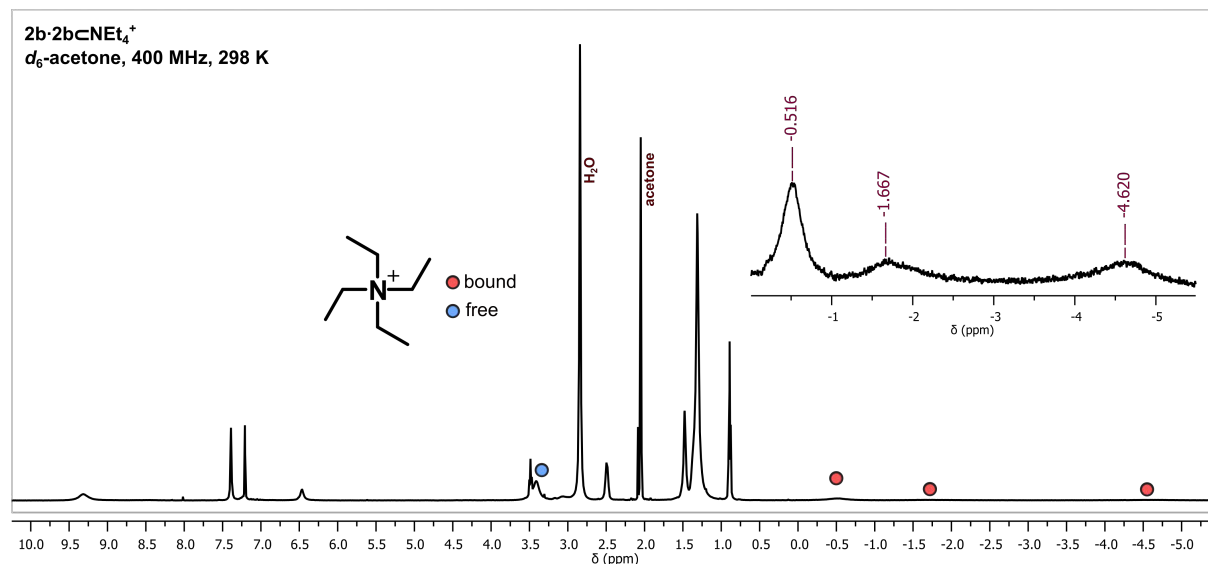


Figure S12. ^1H NMR spectrum (d_6 -acetone, 400 MHz, 298 K) of **2b** and excess NEt_4Br . Signals corresponding to the encapsulated and free guest are marked with red and blue circles, respectively. The methyl signal of the free guest is obscured by the alkyl signals of the host.

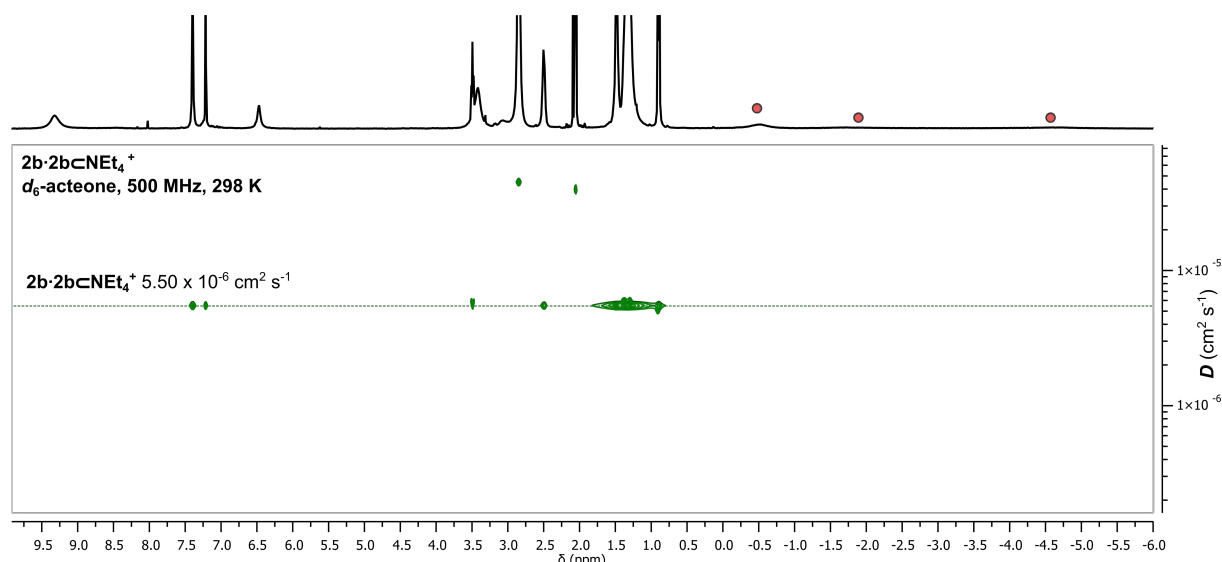


Figure S13. DOSY NMR spectrum (d_6 -acetone, 500 MHz, 298 K) of **2b** and excess NEt_4Br . Signals corresponding to the encapsulated guest are marked with red circles.

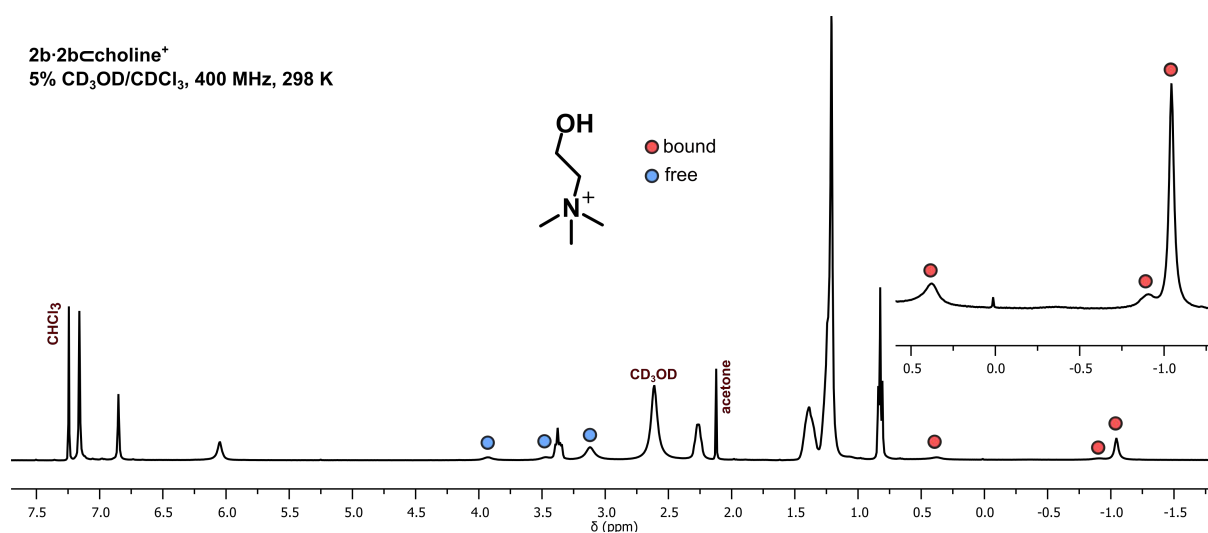


Figure S14. ¹H NMR spectrum (5% v/v CD₃OD/CDCl₃, 400 MHz, 298 K) of **2b** and choline chloride (1:1). Signals corresponding to the encapsulated and free guest are marked with red and blue circles, respectively.

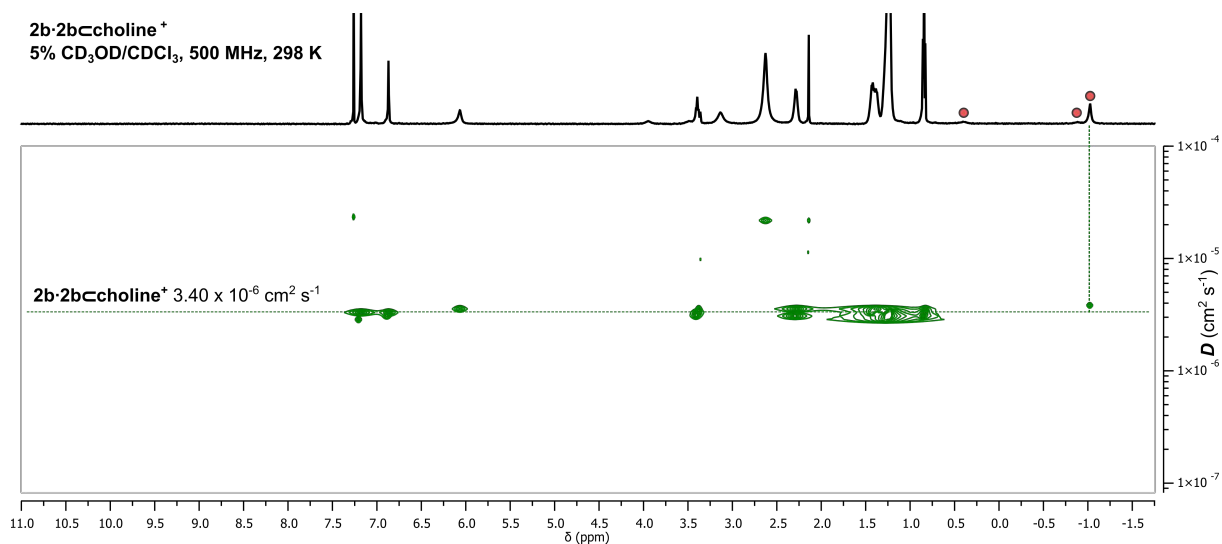


Figure S15. DOSY NMR spectrum (5% v/v CD₃OD/CDCl₃, 500 MHz, 298 K) of **2b** and choline chloride (1:1). Signals corresponding to the encapsulated guest are marked with red circles. The OH protons of the host are not observed due to exchange with CD₃OD.

2b·2b⁺cNMe₄⁺
5% CD₃OD/CDCl₃, 400 MHz, 298 K

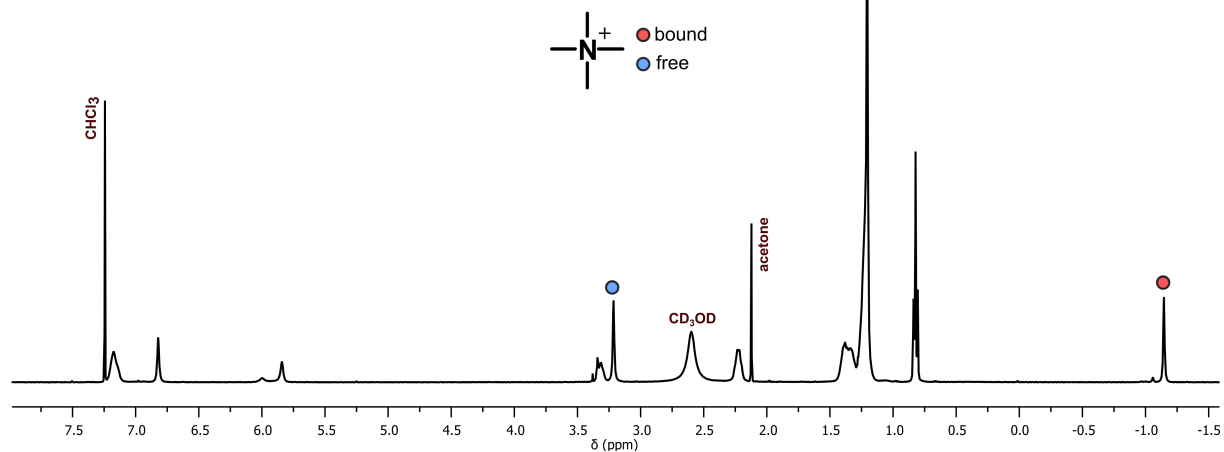


Figure S16. ¹H NMR spectrum (5% v/v CD₃OD/CDCl₃, 500 MHz, 298 K) of **2b** and NMe₄Cl (1:1). Signals corresponding to the encapsulated and free guest are marked with red and blue circles, respectively. The OH protons of the host are not observed due to exchange with CD₃OD.

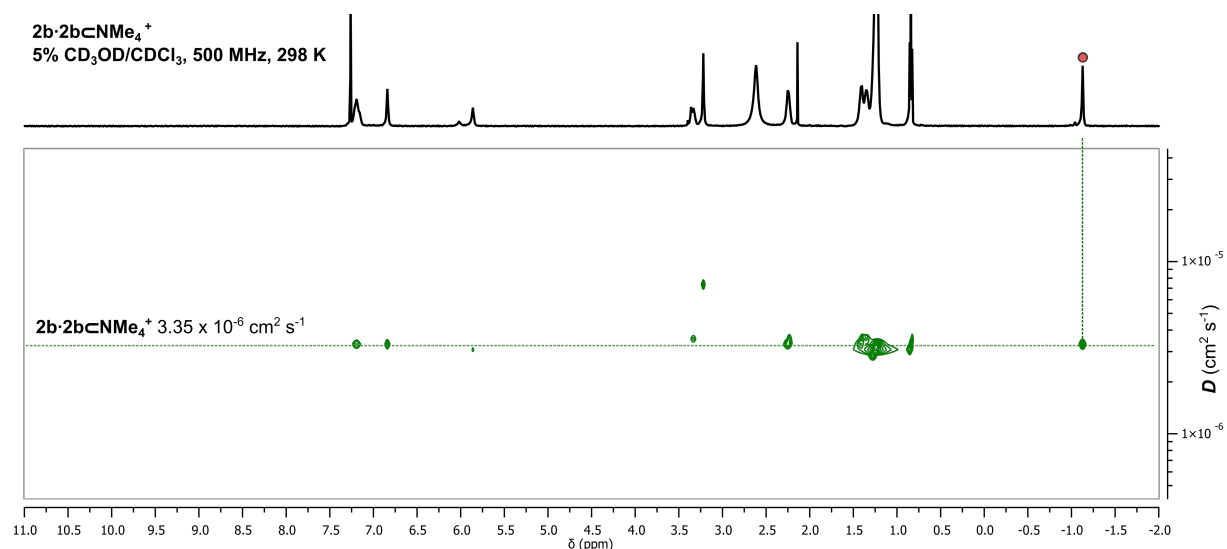


Figure S17. DOSY NMR spectrum (5% v/v CD₃OD/CDCl₃, 500 MHz, 298 K) of **2b** and NMe₄Cl (1:1). Signals corresponding to the encapsulated guest are marked with red circles.

Compound **2a** (R = Et) was combined with 1 equivalent of NEt_4Br in 20% v/v $\text{CD}_3\text{OD}/\text{CDCl}_3$ and the suspension allowed to stir at rt until dissolved (ca 12 hours; Figure S18). Crystals suitable for X-ray diffraction were grown by the layered diffusion of toluene into the $\text{CD}_3\text{OD}/\text{CDCl}_3$ solution at room temperature.

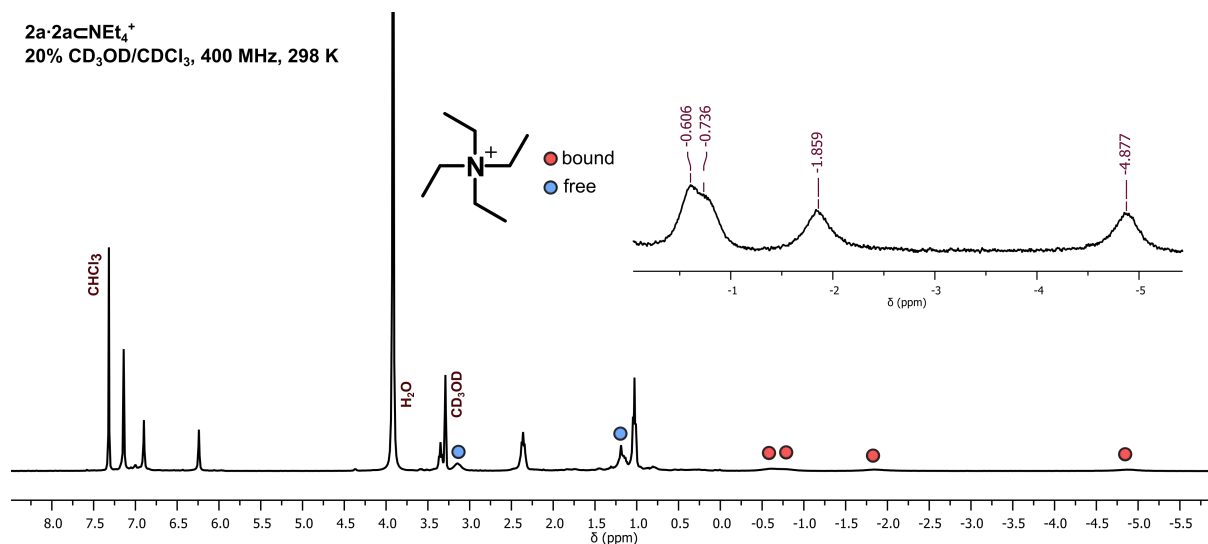


Figure S18. ^1H NMR spectrum (20% v/v $\text{CD}_3\text{OD}/\text{CDCl}_3$, 400 MHz, 298 K) of **2a** and NEt_4Br (1:1), referenced to the residual CHCl_3 signal at 7.26 ppm. Signals corresponding to the encapsulated and free guest are marked with red and blue circles, respectively. The OH protons of the host are not observed due to exchange with CD_3OD .

Cavitand **2b** was combined with 0.5 equiv. of NMe_4Cl , NEt_4Br and choline chloride to assess the competitive preference for the different cationic guests. Only NMe_4^+ and NEt_4^+ are bound in approximately a 1:1.2 ratio (green and orange circles, respectively).

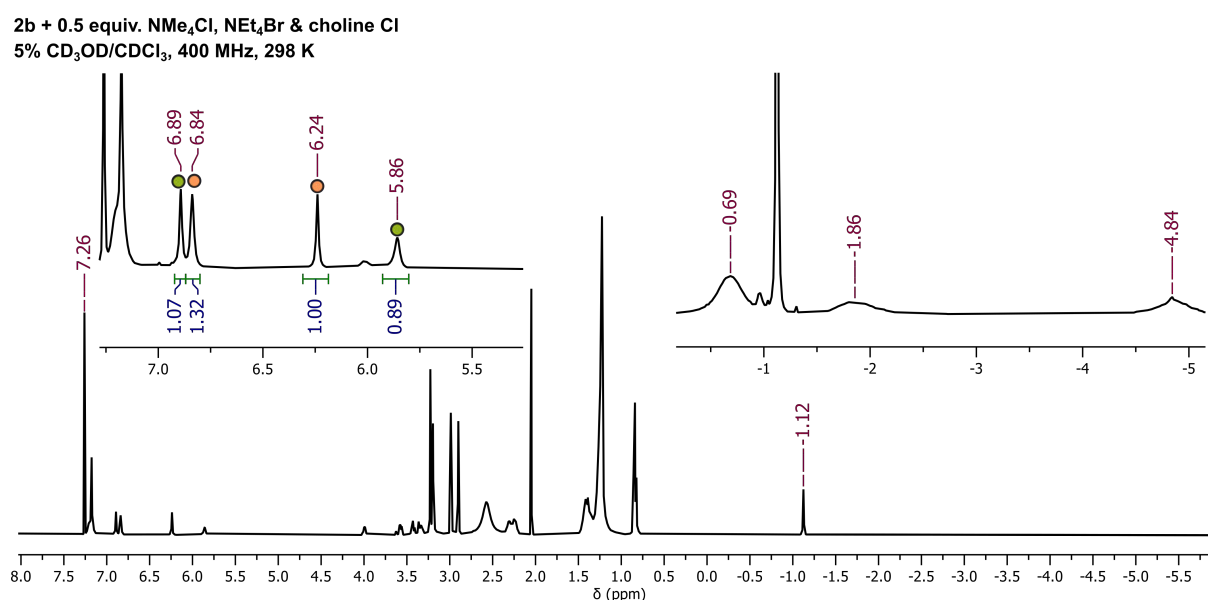


Figure S19. ^1H NMR spectrum (5% v/v $\text{CD}_3\text{OD}/\text{CDCl}_3$, 400 MHz, 298 K) of **2a** and 0.5 equiv. NMe_4Cl , NEt_4Br and choline chloride. Cavitand signals of the complexes of NMe_4^+ and NEt_4^+ are marked with green and orange circles, respectively.

Association constant for the host-guest complex $2b \cdot 2b \subset \text{NEt}_4^+$: UV-visible spectra of **2b** in CHCl_3 with increasing concentrations of NEt_4Br were recorded on an Edinburgh Instruments FS5 Fluorimeter in 1 cm quartz cells at room temperature (20–21 °C; Figure S20). The resulting isotherms (absorbance vs $[\text{G}]_0/[\text{H}]_0$) for wavelengths 261, 268, 275, 303, 309 and 317 nm were fitted using BindFit (<http://supramolecular.org>)⁴ based on a 1:1 binding model ($2b \cdot 2b + \text{NEt}_4^+ \leftrightarrow 2b \cdot 2b \subset \text{NEt}_4^+$) on the assumption that $K_{\text{dimer}} \gg K_a$. The results may be viewed at the following address: <http://app.supramolecular.org/bindfit/view/6ae0e32a-d824-4cb5-832e-12b0e1e3becc>.

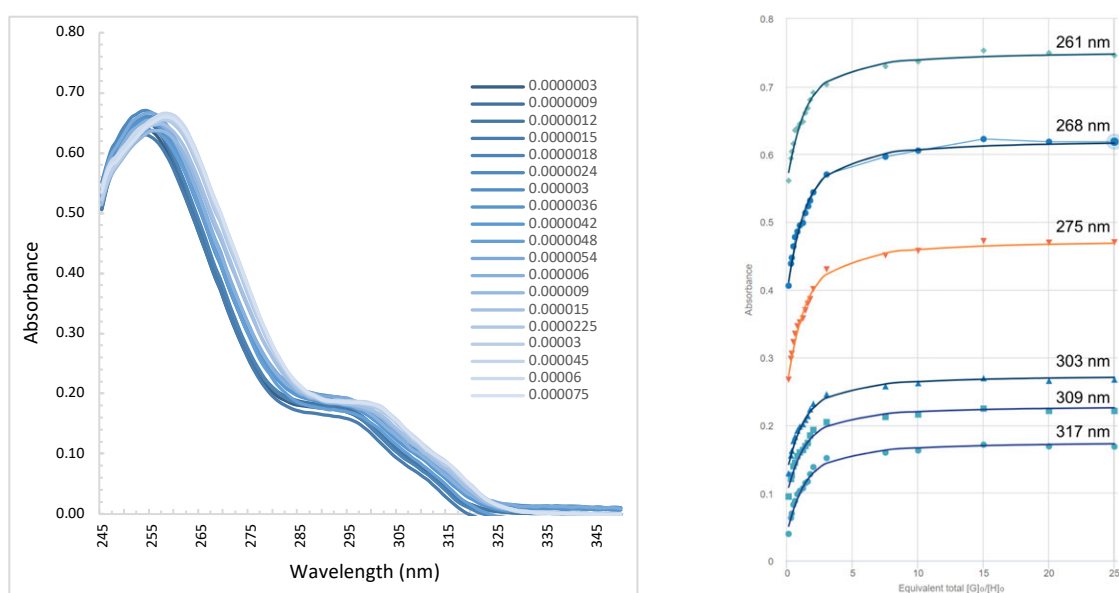


Figure S20. UV-visible spectra of **2b·2b** in CHCl_3 with increasing equivalents of NEt_4Br . The isotherms and their global calculated fit based on 1:1 host guest binding are shown for a range of wavelengths. $K_a = 4.6 \times 10^5 \text{ M}^{-1}$.

ESI-MS spectra of the host-guest complexes were collected on a Shimadzu LCMS-9030 Q-TOF electrospray ionisation mass spectrometer by direct injection of acetone/ CHCl_3 solutions.

$2\mathbf{a} \cdot 2\mathbf{a} \subset \text{NEt}_4^+$

#	Score	Pred. (M)	Pred. m/z	Meas. m/z	Diff. (mDa)	Formulae (M)	Ion	Diff. (ppm)	Iso Score	DBE
1	37.57	1922.82941	1922.82886	1922.83002	1.16	$\text{C}_{128}\text{H}_{116}\text{N O}_{16}$	$[\text{M}]^+$	0.603	30.91	71.5

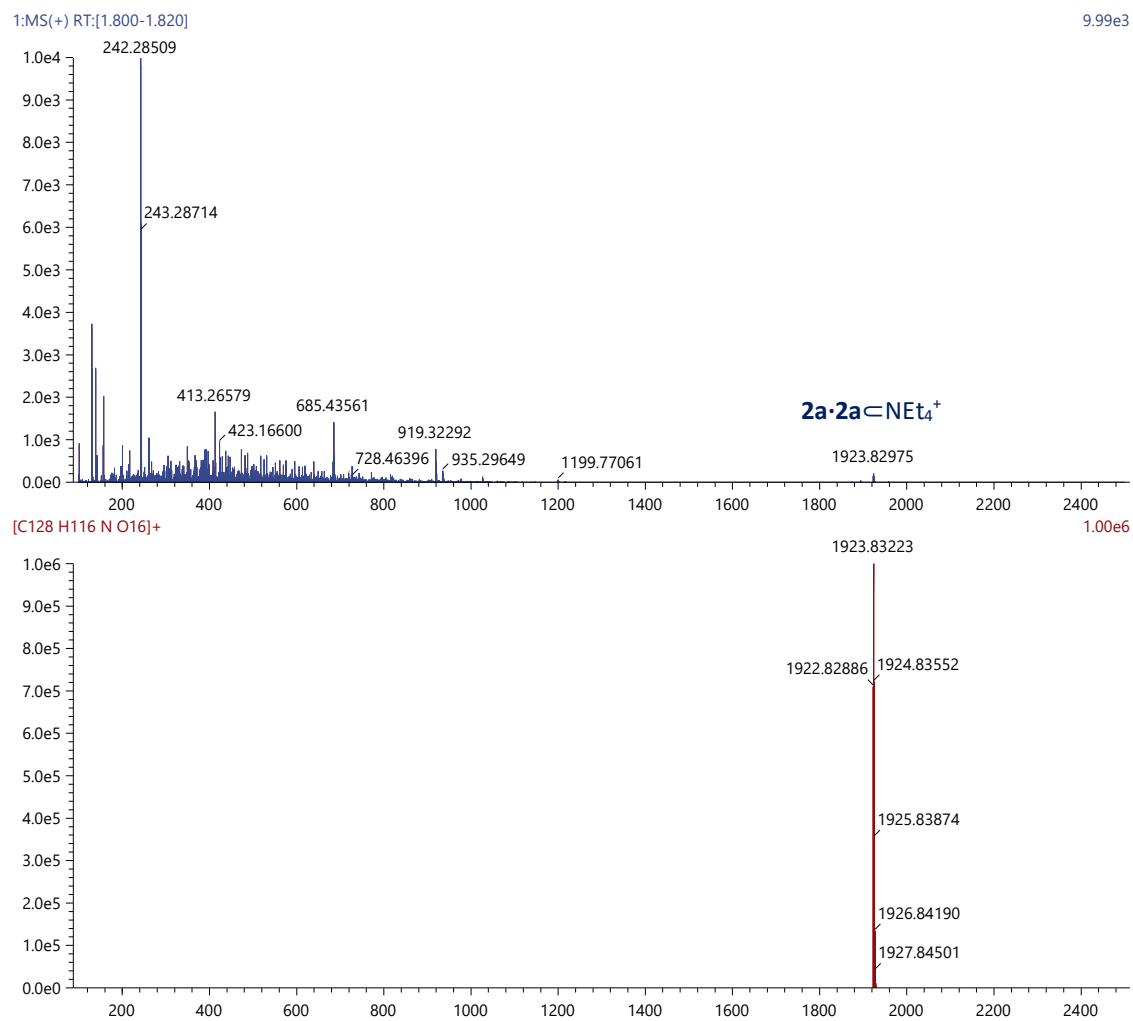
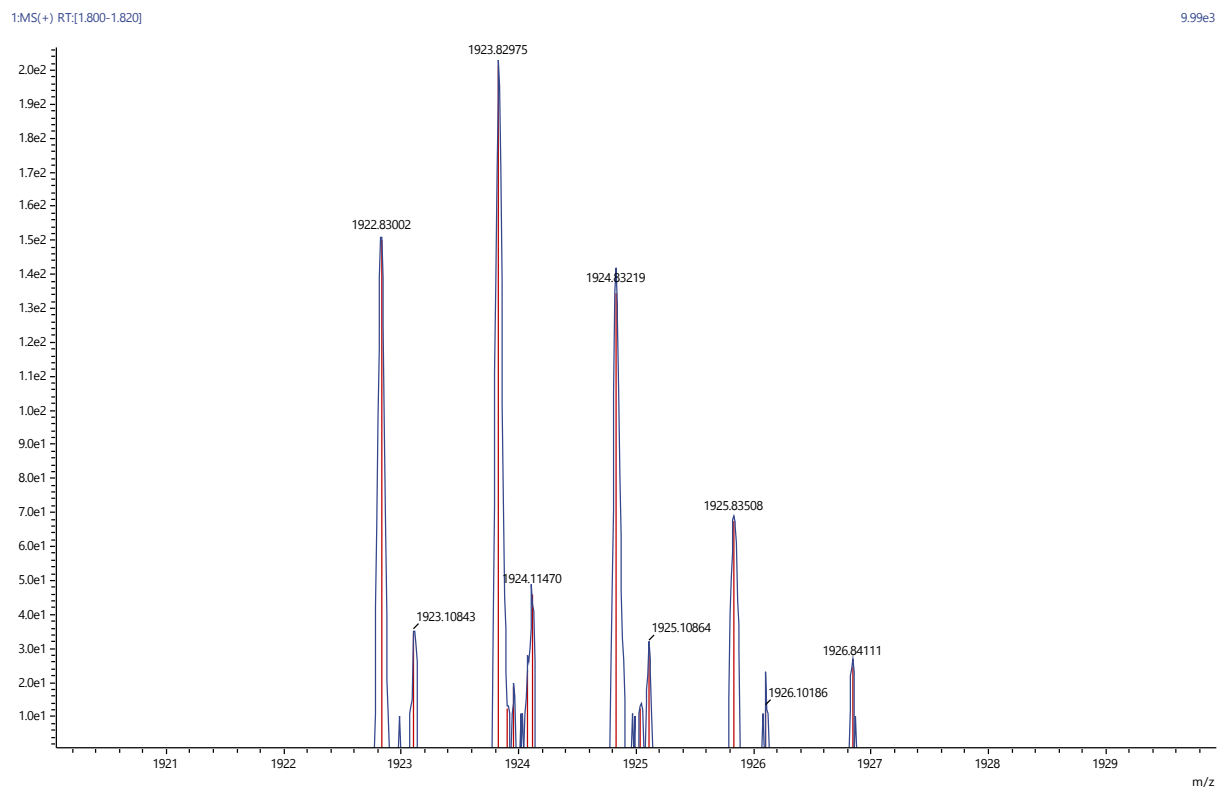


Figure S21. ESI-MS spectra of $2\mathbf{a} \cdot 2\mathbf{a} \subset \text{NEt}_4^+$.

Experimental $2a \cdot 2a \subset \text{NEt}_4^+$



Calculated $2a \cdot 2a \subset \text{NEt}_4^+$

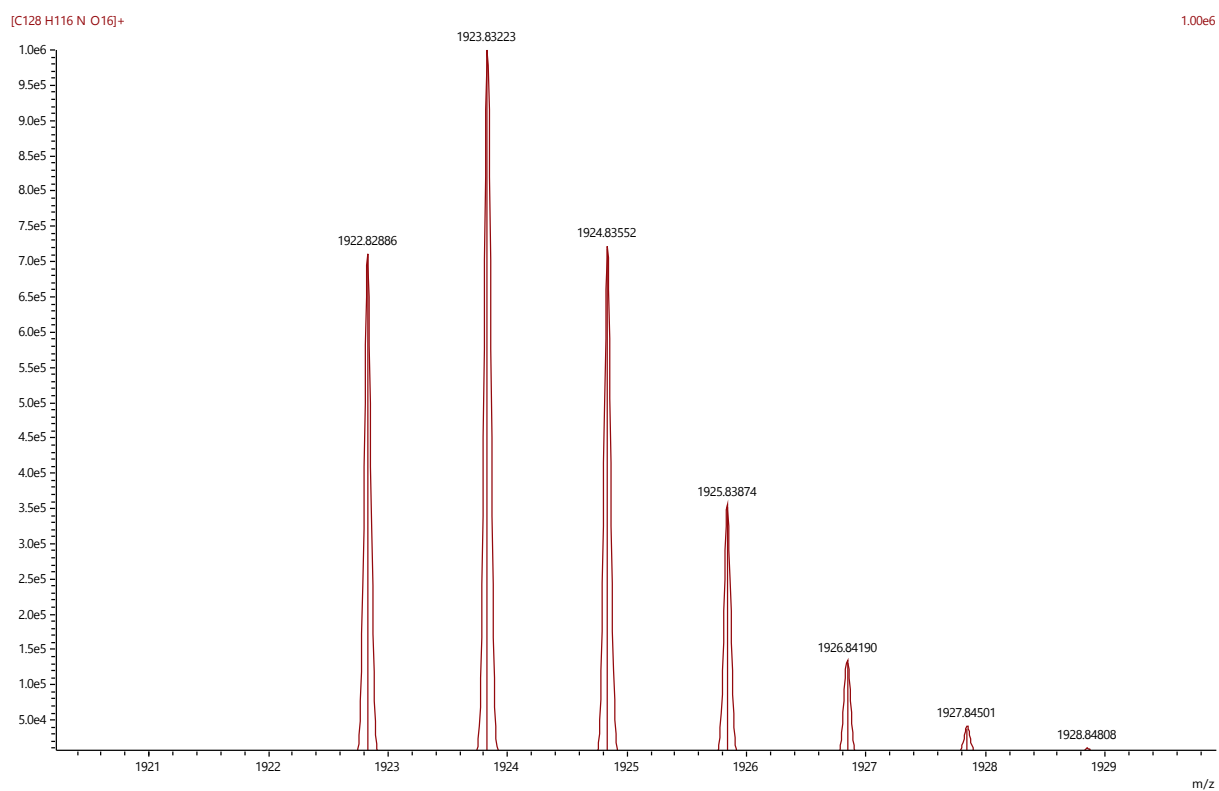


Figure S22. ESI-MS spectra of $2a \cdot 2a \subset \text{NEt}_4^+$.

$2b \cdot 2b \subset \text{NEt}_4^+$

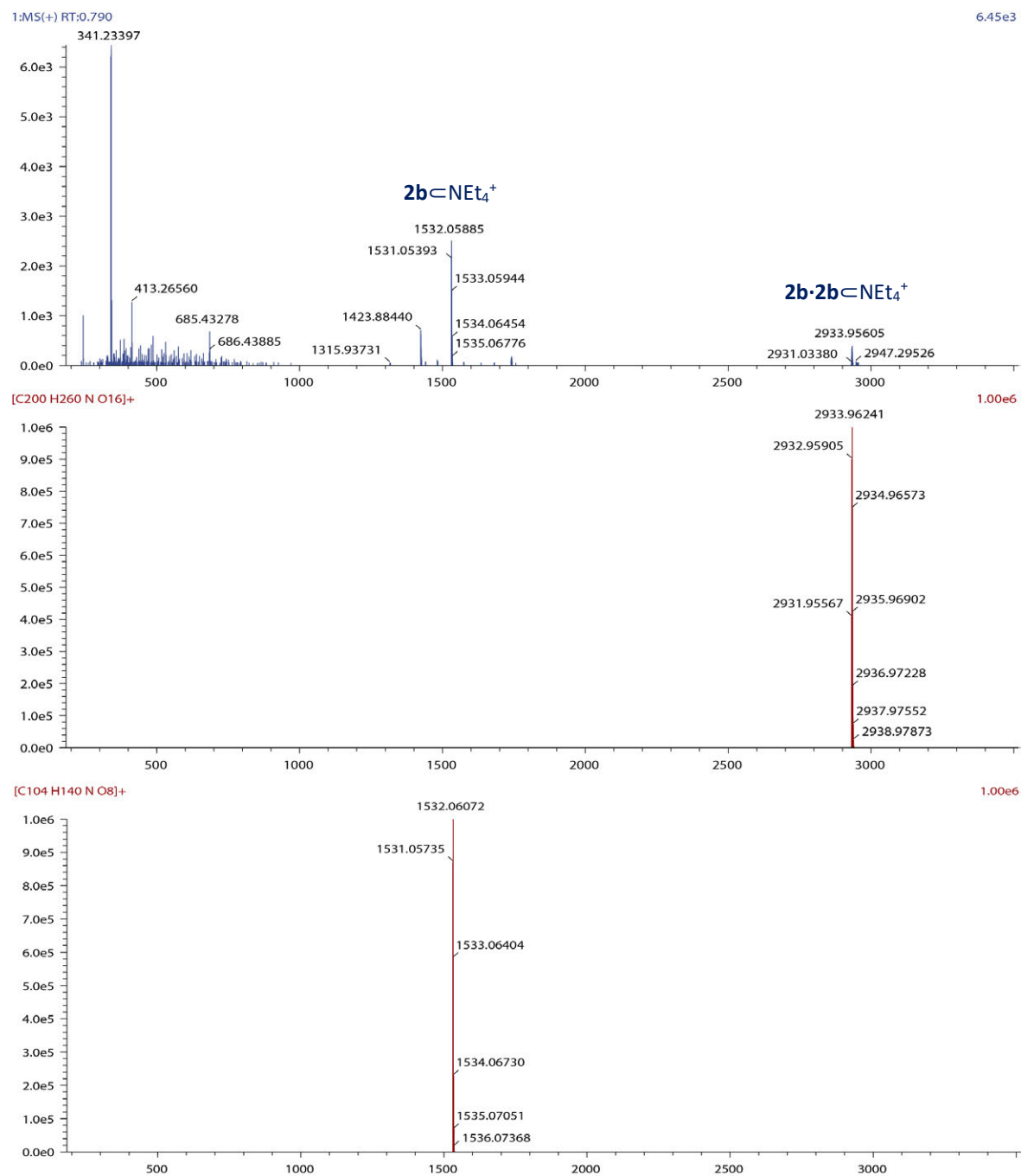
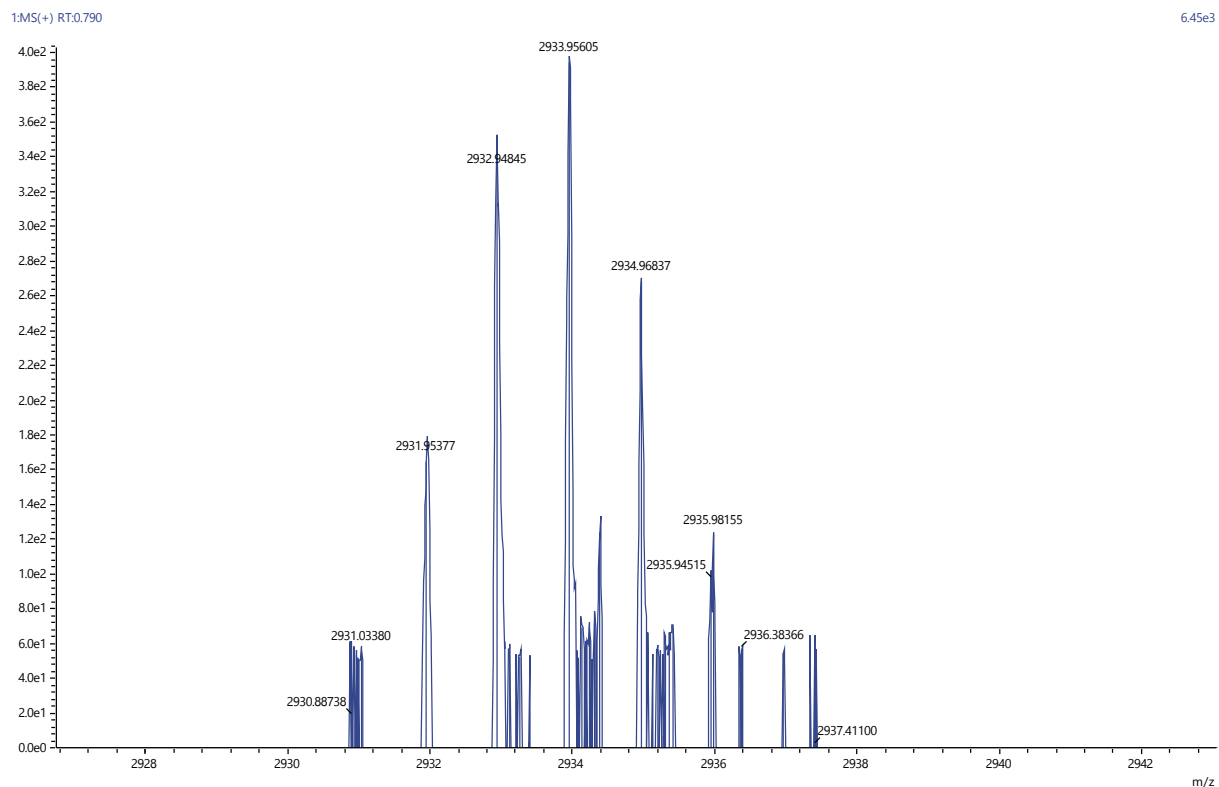


Figure S23. ESI-MS spectra of $2b \cdot 2b \subset \text{NEt}_4^+$, also showing the fragment ion $2b \subset \text{NEt}_4^+$.

Experimental $2b \cdot 2b \subset \text{NEt}_4^+$



Calculated $2b \cdot 2b \subset \text{NEt}_4^+$

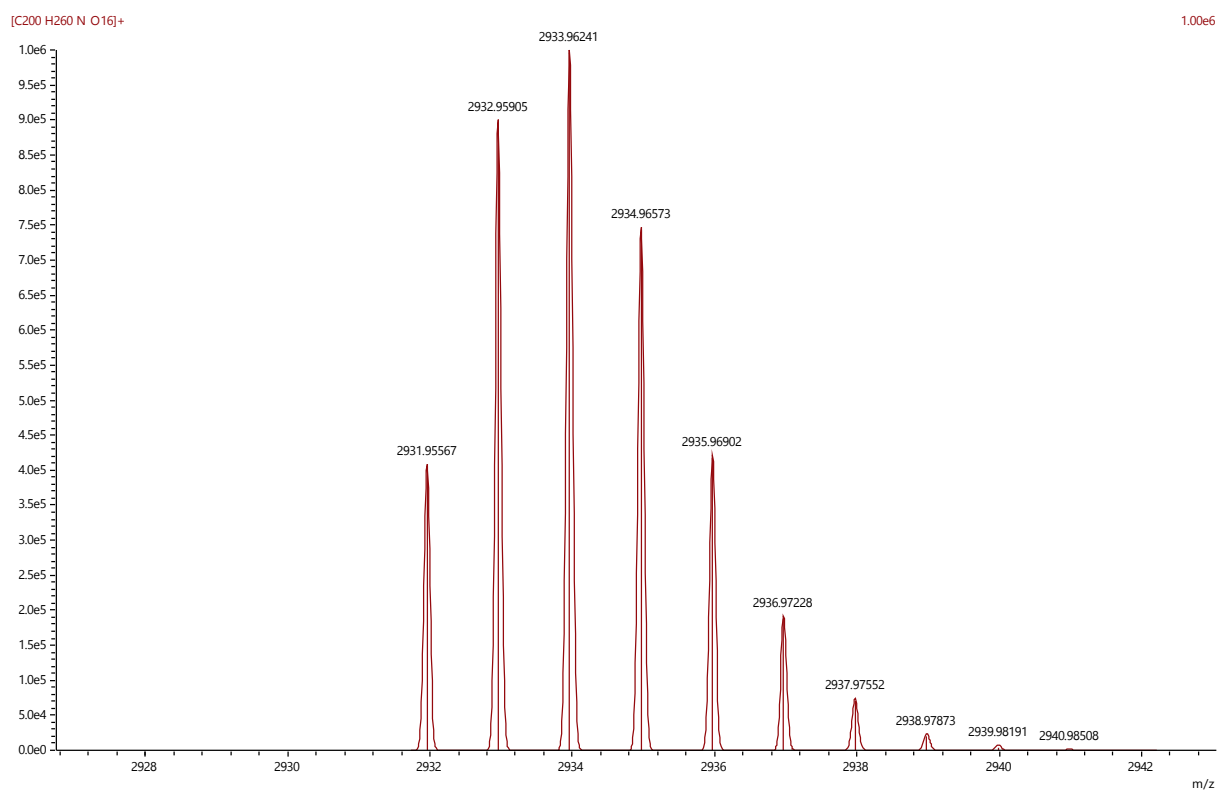


Figure S24. ESI-MS spectra of $2b \cdot 2b \subset \text{NEt}_4^+$.

5. Calculations

Internal cavity volumes for the X-ray crystal structure and energy optimised dimers were calculated using the CAVER Analyst 2.0 beta software (www.caver.cz)⁵ with a probe radius of 1.40 Å and increased volume precision. The volumes of guest molecules were calculated from the X-ray crystal structure (NEt₄⁺) or SPARTAN 14 (MMFF) optimized structures using VEGA ZZ 3.2.1 (www.ddl.unimi.it).⁶⁻⁷ All volumes are rounded up to the nearest integer value and are summarised in Table S1.

Table S1. Summary of capsule cavity and guest volumes.

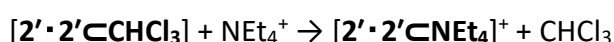
molecule/complex	cavity volume (Å ³)	guest volume (Å ³)
2a·2a CNEt ₄ ⁺ (crystal structure)	235	-
2'·2' CCHCl ₃ (calculated)	175	-
benzene	-	81
chloroform	-	71
NMe ₄	-	94
NEt ₄	-	152
NPr ₄	-	227
choline	-	122
SiEt ₄	-	176
terephthalonitrile	-	116
adamantane	-	147
C ₆ F ₆	-	113

Electronic structure calculations were performed using density functional theory (DFT) *in vacuo*, applying the B3LYP functional calculated with Grimme's D3 corrections for dispersion.⁸ Geometry optimisation from empirical coordinates was performed using the 6-31G(d,p) basis set on all atoms. From the optimised structure, single-point energies were refined at the B3LYP-D3/6-311G++(2d,2p) level of theory. No symmetry constraints were applied to the empirical data, where the Cartesian coordinates of the **2'·2'** capsule (Figure S25) were obtained from X-ray crystallographic data (see X-ray data section) with residual solvent removed. Ethyl pendent groups were substituted for methyl groups for faster geometry convergence. In addition, the energy of the empirical **2'·2'** capsule was compared to an ideal vacant capsule of high symmetry (*S*₈ point group: Figure S26), where the **2'·2'** capsule is predicted +85.48 kJ mol⁻¹ less stable relative to the ideal system *in vacuo*. This higher energy is mainly due to hydrogen bonding displaying less geometric order in the **2'·2'** experiment system.

Guest molecule coordinates were then introduced to the cavity of the previously optimised **2'·2'** capsule structure before geometry re-optimisation (B3LYP-D3/6-31G(d,p)) under zero

symmetry constraints. Single-point energies were again refined at the B3LYP-D3/6-311G++(2d,2p) level of theory. All calculations were performed using the Gaussian09 package⁹ on the NCI computing cluster (using 48 processors).

Using this procedure, the energies of solvent CHCl₃ (Figure S27), and guests NEt₄⁺ (Figure S28), SiEt₄ (Figure S29), choline⁺ (Figure S30) within the 2'·2' capsule were calculated (Table S2). Relative energies of encapsulation ($\Delta E_{\text{interaction}}$) were modelled as a displacement of the chloroform solvent molecule from the cavity by a single guest species, using the difference between the products-reactants systems. For example, equation 3 relates to the encapsulation of NEt₄⁺ displacing CHCl₃:



$$\Delta E_{\text{interaction}} = \{E([2' \cdot 2' \subset \text{NEt}_4]^+) + E(\text{CHCl}_3)_{\text{monomer}}\} - \{E([2' \cdot 2' \subset \text{CHCl}_3]) + E(\text{NEt}_4^+)_{\text{monomer}}\} \quad (3)$$

Guest (monomer) geometries and energies *in vacuo* were calculated using the same procedure (B3LYP-D3/6-31G(d,p)//B3LYP-D3/6-311G++(2d,2p)) using the highest symmetry constraints (CHCl₃: C_{3v}; NEt₄⁺: S₄; SiEt₄: S₄; choline⁺: C_s). Energies of encapsulation relative to the solvent guest 2'·2'⊂CHCl₃ are provided in Table S2.

Electrostatic Potential (ESP) maps were constructed directly from formatted checkpoint files using Gaussview 6.0.16 visualisation package¹⁰ using default parameters for mapping. Images of the empirical capsule (Figure S25), the ideal S₈ capsule (Figure S26), 2'·2'⊂CHCl₃ (Figure S27), 2'·2'⊂NEt₄⁺ (Figure S28), 2'·2'⊂SiEt₄ (Figure S29), and 2'·2'⊂choline⁺ (Figure S30) are provided; showing various orientations and slices of each mapped surface.

Table S2: Single-point energies of experiment cavitand capsules with encapsulated solvent (CHCl₃) and guest (NMe₄⁺, NEt₄⁺, SiEt₄, Choline⁺) at the B3LYP-D3/6-311G++(2d,2p) level *in vacuo*. Interaction energies of the 2xCavitand·1 x Guest systems with respect to empty experiment structure.

	2'·2'	CHCl ₃	NMe ₄ ⁺	NEt ₄ ⁺	SiEt ₄	choline ⁺
E(e) _{monomer} ^a	-14,497,547.31	-3,726,601.47	-562,502.50	-975,485.58	-1,592,542.37	-863,301.36
E(e) _{capsule} ^{a, b}	-	18,224,267.81	15,060,312.79	15,473,323.27	16,090,206.61	15,361,105.72
E(e) _{interaction} ^{a, c}	-	-119.03 (0.00)	-262.98 (-143.95) ^d	-290.38 (-171.35) ^d	-116.94 (+2.09) ^d	-257.05 (-138.02) ^d

^aElectronic Energies in kJ mol⁻¹ (*in vacuo*).

^bExperiment capsule with optimised guest species.

^cE(e)_{interaction} = E(e)_{capsule} - [E(e)_{empty capsule} + E(e)_{guest monomer}].

^dRelative energy of guest molecule displacing encapsulated solvent.

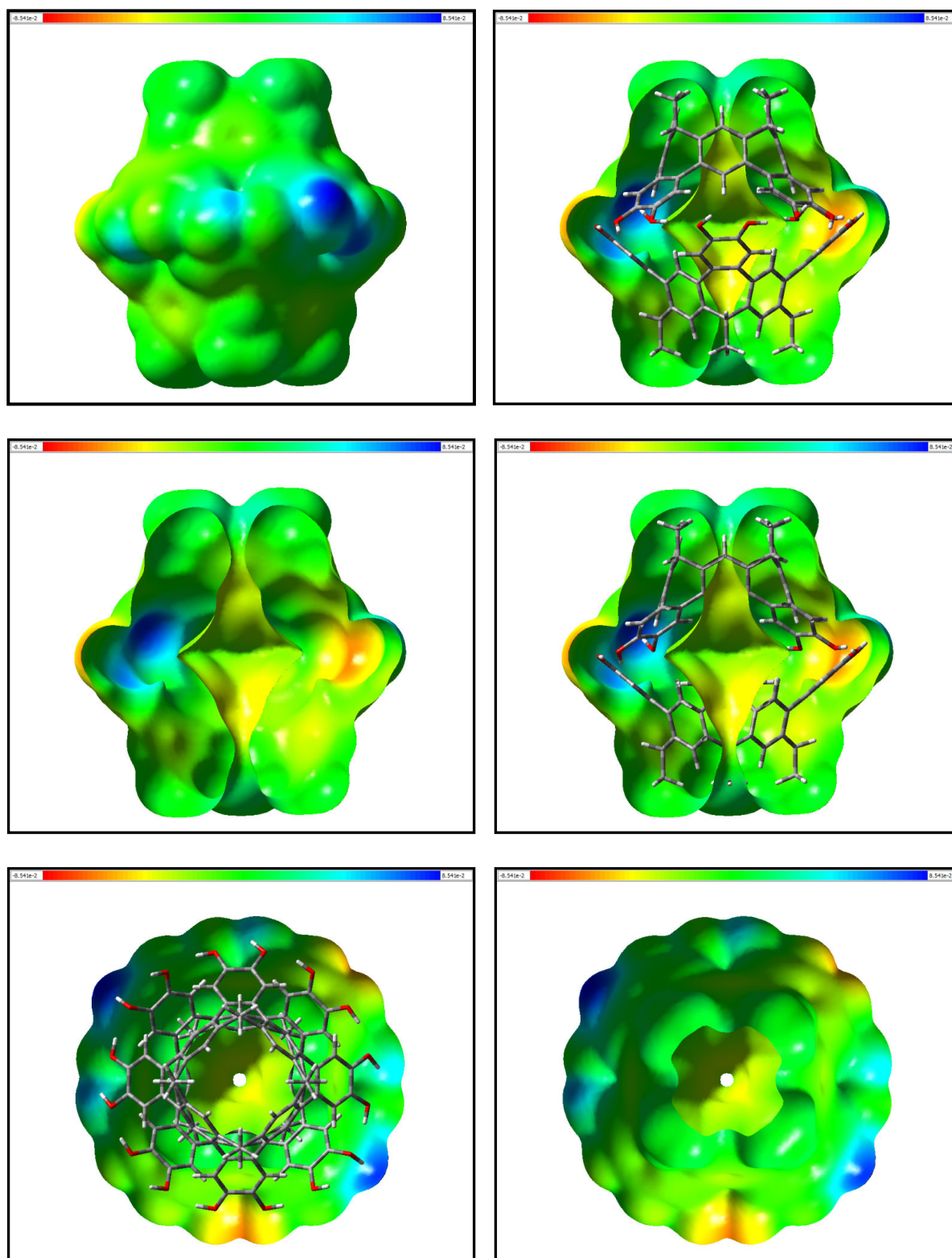


Figure S25. ESPs of the optimised C_1 -symmetric structure $2' \cdot 2'$ based on crystallographic data (solvent and guest removed).

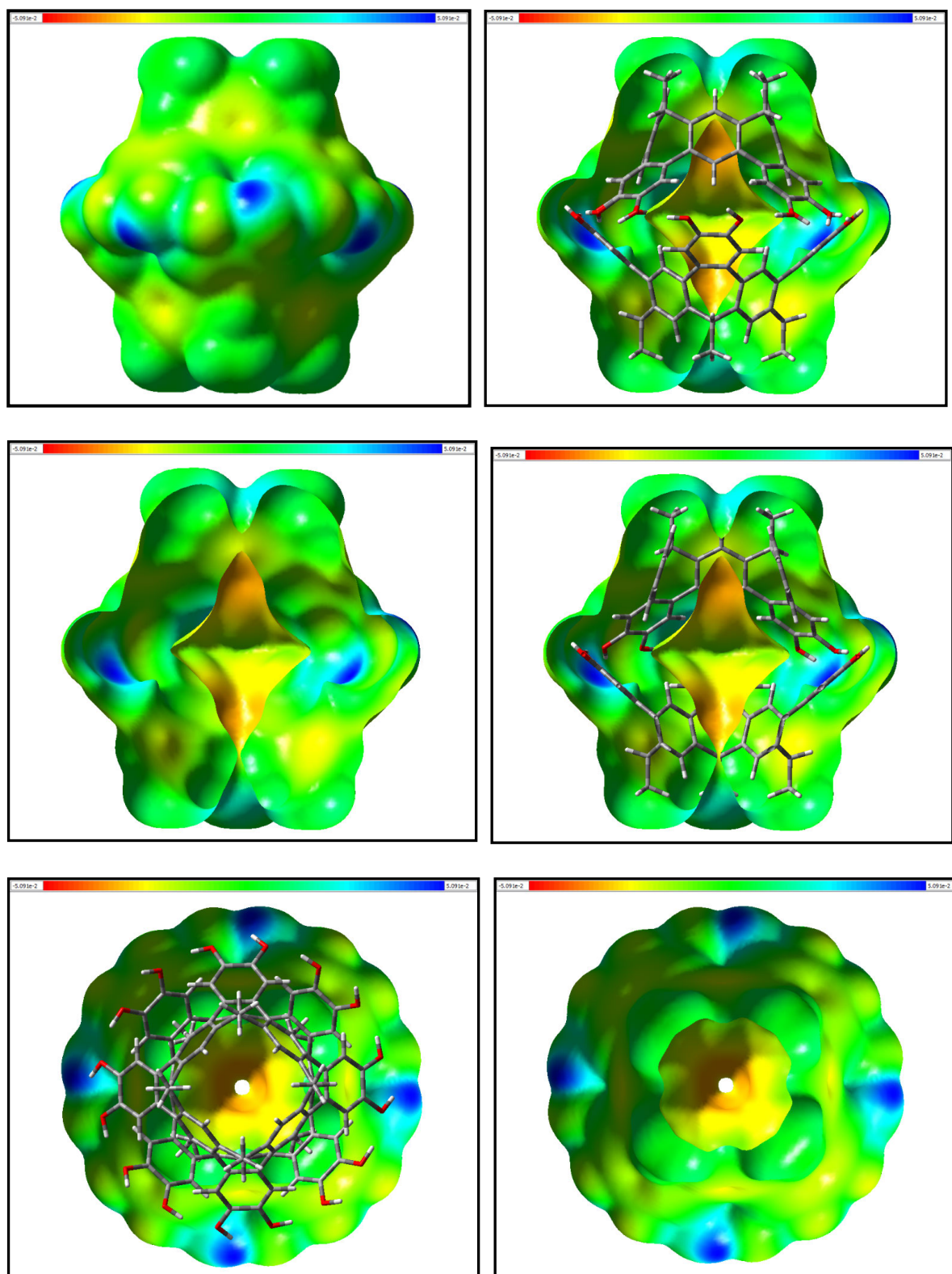


Figure S26. ESPs of the optimised S_8 -symmetric capsule $2' \cdot 2'$.

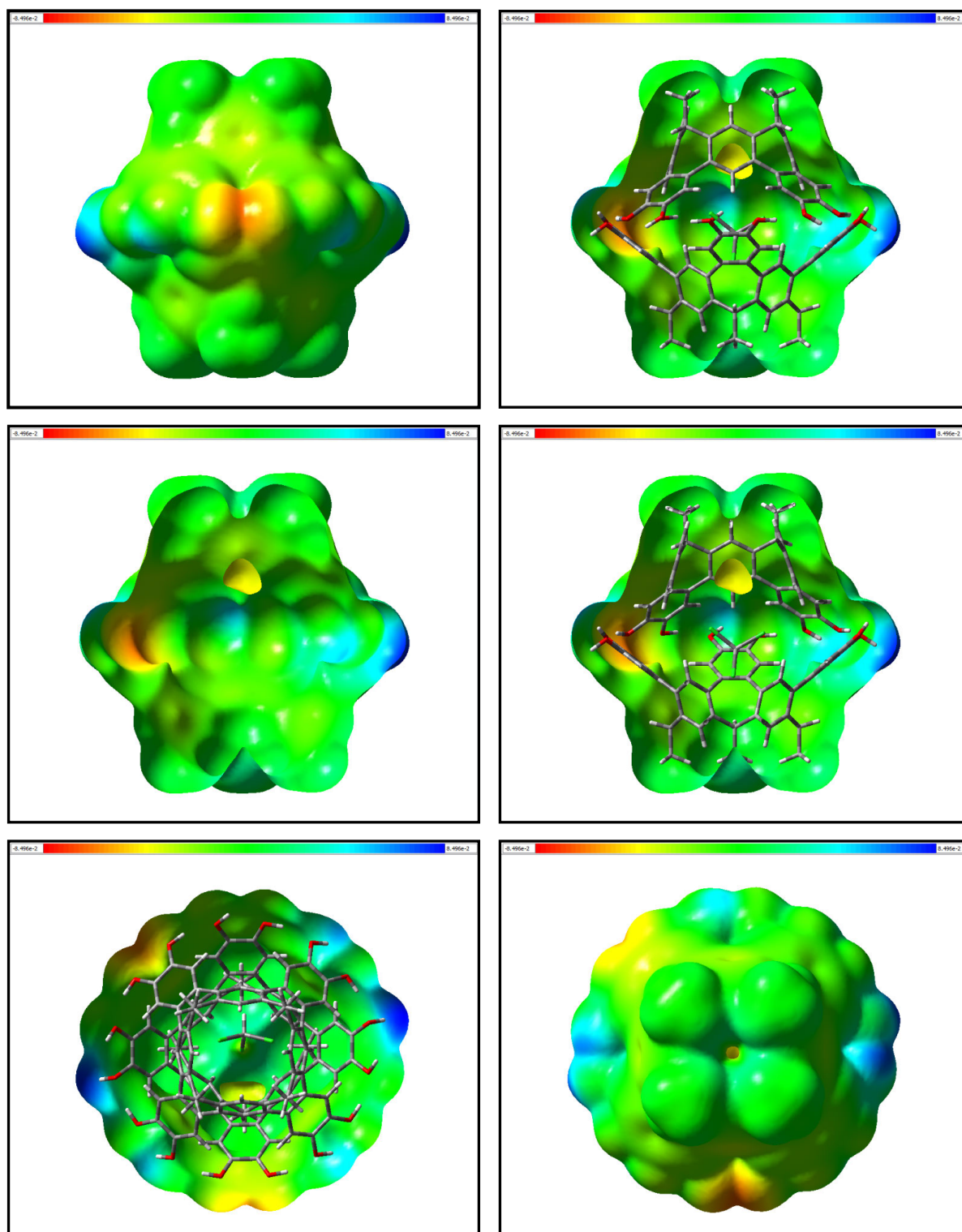


Figure S27. ESPs of the optimised C_1 -symmetric host-guest complex $2' \cdot 2' \subset \text{CHCl}_3$.

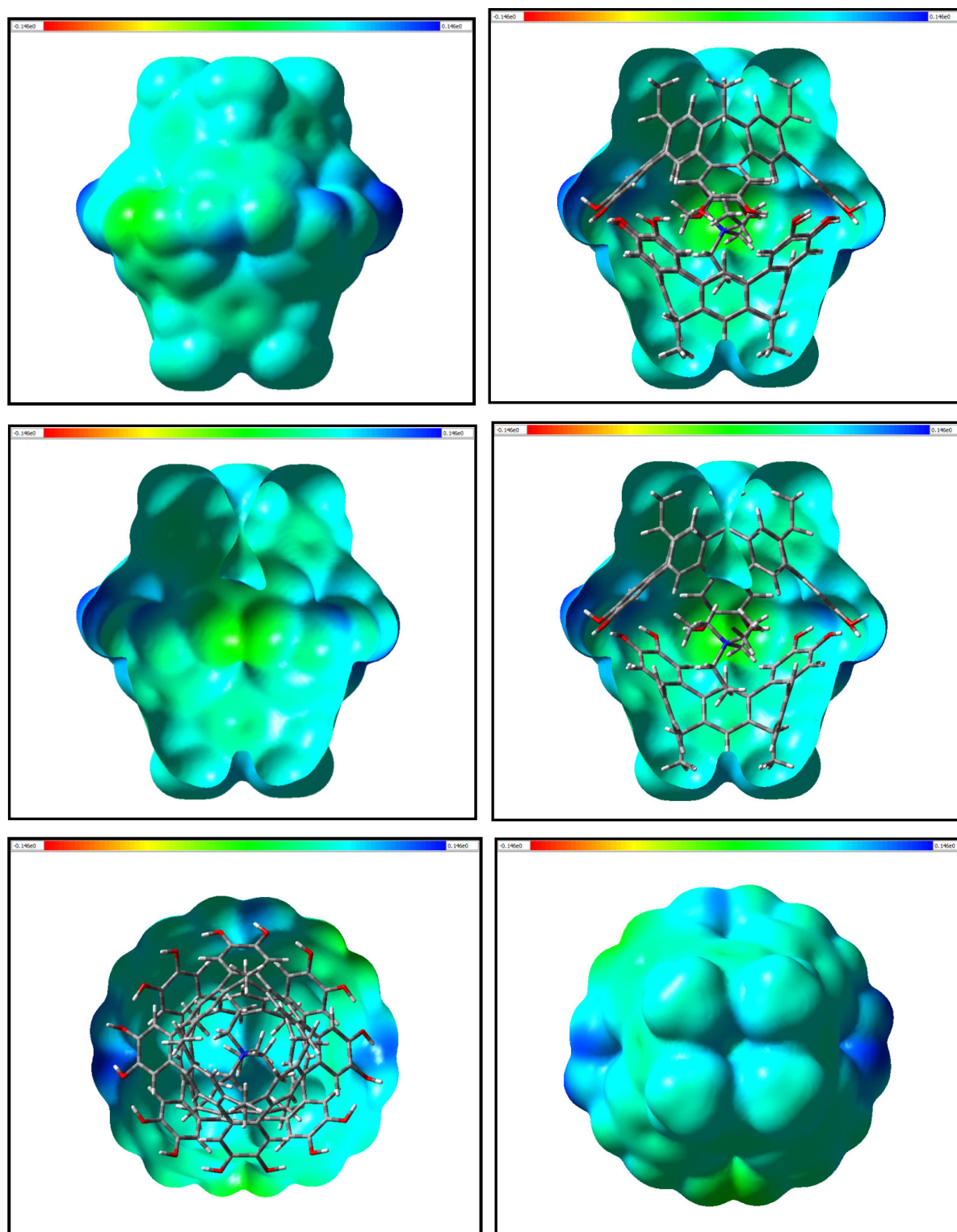


Figure S28. ESPs of the optimised C_1 -symmetric host-guest complex $2' \cdot 2' \subset \text{NEt}_4^+$.

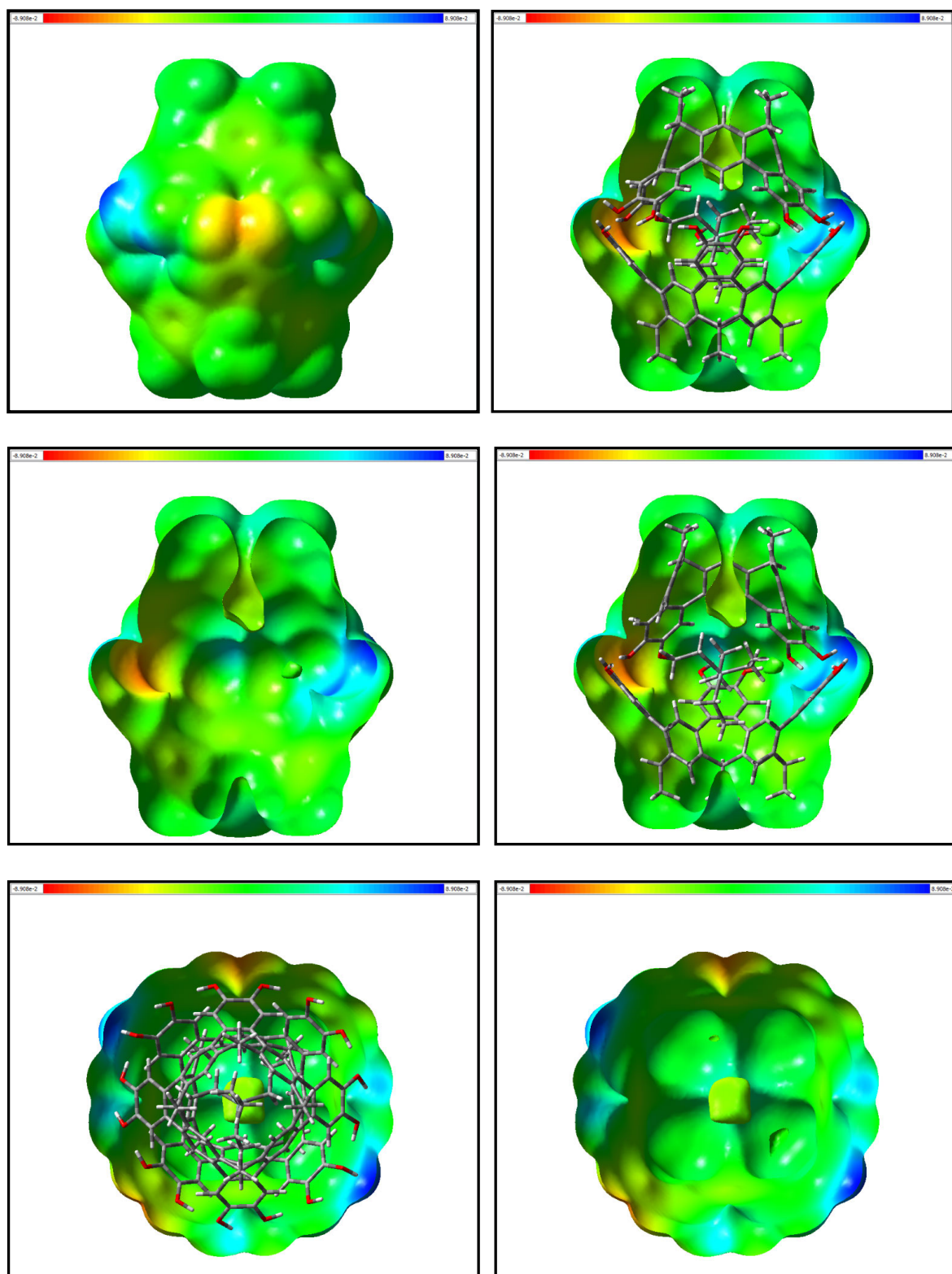


Figure S29. ESPs of the optimised C_1 -symmetric host-guest complex $2' \cdot 2' \subset \text{SiEt}_4$.

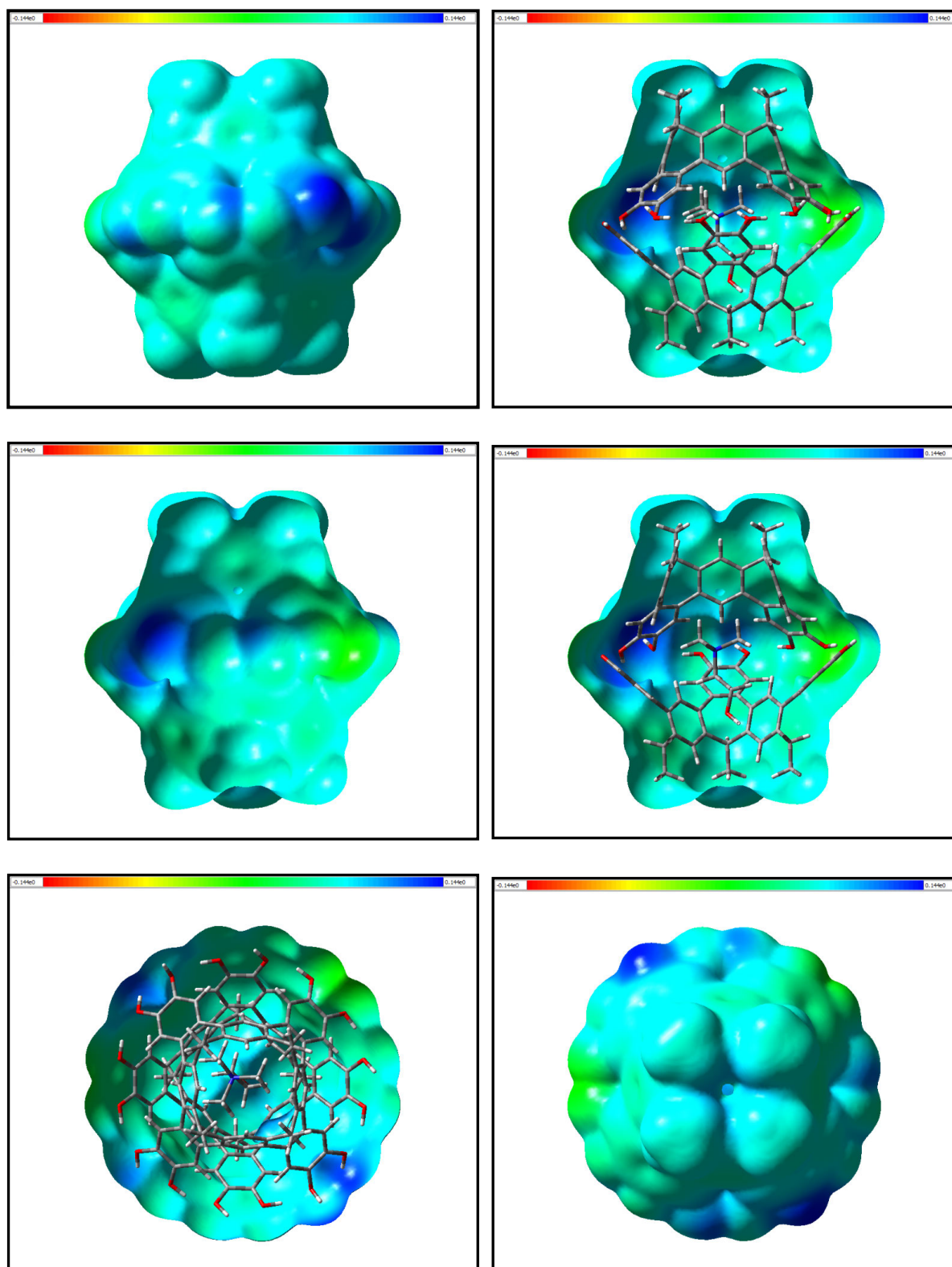


Figure S30. ESPs of the optimised C_1 -symmetric host-guest complex $2' \cdot 2' \subset \text{choline}^+$.

6. X-ray Crystallography

Data were collected on an Agilent SuperNova with Atlas CCD using mirror monochromated microfocus Mo K_{α} radiation ($\lambda = 0.71073 \text{ \AA}$) at 40 W. The data processing was undertaken within CrysAlisPro,¹¹ including a numerical absorption correction over a face-indexed model. The structures were solved by direct methods with SHELXT2014¹²⁻¹³ and extended and refined against all F^2 data with SHELXL2014¹² using the X-Seed¹⁴ interface. The data are summarised in Table S3. The non-hydrogen atoms in the asymmetric unit were modelled with anisotropic displacement parameters. Non-phenolic hydrogen atoms were placed in calculated positions and refined using a riding model with fixed C–H distances (sp^2 CH 0.95 Å, sp^3 CH₃ 0.98 Å, sp^3 CH₂ 0.99 Å; sp^3 CH 1.00 Å,) and isotropic displacement parameters estimated as $U_{\text{iso}}(\text{H}) = 1.2U_{\text{eq}}(\text{C})$, except for CH₃, where $U_{\text{iso}}(\text{H}) = 1.5U_{\text{eq}}(\text{C})$. The phenolic hydrogen atoms of the cavitands were restrained only in the O–H distance (0.84 Å) and $U_{\text{iso}}(\text{H}) = 1.2U_{\text{eq}}(\text{O})$.

The NEt_4^+ guest was disordered over two sites and modelled with the assistance of distance (SAME) and ADP (EADP, RIGU) restraints. A CHCl_3 and MeOH molecule were disordered over the same site, their occupancies refined by free variables. Solvent molecules were restrained with distance (DFIX) and ADP (RIGU, EADP) restraints where necessary.

The structure also contained regions of disordered solvent that could not be effectively modelled and have been treated as a diffuse contribution to the overall scattering using PLATON SQUEEZE.¹⁵ Within the unit cell, void regions of 371 Å³/108 e and 584 Å³/160 e were identified, corresponding to two and three molecules of toluene, respectively.

Figure S31 shows an ORTEP diagram of the structure with 50% probability ellipsoids and labels for key atoms. Figure S32 shows the short contacts between the axial methyl foot of the guest and the aromatic rings of one half of the host.

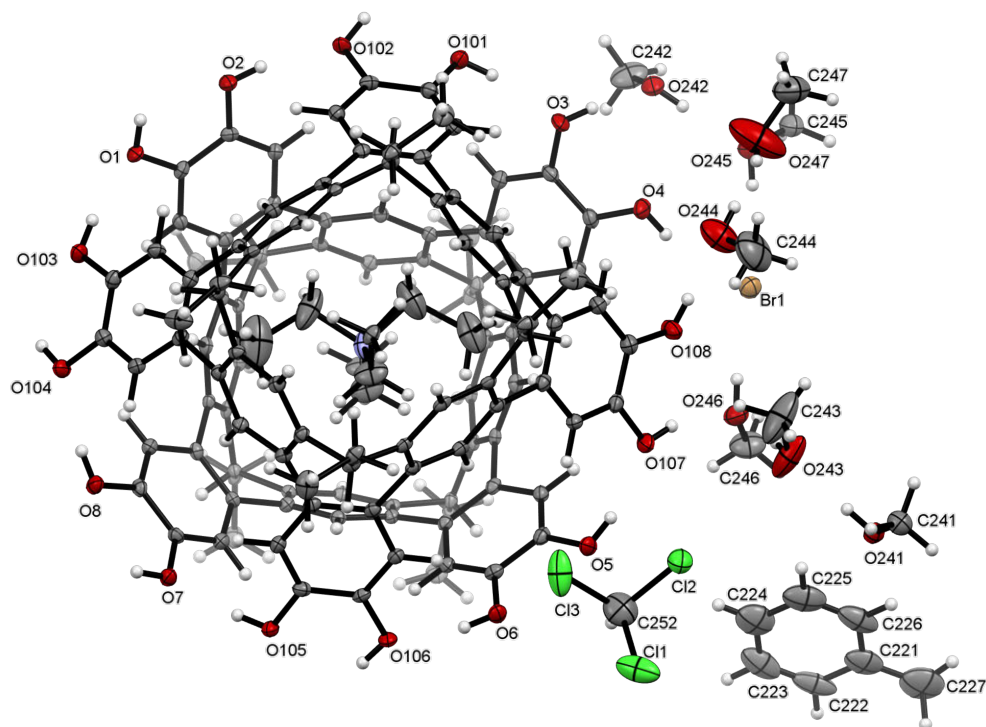


Figure S31. ORTEP diagram of the asymmetric unit $[2b \cdot 2b \cdot C_8H_{20}N] \cdot Br \cdot 7.63(CH_3OH) \cdot 0.37(CHCl_3) \cdot C_7H_8$. The second component of disorder is omitted for clarity.

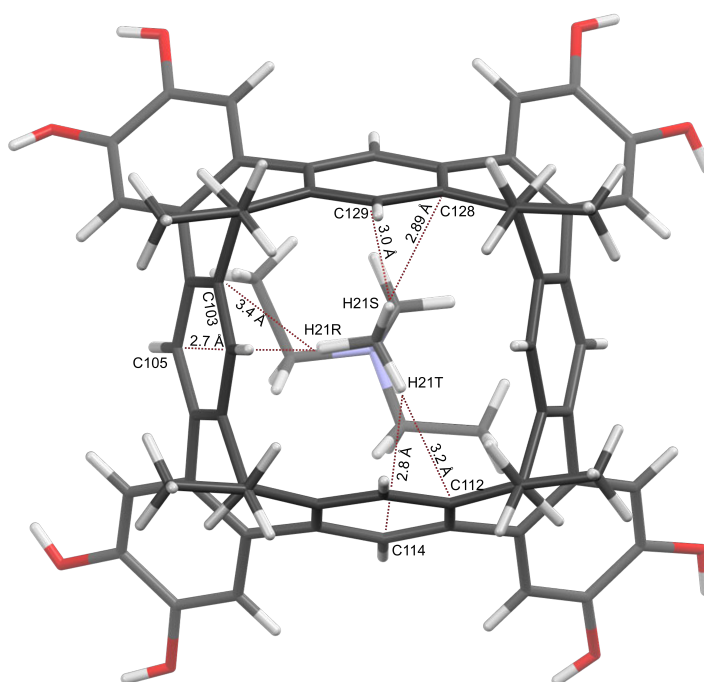


Figure S32. Partial crystal structure of $[2b \cdot 2b \cdot C_8H_{20}N] \cdot Br \cdot 7.63(CH_3OH) \cdot 0.37(CHCl_3) \cdot C_7H_8$, highlighting the short contacts between the axial methyl group of the guest and the aromatic rings of the host. Solvent, one cavitand molecule and the second component of disorder omitted for clarity.

7. References

1. Gottlieb, H. E.; Kotlyar, V.; Nudelman, A., NMR Chemical Shifts of Common Laboratory Solvents as Trace Impurities. *J. Org. Chem.* **1997**, *62*, 7512-7515.
2. Smith, J. N.; Lucas, N. T., Rigid tetraarylene-bridged cavitands from reduced-symmetry resorcin[4]arene derivatives. *Chem. Commun.* **2018**, *54*, 4716-4719.
3. Smith, J. N.; Brind, T. K.; Petrie, S. B.; Grant, M. S.; Lucas, N. T., One-Step Synthesis of C_{2v} -Symmetric Resorcin[4]arene Tetraethers. *J. Org. Chem.* **2020**, *85*, 4574-4580.
4. Hibbert, D. B.; Thordarson, P., The death of the Job plot, transparency, open science and online tools, uncertainty estimation methods and other developments in supramolecular chemistry data analysis. *Chem. Commun.* **2016**, *52*, 12792-12805.
5. Jurcik, A.; Bednar, D.; Byska, J.; Marques, S. M.; Furmanova, K.; Daniel, L.; Kokkonen, P.; Brezovsky, J.; Strnad, O.; Stourac, J.; Pavelka, A.; Manak, M.; Damborsky, J.; Kozlikova, B., CAVER Analyst 2.0: analysis and visualization of channels and tunnels in protein structures and molecular dynamics trajectories. *Bioinformatics* **2018**, *34*, 3586-3588.
6. Pedretti, A.; Villa, L.; Vistoli, G., VEGA: a versatile program to convert, handle and visualize molecular structure on Windows-based PCs. *J. Mol. Graphics Modell.* **2002**, *21*, 47-49.
7. Pedretti, A.; Villa, L.; Vistoli, G., VEGA – An open platform to develop chemo-bio-informatics applications, using plug-in architecture and script programming. *J. Comput. Aided Mol. Des.* **2004**, *18*, 167-173.
8. Grimme, S.; Antony, J.; Ehrlich, S.; Krieg, H., A consistent and accurate ab initio parametrization of density functional dispersion correction (DFT-D) for the 94 elements H-Pu. *J. Chem. Phys.* **2010**, *132*, 154104.
9. Frisch, M. J.; Trucks, G. W.; Schlegel, H. B.; Scuseria, G. E.; Robb, M. A.; Cheeseman, J. R.; Scalmani, G.; Barone, V.; Petersson, G. A.; Nakatsuji, H.; Li, X.; Caricato, M.; Marenich, A.; Bloino, J.; Janesko, B. G.; Gomperts, R.; Mennucci, B.; Hratchian, H. P.; Ortiz, J. V.; Izmaylov, A. F.; Sonnenberg, J. L.; Williams-Young, D.; Ding, F.; Lipparini, F.; Egidi, F.; Goings, J.; Peng, B.; Petrone, A.; Henderson, T.; Ranasinghe, D.; Zakrzewski, V. G.; Gao, J.; Rega, N.; Zheng, G.; Liang, W.; Hada, M.; Ehara, M.; Toyota, K.; Fukuda, R.; Hasegawa, J.; Ishida, M.; Nakajima, T.; Honda, Y.; Kitao, O.; Nakai, H.; Vreven, T.; Throssell, K.; J. A. Montgomery, J.; Peralta, J. E.; Ogliaro, F.; Bearpark, M.; Heyd, J. J.; Brothers, E.; Kudin, K. N.; Staroverov, V. N.; Keith, T.; Kobayashi, R.; Normand, J.; Raghavachari, K.; Rendell, A.; Burant, J. C.; Iyengar, S. S.; Tomasi, J.; Cossi, M.; Millam, J. M.; Klene, M.; Adamo, C.; Cammi, R.; Ochterski, J. W.; Martin, R. L.; Morokuma, K.; Farkas, O.; Foresman, J. B.; Fox, D. J. *Gaussian 09*, Gaussian, Inc.: Wallingford CT, 2016.
10. Dennington, R.; Keith, T.; Millam, J. *GaussView*, 6.0.16; 2009.
11. *CrysAlisPro*, 1.171.40.67a; Agilent Technologies: Yarnton, Oxfordshire, UK, 2019.

12. Sheldrick, G. M., A short history of SHELX. *Acta Crystallogr. Sect. A: Found. Crystallogr.* **2008**, *64*, 112-122.
13. Sheldrick, G. M., SHELXT - Integrated space-group and crystal-structure determination. *Acta Crystallogr. Sect. A: Found. Adv.* **2015**, *71*, 3-8.
14. Barbour, L. J., X-Seed — A Software Tool for Supramolecular Crystallography. *J. Supramol. Chem.* **2001**, *1*, 189-191.
15. Spek, A. L., PLATON SQUEEZE: a tool for the calculation of the disordered solvent contribution to the calculated structure factors. *Acta Crystallogr. Sect. C: Cryst. Struct. Commun.* **2015**, *71*, 9-18.